Doctoral Dissertation

Study on the Synthesis and Biodegradability of Sustainable Poly(lactic acid)-Based Block Copolymers

持続可能なポリ乳酸を基盤としたブロック共重合体の合成および生分解性に関する研究

Atsuki Takagi

July 2025

Graduate School of Engineering,
the University of Osaka

Contents

General Introduction

Environmental Issues

Plastics have become an integral part of our daily lives. Since the mid-20th century, the use of plastics has grown considerably, currently reaching 400 million metric tons (Mt) (**Figure 1**).[1,2] Although plastic is widely used in numerous products, its heavy reliance on petroleum resources raises concerns about its extensive use of fossil resources and the environmental issues caused by improper management of plastic waste.[2,3] Given the critical state of fossil resources, fossil-based plastics, which account for 20% of petroleum consumption and contribute to greenhouse gas (GHG) emissions, have undergone a gradual industrial reduction since the 1980s. In 2018, 33% of plastic waste was recycled, 25% was landfilled, and the rest was incinerated.[3] Mismanagement of other plastic waste has resulted in significant amounts of plastic entering rivers and oceans.[2,4] Marine pollution from plastics, first reported in the early 1970s, has recently become a global issue (**Figure 2**).[4,5] The Global Plastics Outlook, released by the Organization for Economic Co-operation and Development (OECD), reported that 6.1 Mt of plastic waste entered aquatic environments in 2019, with 1.7 Mt reaching marine areas. In addition, 30 Mt of plastic waste has accumulated and is drifting in the oceans. The OECD projects that 11.6 Mt of mismanaged plastics will be discharged into aquatic environments by 2060, with 4 Mt entering the oceans (**Figure 3**).[2] Discharged microplastics can accumulate in organisms through the food chain, potentially affecting human health.[6] Environmentally friendly biodegradable plastics made from sustainable bioresources should be developed to mitigate these issues.

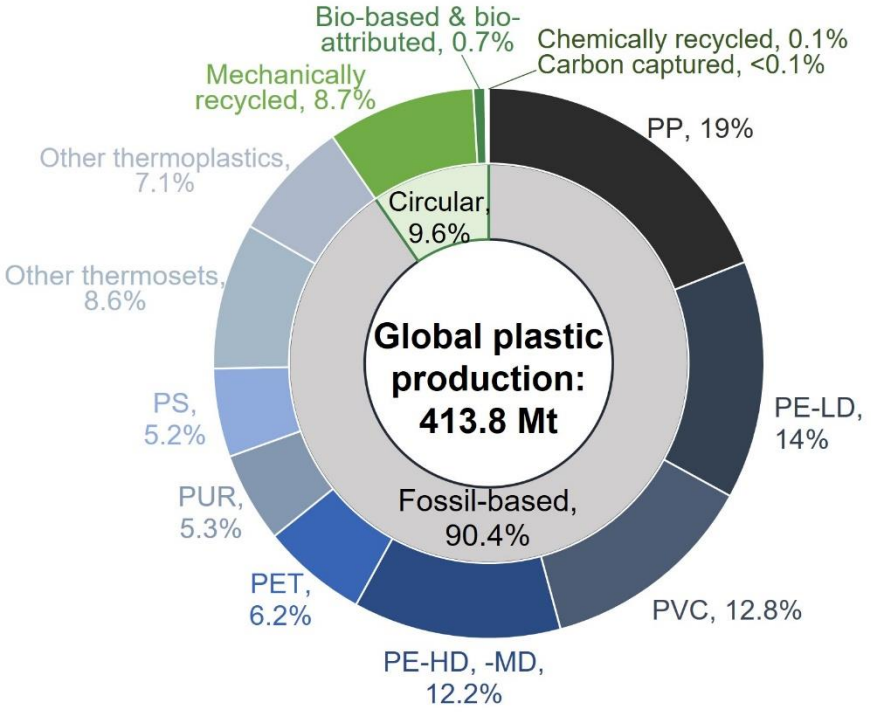

Figure 1. Global plastics production in 2023. Adapted from reference.[1]

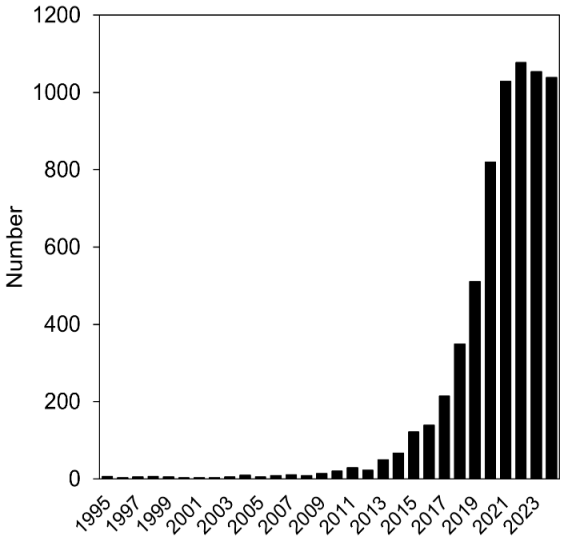

Figure 2. The number of publications about marine plastic pollution (data collected from Web of Science, March 9, 2025).

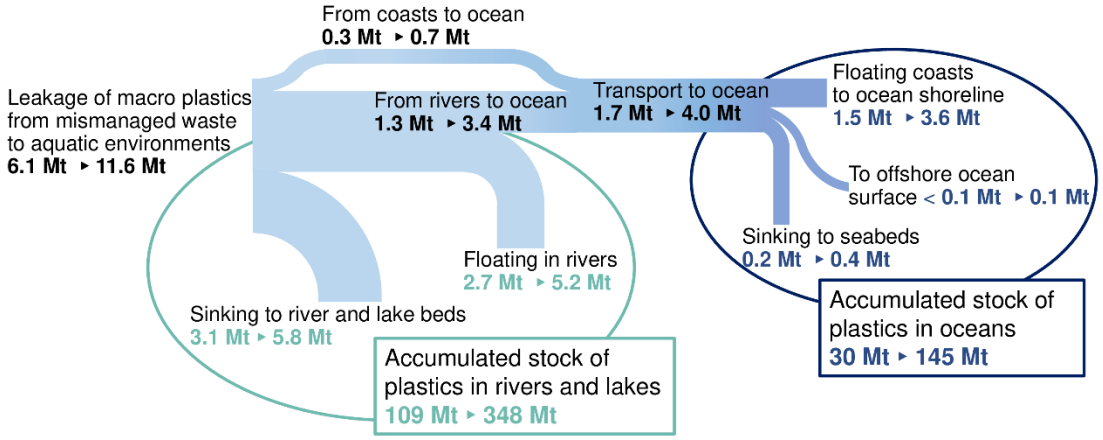

Figure 3. Projected leakage of plastic debris into the aquatic environment. It is projected to double between 2019 and 2060. (2019 ▶2060). Adapted from reference.[2]

Interest in Bioplastics and Inedible Feedstocks

As declared by the 1997 Kyoto Protocol,[7] global warming has become a global issue, prompting various countries to take action. The European Union (EU) introduced the EU Policy Framework on Biobased, Biodegradable, and Compostable Plastics in 2022, which, although not legally binding, outlines the ideal state of plastics from the perspectives of biodiversity and ecodesign.[8] In the United States, initiatives to promote biotechnology and prevent plastic pollution have led to the announcement of the Bold Goals and Priorities to Advance American Biotechnology and Biomanufacturing in 2023[9] and the National Strategy to Prevent Plastic Pollution in 2024.[10] In 2019, Japan formulated the Bioeconomy Strategy and developed a roadmap for the introduction of bioplastics, aiming to build a new

economic society.[11] Consequently, continuing to contribute to a sustainable society while minimizing environmental impact is crucial. Therefore, interest in bioresources is growing, and the production of bioplastics is expected to increase. The feedstocks for biorefineries, which produce bioplastics and other biomass-based products, can be classified into sugar-based feedstocks (e.g., sugarcane and sugar beet), starch-based feedstocks (e.g., rice and corn), and cellulose-based feedstocks (e.g., agricultural residues, wood, and paper waste) (**Figure 4**).[12,13] Sucrose-based feedstocks can be easily used as sugars through simple processes, such as leaching and pressing, whereas starch-based feedstocks can be readily converted into sugars through amylase treatment. These feedstocks are widely used in biorefineries. However, since sucrose- and starch-based feedstocks are food resources, their use in biorefineries leads to competition with food supplies, which poses a significant issue.[12] Approximately 30% of the global food price increase in the 2000s can be attributed to the conversion of grains to biofuels. In the case of corn, nearly 40% of the price increase is linked to the rising demand for biofuels.[14] Conversely, cellulosic feedstocks have attracted considerable attention because they do not compete with food supplies, although their robust structure makes their use challenging.[15] Although approximately 70% of the world's biomass production consists of plant cell walls, their industrial use accounts for only about 2% in the forestry, pulp and paper, and textile industries.[14] Cellulose-based feedstocks have the potential to serve as renewable carbon sources that can gradually reduce reliance on fossil resources.[3,16]

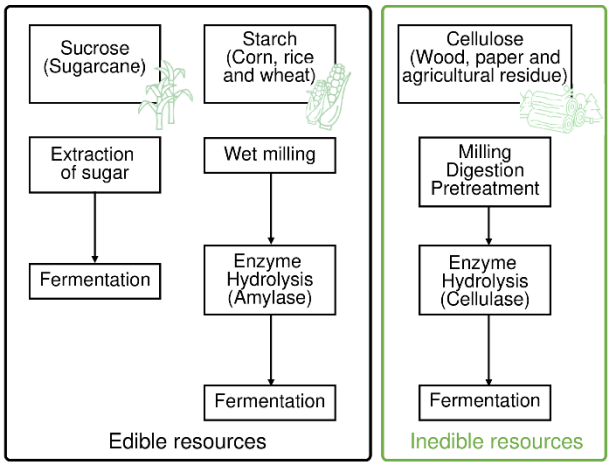

Figure 4. Three raw materials used in biorefineries and their general utilization flow. The raw materials are classified into sucrosear-based, starch-based, and cellulose-based. Adapted from reference.[12]

Environmental Analysis of Bioplastics

Expanding the use of bioplastics requires organizing political (P), economic (E), social (S), and technological (T) perspectives related to bioplastics, in addition to understanding domestic and international market trends and the relevant technological background. In particular, bioplastic feedstock is mainly derived from edible resources, which exacerbates the impact on environmental issues and the geopolitical situation. Therefore, a PEST analysis was conducted to organize the external environment from a macro perspective (**Figure 5**).[17]

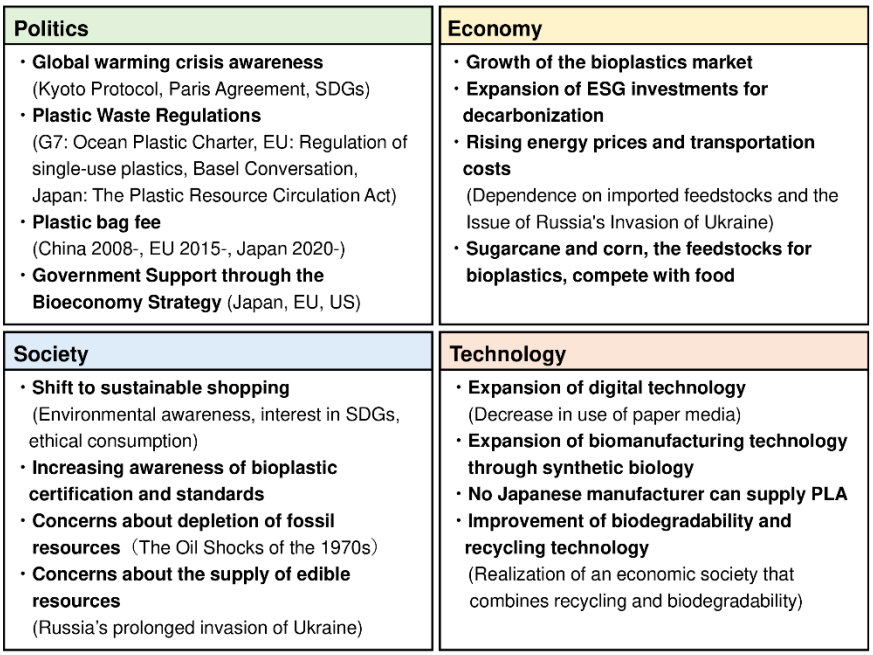

Figure 5. PEST analysis[17] of the environment surrounding PLA and other bioplastics.

Political Factors (P)

Awareness of the global warming crisis has increased since the adoption of the Kyoto Protocol in 1997 and the Paris Agreement and Sustainable Development Goals (SDGs) in 2015,[7,18] resulting in a global promotion of decarbonization efforts. Environmental pollution caused by plastic waste was recognized as a global issue at the G7 Summit, where the Ocean Plastics Charter was approved.[19] To promote a sustainable circular economy, the EU has implemented regulations on single-use plastics since 2021.[20] After the Basel Convention, China and Thailand announced import bans on foreign waste, including plastic waste, to address environmental pollution.[21–23] In addition, the United States established the BioPreferred Program to increase the consumption of biobased products.[24] The EU has set the desired direction for plastics in its policy framework on biobased, biodegradable, and compostable plastics.[8] Japan enacted the Plastic Resource Circulation Act to promote plastic resource circulation.[25] In addition, as in other countries, a plastic bag fee was introduced in 2020.[26] The Roadmap for Bioplastics Introduction was formulated based on the Cabinet Office's Bioeconomy Strategy 2019[11] to achieve a new economic society with highly sustainable bioplastics.[27] Because bioplastics are produced on a smaller scale and at a higher cost than fossil-based plastics, their introduction will not be driven solely by cost competition. Therefore, legal regulations such as a plastic bag fee system introduced by the Japanese government in 2020 are essential to support their introduction.

Economic Factors (E)

The global production capacity of bioplastics, including sustainable biomass plastics and biodegradable plastics, is expected to increase from 2.47 Mt in 2024 to 5.73 Mt in 2029 (**Figure 6**).[28,29] In

2023, the distribution of bioplastic applications was as follows: packaging accounted for approximately 42.9%, textiles for 20.7%, consumer goods for 13.4%, automotive and transportation for 9.7%, agriculture and horticulture for 4.5%, electronics for 3.6%, coatings and adhesives for 1.2%, construction materials for 0.6%, and other uses for 3.4%.[28] Environmental, social, and governance (ESG) investments are increasing globally, from 66.2 billion yen at the end of 2015 to 928.1 billion yen at the end of 2021.[30] These investments are also increasing in Japan, with several companies adopting ESG-focused strategies. For example, the Oji Group has increased its ESG investments through a strategy aimed at creating value from forests. The rise in ESG investments has heightened the demand for environmentally friendly technologies and materials, including bioplastics such as poly(lactic acid) (PLA), which utilize forest resources.[31]

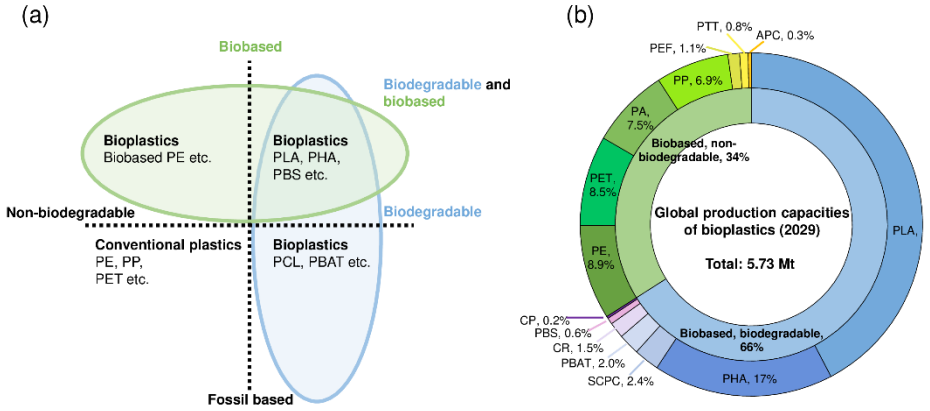

Figure 6. (a) Classification of polymers according to whether biobased or fossil-based, biodegradable or non-biodegradable, adapted from reference.[29] (b) Global production capacity forecast for bioplastics in 2029, adapted from reference.[28]

Russia's invasion of Ukraine has disrupted the global energy situation, leading to higher energy prices.[32] High transportation costs and reliance on imports have raised the prices for bioplastics such as PLA, which lack a production base in Japan.[33] The main feedstocks for bioplastics, such as sugarcane and corn, are also used as food sources. Therefore, overuse of bioplastics could lead to fluctuations in feedstock prices and competition for resources with food supplies. It is essential to always consider the optimal balance and seek the use of inedible biomass from a medium- to long-term perspective.[34]

Social Factors (S)

Ethical consumption, characterized by a preference for sustainable materials and recyclable products, is gaining momentum with increasing interest in the SDGs among consumers and businesses worldwide. Although increasing awareness of bioplastics remains a challenge, certifications and standards for biodegradability and biomass content are being standardized, primarily by European organizations, including Technischer Überwachungsverein (TÜV),[35] Deutsches Institut für Normung (DIN) Certco,[36] European Bioplastics,[29] Nederlands Normalisatie instituut (NEN),[37] and The Biodegradable Products Institute (BPI),[38] to promote proper usage and product proliferation (**Tables 1 and 2**). Similar schemes are being implemented in the United Kingdom (Renewable Energy Assurance Ltd.[39]) and other countries,

including Australia[40] and Italy.[41] In Japan, according to a 2018 survey by the Ministry of the Environment, approximately 60% of respondents reported that they would accept higher prices for ethical goods and services compared with conventional products.[42] In 2019, another public opinion survey on plastic waste issues revealed that 36.6% of respondents would purchase alternatives such as plant-based plastics "even if they are more expensive," which indicates a growing awareness of ethical consumption and the increasing purchase of environmentally friendly products and services.[43] The certification for marine biodegradable plastics[44]—operated by the Japan BioPlastics Association (JBPA) in 2013—reflects the growing awareness of environmental issues, such as marine plastic pollution caused by microplastics, and the increasing interest in bioplastic certification (**Table 2**).

Given the finite nature of fossil resources, there is growing concern that economic and population growth will intensify competition for these resources, leading to their depletion. Given the political instability in the Middle East, supply disruptions and fluctuations in oil prices are likely to occur, similar to the oil shocks of the 1970s.[45] Furthermore, Russia's prolonged invasion of Ukraine has reduced exports of agricultural products and fertilizers from Ukraine and Russia, leading to price increases in food resources and raising concerns about a potential food crisis.[46] Ukrainian corn production in 2024/2025 is projected to be 36% lower than in 2021/2022 (the year before the invasion), and exports are projected to be 11% lower.[47] Therefore, it is essential to always consider the optimal balance with edible feedstocks and to use inedible feedstocks to avoid competition for food resources.

Table 1. Global biobased plastics certification.[48,49]

Certification bodies	Certification systems	Certification marks	standards	Biobased Content Certification
JBPA (Japan)	Biomass plastic mark		ISO 16620-3	Biomass plastic degree of 25% or more.
JORA (Japan)	Biomass mark		ISO16620-4	Biomass degree of 10% or more.
TÜV (Austria)	TÜV OK-Biobased		ASTM D 6866 ISO 16620-2	Classification by the proportion of biobased carbon. 1 star: Biobased 20% - 40% 2 stars: Biobased 40% - 60% 3 stars: Biobased 60% - 80% 4 stars: Biobased > 80%
NEN (Netherlands)	NEN Biobased	biobased %	NCS 16785 (en)	Biobased content (based on biomass, not just biobased carbon).
DIN Certco (Germany)	DIN-Geprüft biobased		ASTM D 6866 ISO 16620-2 CEN/TS 16137	Classification by the proportion of biobased carbon. Biobased 20 – 50 % Biobased 50 – 85 % Biobased > 85 %
USDA (USA)	USDA BioPreferred Certification		ISO 16620-2	Meets the minimum biobased content for the product category or contains at least 25% biobased raw materials.

Table 2. Global certification of biodegradable plastics.[49]

Certification bodies	Certification systems	Environment	Certification marks	Standards	Biobased Content Certification
JBPA (Japan)	Biodegradable Plastic Identification and Labeling System	Compost, Soil, Water		OECD 301C, ISO 14851, ISO 14852, ISO 17556, ISO 14855-1, ISO 14855-2	Over 60% biodegradable in specified tests
JBPA (Japan)	Marine Biodegradable Plastic Identification and Labeling System	Seawater		ISO22403	Over 90% biodegradable in 2 years (max. 28° C).
TÜV (Austria)	OK compost INDSTRIAL	Industrial composting		EN 13432: 2000	Over 90% biodegradable in 6 months (max. 58° C).
TÜV (Austria)	OK compost HOME	Home composting		No official standards. (AS 5810, NF T 51800, EN 17427)	Over 90% biodegradable in 12 months (max. 28° C).
TÜV (Austria)	OK biodegradable SOIL	Soil		No official standard. (ISO 17556)	Over 90% biodegradable in 2 years (max. 25° C).
TÜV (Austria)	OK biodegradable WATER	Fresh water		No official standard. (ISO 14851, ISO 14852)	Over 90% biodegradable in 56 days (max. 21° C).
TÜV (Austria)	OK biodegradable MARINE	Marine		No official standard. (ASTM D6691)	Over 90% biodegradable in 6 monts (max. 30° C)..
DIN Certco (Germany)	Industrial Compostable	Industrial composting		EN 13432	Over 90% biodegradable in 6 months (max. 58° C).
DIN Certco (Germany)	Home Compostable	Home composting		NF T51-800	Over 90% biodegradable in 12 months (max. 28° C).
DIN Certco (Germany)	Biodegradable in soil	Soil		EN 17033	Over 90% biodegradable in 2 years (max. 25° C).
DIN Certco (Germany)	Biodegradable in Marine Environments	Marine		ISO 22403	Over 90% biodegradable in 2 years (max. 28° C).
European Bioplastics (EU)	Seedling	Industrial composting		EN 13432	Industrial composting plants (55-60° C).
BPI (USA)	Certified Compostable	Industrial composting		ASTM D6400 ASTM D6868	Biodegradation within 180 days

Technological Factors (T)

The COVID-19 pandemic accelerated digital transformation worldwide, with the expansion of online payments, e-advertising, and web conferencing, leading to the automation of various technologies and the shift from paper to electronic media. For example, digitalization has accelerated in Japan, resulting in a 45% decrease in the production volume of paper products (e.g., newsprint) in 2023 compared to its peak in 2000.[50] Consequently, paper companies are working to develop new materials (e.g., sugar, ethanol, and PLA) that can substitute for paper, leveraging abundant wood resources.[34] Japanese PLA suppliers began mass-producing PLA using edible resources in the 1990s. However, they have already withdrawn from the

PLA manufacturing business due to low demand and high manufacturing costs at the time.[51] Consequently, Japan's supply of bioplastics lags behind that of Europe, the United States, and China.[52] However, recent advances in information technology and artificial intelligence have enabled the use of highly designed genomes in biomanufacturing processes.[53,54] These technologies are expected to support the production of bioplastics from abundant forest resources,[34] contributing to the Japanese government's goal of a bioeconomy by increasing the supply of domestically produced bioplastics.[11,27]

There is a growing global momentum for closed-loop recycling, in which producers collect and reuse used products, driven by advances in chemical and material recycling technologies.[55–57] In 2021, 87% of waste plastics in Japan were recycled, of which only 4% involved chemical recycling and 21% were material recycling, with the majority used for thermal recovery.[58] Interest is growing in biodegradable materials and materials that enable closed-loop recycling, including PLA,[2,55,59] to address issues such as import restrictions on plastic waste under the Basel Convention, the increase in dirty plastics unsuitable for recycling, and environmental plastic leakage caused by insufficient waste management infrastructure in developing countries.[2,21]

Overview of PLA

PLA is widely used as a representative bioplastic because it ultimately biodegrades into H_2O and CO_2 in compost environments, making it an excellent alternative to conventional fossil-based plastics.[60] PLA is biocompatible and produced from renewable resources, thus saving energy and reducing GHG emissions.[61] The basic structural unit of PLA is lactic acid or lactide produced by fermenting glucose obtained from various resources such as corn and sugarcane. Lactic acid has two enantiomers: L-lactic acid and D-lactic acid.[62] Methods such as direct polymerization[62,63] and ring-opening polymerization of lactide for high-molecular-weight PLA[64] are used. PLA is used in major applications, including food and medical product packaging, medical devices, textiles, agricultural plastics, and automotive parts.[62]

Markets of PLA

In response to this global trend, PLA—a representative bioplastic—accounted for 37.1% of the world's bioplastic production in 2024, with a production capacity of approximately 0.81 Mt. By 2029, PLA is expected to account for 42.3%, with a production capacity of roughly 2.42 Mt, and it is on the trend of increase (**Figure 7**).[28] Companies such as NatureWorks, TotalEnergies Corbion, and Zhejiang Hisun Biomaterials are meeting global demand. According to a 2022 survey, 60.6% of PLA was used for packaging, 14% for textiles, 8% for agriculture, 5% for biomedical, 1.4% for electronics, and 11% for other applications.[65] The biodegradability of PLA has led to its increased use in the biomedical industry. In Japan, the shipment volume of bioplastics increased from 47,000 tons in 2019[43] to 89,000 tons in 2021.[61] However, this remains below the Japanese government's target of expanding the domestic biomass plastics market to

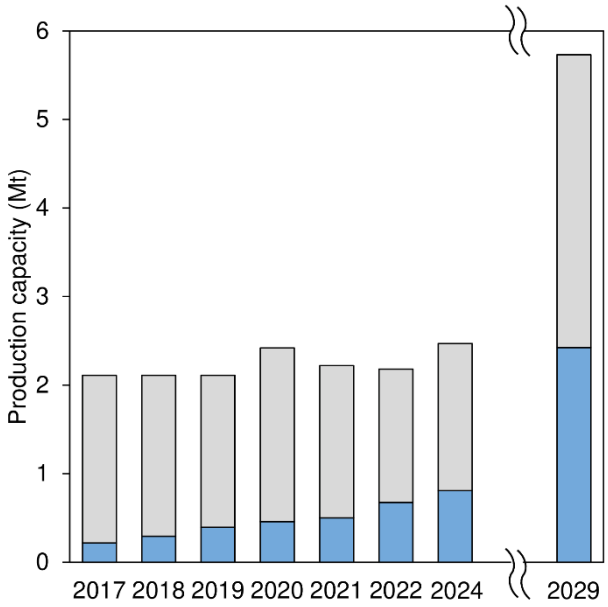

Figure 7. Global production capacity of bioplastics. The blue bars indicate PLA, and the gray bars indicate bioplastics other than PLA. The data[28] were surveyed annually.

approximately 2 Mt by 2030, as outlined in the Bioplastics Introduction Roadmap.[27] Demand for PLA is growing in Japan due to increasing environmental awareness. However, shipments totaled approximately 5,000 tons in 2019, which is low compared with global production capacity.[43] Distribution is low in Japan due to the absence of domestic PLA suppliers caused by technical or market difficulties, resulting in almost total dependence on imports. From 2014 to 2023, PLA imports have hovered around 5,000 tons, indicating that all shipments are dependent on imports (**Figure 8a**).[33] Imports from the United States have been declining. Almost all imports are believed to come from NatureWorks' production facilities in the United

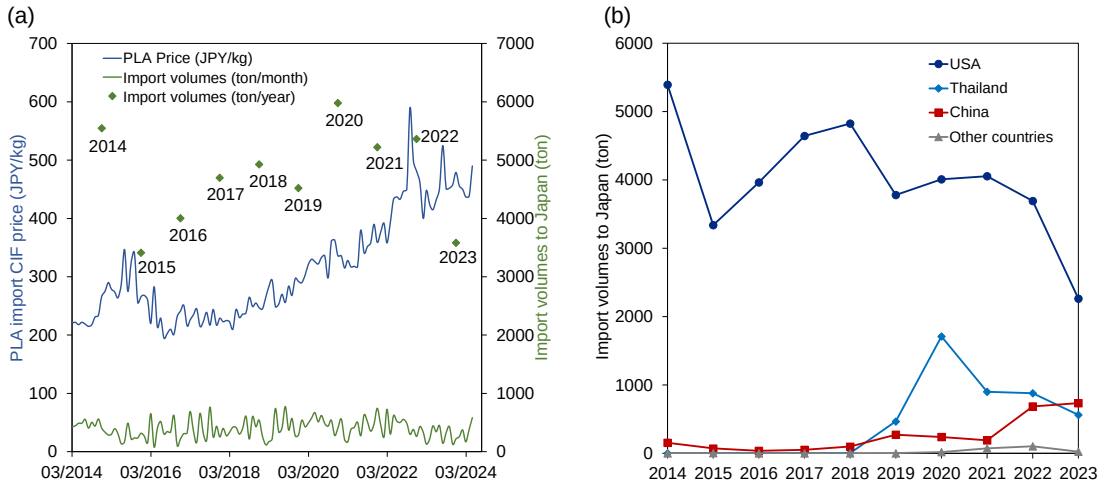

Figure 8. Trends in PLA imports to Japan over the past decade. (a) Variations in PLA import prices (blue line) and import volumes to Japan (monthly import volumes in green line; annual import volumes in green diamonds). (b) Import volumes from the United States (navy circles), Thailand (blue diamonds), China (red squares), and other countries (gray triangles). The data[33] were obtained from the Ministry of Finance Trade Statistics.

States. Imports from Thailand began around 2018 and have increased as imports from the United States have declined, with almost all imports originating from TotalEnergies Corbion's production facilities. In addition, imports from China have increased and surpassed those from Thailand in 2023. Products from companies such as Zhejiang Hisun Biomaterials and BBCA Group & Futerro, which are expanding their production capacity, are expected to be imported. With increasing demand for PLA in countries where these suppliers are based, exports may decrease. Consequently, obtaining PLA in Japan amid rising demand is becoming challenging. Even where imports are possible, soaring fuel prices are further increasing import costs (**Figure 8b**).[66] With growing environmental awareness, the necessity to move away from fossil fuels becomes more pressing, leading to an expected expansion in the demand for bioplastics. The use of abundant inedible biomass has recently been considered to expand bioplastics production capacity, address concerns about competition with edible feedstocks, and diversify sustainable bioresources. In the past, given the lack of industrial biomass in Japan, the Functional Lignocellulosic New Material Technology Research Association led by Ebara Corporation investigated the production of PLA from agricultural residues and thinned wood (**Figure 9**).[67] Oji Holdings is working toward becoming a PLA supplier in Japan by industrializing PLA production from woody resources. Accordingly, LCA calculations revealed that PLA derived from inedible biomass can reduce CO_2 emissions compared with PLA derived from corn.[68] The realization of PLA production from inedible feedstocks in Japan is expected to change the market structure.

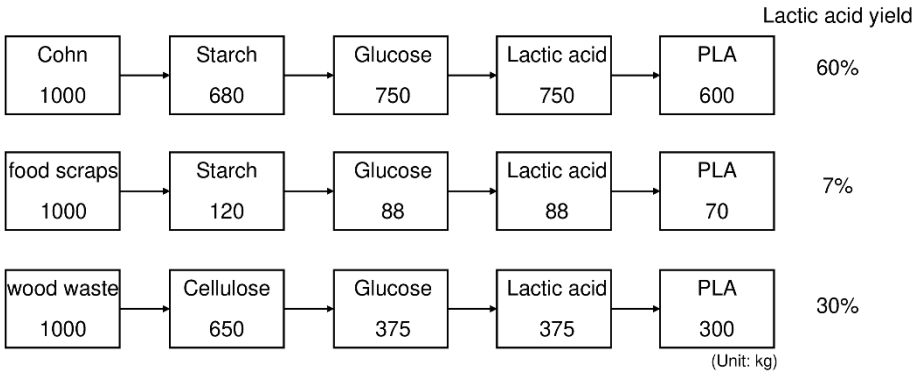

Figure 9. Yields of PLA from various biomass types predicted by the Functional Lignocellulosic New Material Technology Research Association in Japan, adopted from reference.[67]

History and Development of PLA

The development of PLA has a long history characterized by numerous technological advances, which have established it as a sustainable material (**Figure 10**). This development dates back to 1845 when French chemist Théophile-Jules Pelouze first synthesized PLA through the condensation of lactic acid.[52] In 1932, DuPont scientist Wallace Carothers developed a method for producing PLA by polymerizing lactide.[69] Although DuPont gained various fundamental insights into the properties and production processes of PLA, its commercial production was limited to medical applications.[69,70] Growing concerns about plastic pollution led to significant attention to PLA, along with starch-based polymers and polyhydroxyalkanoates (PHA), particularly in the early 1990s.[64,70] In 1994, the agribusiness company

Cargill established a PLA production facility in Minnesota, United States. In 1997, Cargill Dow LLC, a joint venture with Dow Chemical, was formed.[71] Lactic acid manufacturer Galactic began researching PLA in a pilot plant in the 1990s.[52] In the 1990s, Mitsui Chemicals announced the production of PLA through direct polymerization, targeting the food packaging market, but later discontinued its development.[51,63] Since 2002, the PLA market has grown slowly, recently reaching a significant turning point. In late 2001, Cargill Dow LLC announced a commercial facility with a production capacity of approximately 150 kilotons (kt), making it the world's largest PLA producer.[71] In early 2005, the company was renamed NatureWorks after Dow withdrew from the joint venture.[70] NatureWorks began building a second PLA facility in Thailand with a capacity of approximately 75 kt.[72] In addition, Galactic established a joint venture with Total Petrochemicals;[72] however, Total Petrochemicals withdrew from the joint venture in 2016.[73] In December 2018, Futerro, Sulzer, and TechnipFMC formed the PLAnet™ initiative to provide integrated PLA technology, with Futerro providing lactic acid and lactide production technology, Sulzer handling lactide separation and polymerization, and TechnipFMC offering technology integration and engineering packages.[74]

In the 1990s, semicommercial PLA producers were limited to Cargill and Galactic. However, Purac began supplying D- and L-lactide to PLA producers in 2008, thereby establishing a more stable position in the PLA sector.[52,69] In 2009, Purac built a PLA plant in collaboration with Sulzer in Switzerland and Synbra in the Netherlands.[70] In 2016, Corbion Purac and TotalEnergies established a joint venture named TotalEnergies Corbion to produce and sell PLA.[75] In 2019, they built a 75-kt PLA plant in Thailand.[75] In addition, PLA suppliers in China, including Zhejiang Hisun Biomaterials and BBCA, announced plans to increase PLA production.[75] In Japan, Mitsui Chemicals and Shimadzu Corporation had been operating a PLA production plant. However, Shimadzu sold its PLA business to Toyota Motor Corporation in 2002.[67] In 2004, Toyota built a demonstration plant with an annual production capacity of 1 kt; however, it withdrew in 2008 and transferred the manufacturing technology to Teijin.[67,76] Teijin also withdrew from PLA production in 2018 and announced the transfer of the technology to TotalEnergies Corbion.[77]

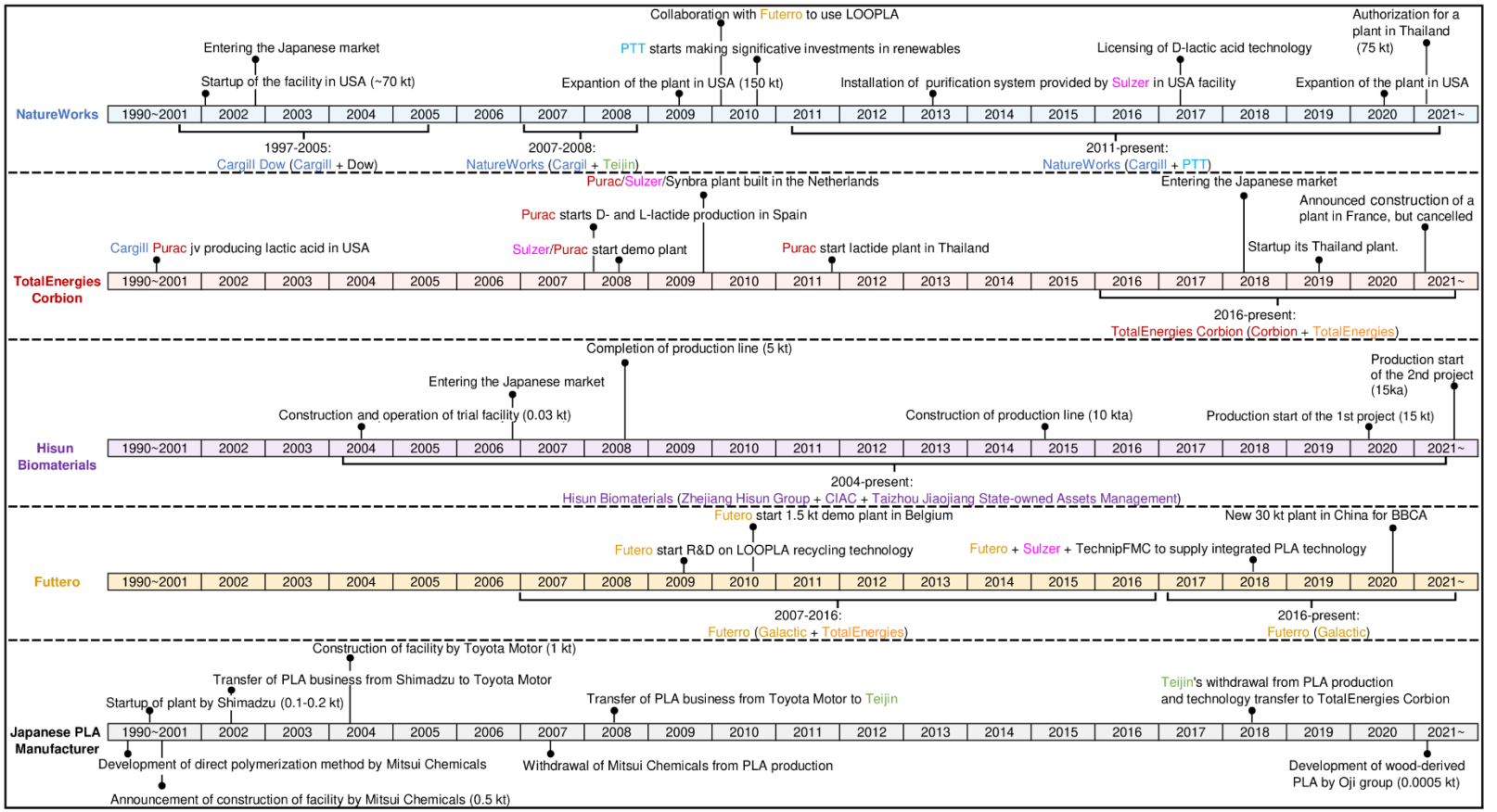

Figure 10. Milestones in the development of major PLA manufacturers. Compiled and adapted from reference.[55]

Major PLA Suppliers

Although several companies identified business opportunities in PLA (**Figure 10**), the majority of current PLA production capacity is dominated by major suppliers, including NatureWorks LLC, TotalEnergies Corbion, and Zhejiang Hisun Biomaterials (**Table 3**).

Table 3. Major suppliers of PLA.

Company	Country	Production capacity (kt)	Raw materials	Manufacturing base
NatureWorks	The United States	150	Corn	The United States
		(+75)	Sugarcane	Thailand
TotalEnergies Corbion	Netherlands	75	Sugarcane	Thailand
Zhejiang Hisun Biomaterials	China	65	Corn	China

NatureWorks is the world's largest PLA producer, with joint investment from global agribusiness giant Cargill and Thailand's largest chemical company, Petroleum Authority of Thailand (PTT) Global Chemical.[68] NatureWorks has been operating a manufacturing facility in the United States under the PLA brand name Ingeo™.[71,72,78] Currently, a second plant is under construction in Thailand with an annual production capacity of 75 kt.[72] Technologically, NatureWorks polymerizes lactic acid derived from the saccharification and fermentation of starch crops (e.g., corn) to supply PLA with 100% biomass content (**Figure 11**).[75,78] Concerns have been raised regarding the environmental impact of genetically modified (GMO) corn.[78] To address these concerns, in Thailand, NatureWorks plans to use sugarcane, a major crop and non-GMO product, as an additional raw material. By adjusting the D-lactide content, the company controls the melting point and melt flow rate to produce PLA suitable for various applications.[72] Regarding the disposal of PLA products, options include material recycling and composting. In addition, NatureWorks possesses chemical recycling technology that hydrolyzes PLA back into lactic acid.[57] NatureWorks entered the Japanese market in 2002, supplying major processing manufacturers, including Unitika and Toray. For example, Unitika markets PLA compounds under the brand name Terramac that are suitable for various industrial applications under the brand name Terramac.[67]

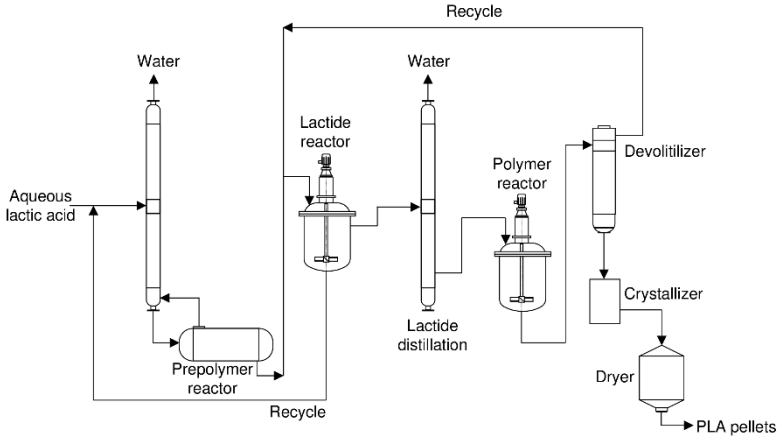

Figure 11. PLA production facility by NatureWorks, adapted from reference.[75]

TotalEnergies Corbion is a joint venture established by TotalEnergies, one of the six major international oil companies and a leading French petrochemical company, and Corbion, a leading lactic acid producer in the Netherlands. The PLA brand name of TotalEnergies Corbion is Luminy.[55] TotalEnergies Corbion primarily uses sugarcane as a raw material to produce PLA. In addition to standard grades, they developed heat-resistant grades using microorganisms that produce only L-lactic acid, as well as low-melting-point grades containing D-lactic acid. Additionally, TotalEnergies Corbion possesses the technology for the formation of the PLA stereocomplex, licensed from Teijin, which previously manufactured PLA, to improve heat resistance.[77] Furthermore, they are developing PLA that can be chemically recycled by collecting used PLA and converting it back to monomer lactic acid.[55] In Japan, TotalEnergies Corbion entered the market in 2018, selling PLA through distributors such as NAGASE & Co.[79]

Zhejiang Hisun Biomaterials, established in 2004 in Taizhou, Zhejiang Province, is a high-tech enterprise focused on the development and manufacturing of PLA under the brand name REVODE.[80] It was founded by three companies and institutions: the Zhejiang Hisun Group, the Changchun Institute of Applied Chemistry of the Chinese Academy of Sciences, and Taizhou Jiaojiang State-Owned Assets Management.[81] The Zhejiang Hisun Group is primarily engaged in the production and sale of biopharmaceuticals and biopesticides. Zhejiang Hisun Biomaterials was the first company to manufacture PLA in China, with a production capacity of 65 kt per year.[82] Zhejiang Hisun Biomaterials produces PLA from raw materials such as corn. It offers a range of products, including standard extrusion grades, high optical purity grades with minimal D-lactide content, and compounded products. The PLA content in their compounds ranges from 30% to 70%, and these are used in various applications, such as injection molding and extrusion.[80] Zhejiang Hisun Biomaterials is believed to have previously sourced lactic acid from Corbion and various domestic lactic acid manufacturers in China.[75] However, to optimize costs, Zhejiang Hisun Biomaterials has transitioned to producing lactic acid from corn and manufactures PLA in an integrated production process. Additionally, Zhejiang Hisun Biomaterials entered the Japanese market, importing and selling PLA through Kobe Fine Chemical.[80] Other Chinese manufacturers, including BBCA & Futerro, have also expanded production in recent years. HighChem has been handling marketing in Japan, specializing in the Japan–China chemical trade.[83]

Technical Challenges of PLA

The global production of PLA has grown substantially, primarily driven by the aforementioned companies (**Table 3**). Although PLA is considered a promising material, it has technical challenges, including brittleness and rigidity, which limit its use as a polymer and require further improvement to expand its applications.[84] PLA also faces challenges in terms of biodegradability: it does not readily degrade in marine or soil environments and exhibits optimal biodegradability only in controlled environments, such as compost.[85] A deep understanding of the degradation mechanisms of polymers is required to improve the biodegradability of PLA. The degradation behavior of polymers typically involves irreversible changes in

the chemical structure, physical properties, and visual appearance caused by the chemical cleavage of polymers *via* multiple mechanisms.[86–88] In addition to biological degradation, these mechanisms include mechanical degradation, photodegradation, thermal degradation, and chemical degradation, such as hydrolysis (**Figure 12**).[87–91] External factors related to the environment, such as heat, humidity, radiation, acidity, and alkalinity, can affect the abiotic degradation process and its rate. These abiotic degradation mechanisms (e.g., photodegradation, hydrolysis, and mechanical degradation) can enhance the biotic degradation process by increasing the surface area for biofilm formation or reducing the molecular weight.[86–88,92,93] Unlike non-biodegradable plastics, biodegradable plastics are broken down into small molecules that microorganisms use as sources of carbon and energy.

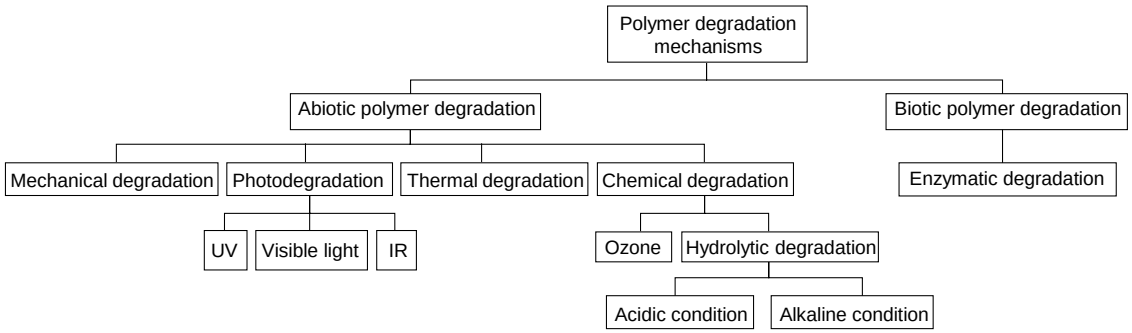

Figure 12. Main mechanism of polymer degradation. Compiled and adapted from reference.[88]

Biodegradable plastics can be classified into three categories based on feedstocks and synthesis methods (**Figure 13**).[85] The first category includes polymers derived from renewable feedstocks, such as natural polymers (e.g., starch and cellulose),[85] and PHA, such as polyhydroxybutyrate[94] produced by microbial fermentation processes. The second category includes biodegradable plastics synthesized from

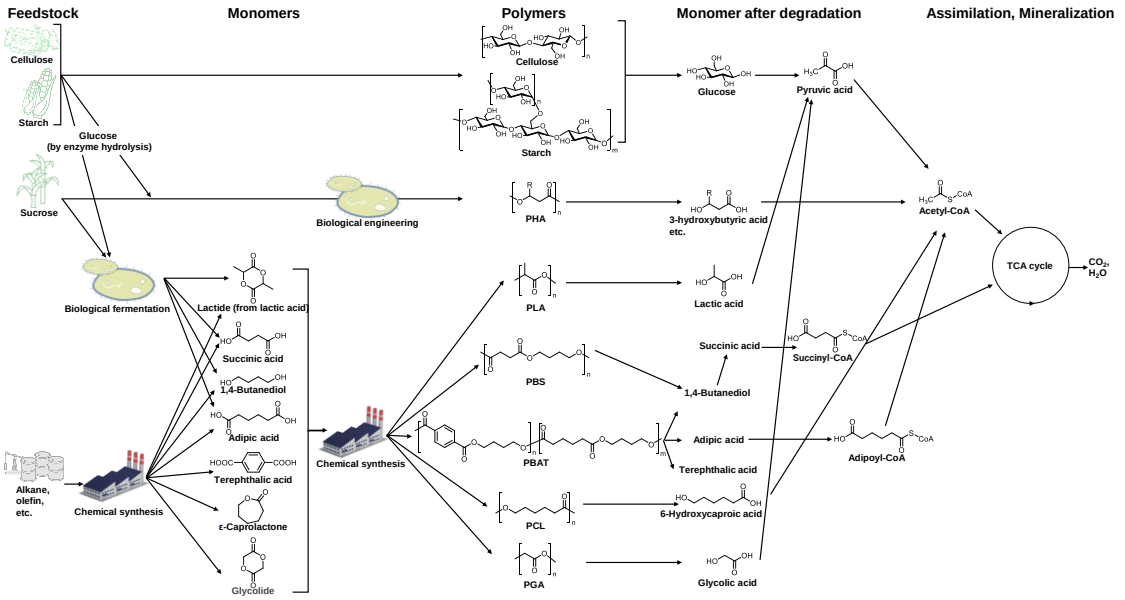

Figure 13. Structure and sources of biodegradable polymers and the main tentative biodegradation pathways under aerobic conditions. Compiled and adapted from references.[86,88,94]

renewable monomers through industrial processes, such as PLA[94] and biobased poly(butylene succinate) (PBS).[94] The third category includes biodegradable plastics synthesized from petrochemical resources, such as polycaprolactone (PCL),[95] poly(butylene adipate-*co*-terephthalate) (PBAT),[94,96] and polyglycolide (PGA)[75,85] When these biodegradable plastics become bioassimilable, they are metabolized by the tricarboxylic acid (TCA) cycle to produce CO_2 and H_2O under aerobic conditions and CO_2, H_2O, and CH_4 under anaerobic conditions (**Figure 13**).[88,95,97] **Figure 14** shows a hypothetical degradation pathway for the most common biobased or fossil-based biodegradable polymers, which are reported to be depolymerized by certain microorganisms after biofilm formation by bacteria.[88]

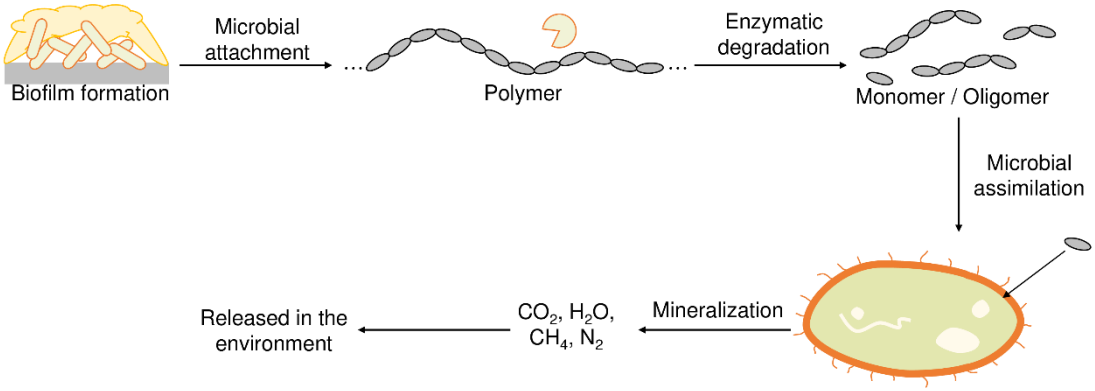

Figure 14. Schematic representation of biodegradation process. Compiled and adapted from references.[98,99]

Biotic and abiotic mechanisms facilitate the degradation process, resulting in biofilm formation in the environment, molecular weight reduction through hydrolysis and enzymatic degradation by microorganisms, and subsequent microbial metabolism.[98,99] Optimal degradation of PLA is only achieved in controlled environments, such as compost.[100] In PLA, hydrolysis and enzymatic action by proteases, lipases, and esterases result in oligomers with molecular weights below 20,000, which serve as substrates for bioassimilation (**Table 4**).[101,102] When these oligomers and monomers become available for microbial bioassimilation, lactic acid is transported through semipermeable membranes, oxidized to pyruvate by dehydrogenation reactions, and then metabolized through the TCA cycle, ultimately being mineralized to CO_2 and H_2O (**Figure 15**).[88,94,103] However, the bottlenecks are PLA's glass transition temperature (T_g), pH, molecular weight, and crystallinity, which make it difficult to lower the molecular weight of PLA.[61,87,100] Therefore, PLA may not be degraded in low-temperature environments with few microorganisms, such as marine environments. Recent studies have reported the potential biodegradability of PLA in marine environments.[104–106] Melt blending and copolymerization with biodegradable materials are considered practical approaches to enhance the potential marine biodegradability of PLA. Melt blends with water-soluble and degradable thermoplastic starch[107] or polyvinyl alcohol[108] take advantage of the readily degradable nature of the material, with the biodegradable domains degraded primarily by the incorporated material, whereas PLA remains stable. Additionally, inspired by the intramolecular transesterification

mechanism of ribonucleic acid (RNA), which rapidly hydrolyzes due to its phosphate ester linkages, an attempt has been made to improve its degradability in seawater by introducing synthetic phosphate linkages as breaking points into PLA through copolymerization.[109]

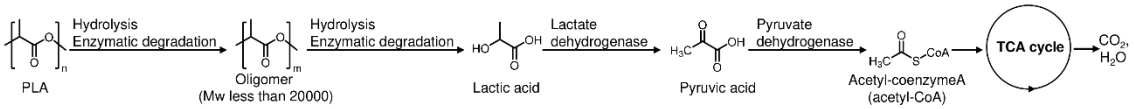

Figure 15. Biodegradation pathway for PLA in aerobic conditions, adapted from references.[88,94,101–103]

Table 4. Microorganisms and enzymes with PLA-degrading activity. Parameters include microbial species, enzymes released, thermophilic conditions, environment or location where microorganisms were isolated, and reported literature. Data were collected from the Plastic Database, a plastic-degrading enzyme database, on April 2, 2025.[110]

Microorganisms	Enzymes	Isolation environment	Isolation location	Ref.
Paenibacillus amylolyticus	PLA depolymerase	-	-	[111]
Cryptococcus sp.	Cutinase	-	-	[112]
Uncultured bacterium	PLA depolymerase	-	-	[113]
Saccharomonospora viridis	Cutinase	Compost	Japan	[114]
Saccharomonospora viridis	Cutinase	-	-	[115]
Aspergillus fumigatus	Esterase	Hot spring	Taiwan	[116]
Bacillus licheniformis	Esterase	Compost	-	[117]
Rhizopus oryzae	Lipase	-	-	[118]
Pseudomonas sp.	-	Soil	Taiwan	[119]
Absidia sp.	-	Soil	Slovakia	[120]
Acinetobacter ursingii	-	Soil	Slovakia	[120]
Actinomucor elegans	-	Soil	Slovakia	[120]
Amycolatopsis alba	-	Culture collection	-	[121]
Amycolatopsis azurea	-	Culture collection	-	[121]
Amycolatopsis coloradensis	-	Culture collection	-	[121]
Amycolatopsis fastidiosa	-	Culture collection	-	[121]
Amycolatopsis mediterranei	-	Culture collection	-	[121]
Amycolatopsis methanolica	-	Culture collection	-	[121]
Amycolatopsis orientalis	-	Culture collection	-	[121,122]
Amycolatopsis sp.	-	Culture collection	-	[121,123]
Amycolatopsis thailandensis	-	Soil	Thailand	[124]
Amycolatopsis tolypomycina	-	Culture collection	-	[121]
Aneurinibacillus aneurinilyticus	-	Soil	Taiwan	[125]
Arthrobacter oryzae	-	Soil	Slovakia	[120]
Aspergillus awamori	-	Culture collection	-	[126]
Aspergillus calidoustus	-	Culture collection	-	[127]
Aspergillus foetidus	-	Culture collection	-	[126]
Aspergillus nidulans	-	Culture collection	-	[126]
Aspergillus niger	-	Culture collection	-	[126]
Aspergillus oryzae	-	Culture collection	-	[126]
Aureobasidium pullulans	-	Soil	Slovakia	[120]
Bacillus licheniformis	-	Soil	Slovakia	[120]
Priestia megaterium	-	Soil	Slovakia	[120]
Bacillus pumilus	-	Soil	The United States	[128,129]
Bacillus sp.	-	Soil	Slovakia/Japan	[120,130]
Bacillus sp.	-	Sewage/sludge	South Korea	[131]
Bacillus subtilis	-	Soil	Slovakia	[120]
Bjerkandera adusta	-	Soil	Slovakia	[120]
Bordetella petrii	-	Soil	South Korea	[132]
Burkholderia cepacia	-	Culture collection	-	[133]
Cladosporium sphaerospermum	-	-	India	[134]
Cladosporium subcinereum	-	Soil	Slovakia	[120]
Fusarium equiseti	-	Soil	Slovakia	[120]
Fusarium moniliforme	-	Culture collection	-	[126]
Fusarium oxysporum	-	Soil	Slovakia	[120]
Fusarium solani	-	Soil	Slovakia	[120]
Kibdelosporangium aridum	-	Culture collection	-	[122,135]
Lentzea albidocapillata	-	Culture collection	-	[122]
Lentzea waywayandensis	-	Culture collection	-	[136]

Mortierella sp.	-	Soil	Slovakia	[120]
Paenibacillus sp.	-	Soil	Slovakia	[120]
Parengyodontium album	-	Culture collection	Russia/-	[127,137]
Penicillium aurantiogriseum	-	Culture collection	Ukraine	[127]
Penicillium chrysogenum	-	Culture collection	Russia	[127]
Penicillium chrysogenum	-	-	India	[134]
Penicillium roqueforti	-	Soil	Japan	[138]
Penicillium roqueforti	-	Culture collection	-	[126]
Penicillium sp.	-	Culture collection	-	[126]
Phanerochaete chrysosporium	-	Culture collection	-	[139]
Pseudomonas frederiksbergensis	-	Soil	Svalbard	[129]
Pseudomonas sp.	-	Sewage/Sludge	South Korea/China	[131,140]
Pseudomonas sp.	-	Soil	Svalbard	[129]
Pseudonocardia alni	-	Culture collection	-	[141]
Rhizopus oligosporus	-	Culture collection	-	[126]
Rhodococcus sp.	-	Soil	Slovakia	[120]
Rhodotorula mucilaginosa	-	-	India	[134]
Saccharothrix australiensis	-	Culture collection	-	[122]
Saccharothrix coeruleofusca	-	Culture collection	-	[122]
Saccharothrix cryophilis	-	Culture collection	-	[122]
Saccharothrix espanaensis	-	Culture collection	-	[122]
Saccharothrix longispora	-	Culture collection	-	[122]
Saccharothrix mutabilis	-	Culture collection	-	[122]
Saccharothrix syringae	-	Culture collection	-	[122]
Saccharothrix texasensis	-	Culture collection	-	[122]
Saccharothrix waywayandensis	-	Culture collection	Japan/-	[122,142]
Saccharothrix waywayandensis	-	-	-	[143]
Serratia marcescens	-	-	India	[134]
Stenotrophomonas maltophilia	-	Soil	South Korea	[144]
Streptoalloteichus hindustanus	-	Culture collection	-	[122]
Streptomyces ciscaucasicus	-	Soil	Slovakia	[120]
Streptomyces cyaneogriseus	-	Soil	Slovakia	[120]
Streptomyces lateritius	-	Soil	Slovakia	[120]
Trichoderma harzianum	-	Soil	Slovakia	[120]
Trichoderma harzianum	-	Culture collection	-	[126]
Trichoderma sp.	-	Culture collection	-	[126]
Trichoderma viride	-	Soil	-	[145]
Tritirachium album	-	-	-	[143]
Actinomadura keratinilytica	-	Soil	Thailand	[146,147]
Actinomadura sp.	-	Compost	Thailand	[148]
Bacillus brevis	-	Soil	Japan	[149]
Bacillus licheniformis	-	Others	-	[150]
Bacillus licheniformis	-	Soil	Thailand	[147]
Bacillus stearothermophilus	-	Soil	Japan	[151]
Geobacillus thermocatenulatus	-	Soil	Japan	[152]
Geobacillus thermoleovorans	-	Compost	-	[153]
Laceyella sacchari	-	Soil	Thailand	[147,154]
Micromonospora echinospora	-	Soil	Thailand	[147]
Micromonospora viridifaciens	-	Soil	Thailand	[147]
Nonomuraea fastidiosa	-	Soil	Thailand	[147]
Nonomuraea terrinata	-	Soil	Thailand	[147]
Pseudonocardia sp.	-	Culture collection	Thailand	[155]
Streptomyces sp.	-	Compost	Thailand	[148]
Thermoactinomyces vulgaris	-	Soil	Thailand	[147]
Thermopolyspora flexuosa	-	Compost	Czech Republic	[156]
Amycolatopsis orientalis	PLA-degrading enzyme	Culture collection	-	[157]
Amycolatopsis sp.	PLA-degrading enzyme	Soil	Thailand	[158]
Amycolatopsis sp.	PLA depolymerase	Soil	Japan	[159]
Bacillus smithii	PLA depolymerase	Plastic waste dumping site	Japan	[160]
Stenotrophomonas geniculata	Protease	Soil	Thailand	[161]
Stenotrophomonas pavanii	Protease	Soil	Thailand	[161]
Paenibacillus amylolyticus	Protease and esterase	Soil	Japan	[162]
Delftia acidovorans	PUR esterase	Culture collection	-	[163]
Thermobifida cellulosilytica	Cutinase	-	-	[164]
Amycolatopsis orientalis	Protease	-	-	[165]
Alcanivorax borkumensis	Hydrolase	-	-	[166]
Rhodopseudomonas palustris	Hydrolase	-	-	[166]
Parengyodontium album	Protease	-	-	[167]
Lederbergia lenta	Protease	-	-	[168]

Bacillus licheniformis	Protease	-	-	[168]
Alcanivorax borkumensis	Esterase	-	-	[169]
Uncultured bacterium	Esterase	-	-	[169]
Moraxella sp.	Polyester hydrolase	-	-	[170]
Nocardioides zeae	-	Plastic waste dumping site	Thailand	[171]
Stenotrophomonas pavanii	-	Plastic waste dumping site	Thailand	[171]
Gordonia desulfuricans	-	Plastic waste dumping site	Thailand	[171]
Chitinophaga jiangningensis	-	Plastic waste dumping site	Thailand	[171]
Pseudomonas chlororaphis	Lipase	Soil/plant associated	-	[172,173]
Pseudomonas chlororaphis	PHA depolymerase	Plant associated	-	[173]
Lachnellula sp.	-	Soil	Switzerland	[174]
Pseudogymnoascus verrucosus	-	Soil	Greenland	[174]
Lachnellula sp.	-	Soil	Switzerland	[174]
Neodevriesia sp.	-	Arctic shore	Norway	[174]
Amycolatopsis sp.	-	Soil	Switzerland	[174]
Bacillus safensis	-	Soil	China	[175]
Phanerochaete chrysosporium	-	Culture collection	-	[176]
Lihuaxuella thermophila	PHB depolymerase	-	-	[177]
Bacillus amyloliquefaciens	-	Culture collection	Korea	[178]
Brevibacillus brevis	-	Culture collection	Korea	[178]
Streptomyces gougerotii	-	Marine	Portugal	[105]
Micromonospora matsumotoense	-	Marine	Portugal	[105]
Nocardiopsis prasina	-	Marine	Portugal	[105]

Intellectual Property Applications in Japan

An examination of the status of intellectual property (IP) applications for general biodegradable plastics in Japan from 1988 to 2024[179] identified 10,336 applications. Applications for technological developments in biodegradable plastics began to increase in the 1990s when mass production of PLA was first considered in Japan, peaking around 2002 (**Figure 16**). The trend in the number of patents indicates that the development of biodegradable plastic technology has reached a certain level of maturity.

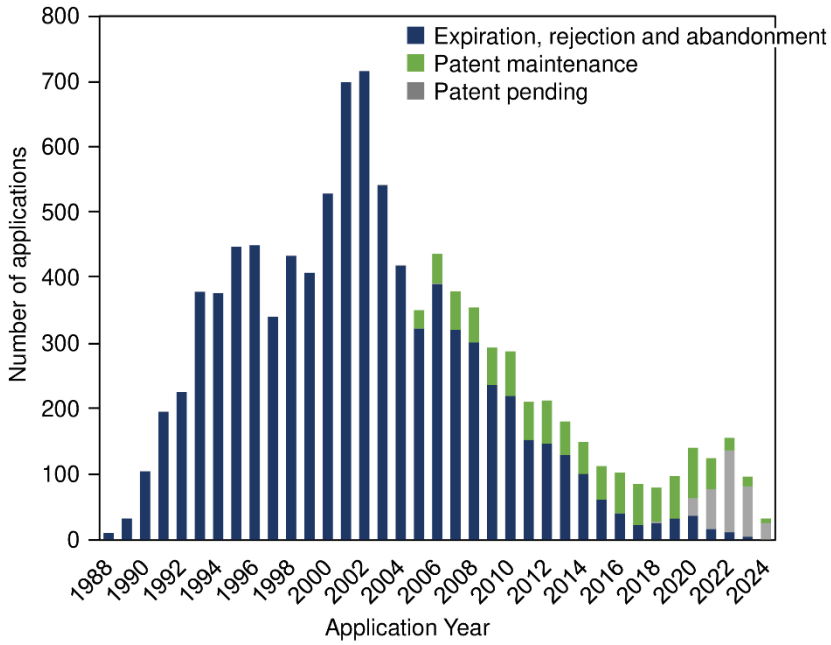

Figure 16. Trend in the number of applications for biodegradable plastics in Japan. The number of applications from 1988 to 2024 was investigated using the patent database (Patent Search Webservice, CKS Web)[179] with the search formula: Japan × Patent × F-term = 4J200 (biodegradable polymer). The total number of hits was 10,336.

Furthermore, the number of patents maintained has reached a plateau, indicating that patent selection is progressing after patents are granted.

Patents related to PLA production in Japan were examined to further analyze application trends and patent holders[180] (**Figure 17**). The development of technologies for lactic acid and PLA increased around 2000, after the initial interest in biodegradable plastics, and peaked by 2010. These technologies have reached a level of maturity. Patents related to Mitsui Chemicals, which had been involved in PLA production since the 1990s, and Shimadzu Corporation, which has transferred rights to other companies, were prominent. Mitsui Chemicals, which developed the direct polymerization method,[63] has had few recent applications. In contrast, Toyota, which inherited Shimadzu's technology,[181] and Teijin, which inherited Toyota's manufacturing technology, have filed patents related to PLA production.[182] Teijin has withdrawn from PLA production, and recent applications are limited, focusing on applications such as PLA fibers and their manufacturing methods.[183] Numerous patents filed by early pioneers, such as Mitsui Chemicals and Shimadzu Corporation, are over 20 years old and have expired. Although Toray and Unitika do not have manufacturing facilities, they have a history of collaboration with Cargill (now NatureWorks).[184] Recent applications have decreased; however, Unitika's patents are related to film and nonwoven fabric manufacturing methods,[185] and Toray has several patents on proprietary purification processes using membranes.[186] Although NatureWorks has filed patents under the Cargill name,[187] few applications have been submitted in Japan by major PLA suppliers, such as Zhejiang Hisun Biomaterials. However, TotalEnergies Corbion, through its group company Purac Biochem, has filed patents covering the entire process from saccharification to lactic acid and PLA production.[188] Although the number of applications has decreased, the company continues to file applications consistently. The development and

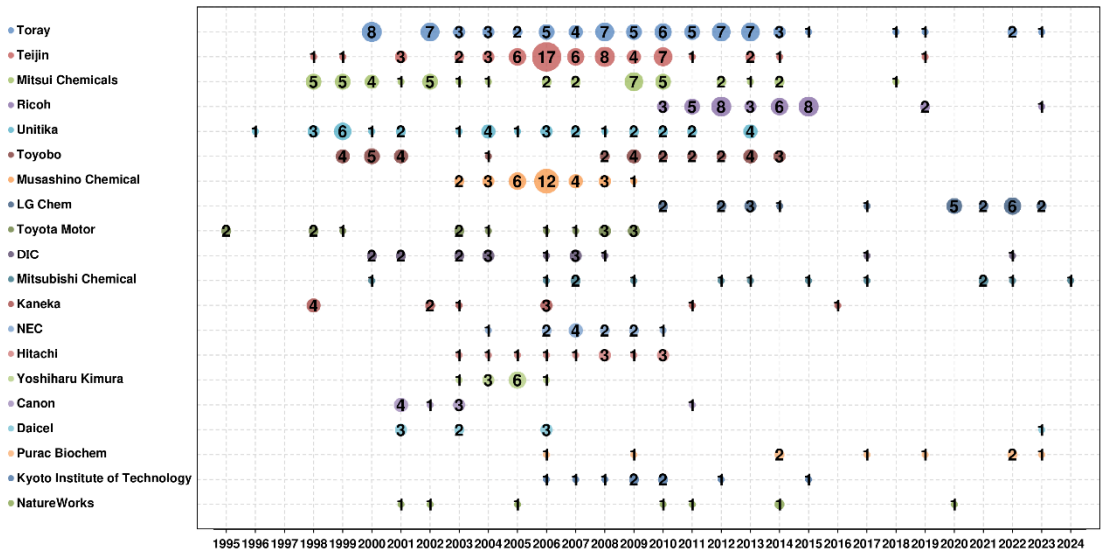

Figure 17. Trends in the number of applications for lactic acid production by applicants in Japan. The number of applications from 1995 to 2024 was investigated using the patent database (Patent Information Providing Service, Shareresearch)[180] with the search formula: Japan × Patent × F-term = 4B064AD33 (microbial production of compounds → lactic acid) + IC = C12P7/56 (production of organic compounds containing oxygen → lactic acid). The total number of hits was 664.

commercialization of new technologies and collaboration with past and overseas suppliers should be promoted to revitalize the Japanese market and realize a sustainable society.

PLA-Based Block Copolymers

The mechanical properties, biodegradability, and thermal stability of PLA are limited, which restricts its wider application. Numerous studies have reported on block copolymerization of PLA with other polymers to overcome these limitations. For instance, the introduction of aromatic components, such as terephthalic acid, into polymers enhances their thermal properties (e.g., T_g). Poly(ethylene terephthalate) (PET)-*co*-PLA is synthesized by the polycondensation of bis(2-hydroxyethyl terephthalate) (BHET), a degradation product of PET, with oligo(lactic acid) (OLA).[189] Copolymerization with poly(trimethylene terephthalate[190] and poly(butylene terephthalate) (PBT)[191] has also been reported. Additionally, the use of the bio-based monomer 2,5-furandicarboxylic acid (FDCA) as a substitute for terephthalic acid has been explored for the synthesis and degradability of copolymers (e.g., poly(ethylene-2,5-furandicarboxylate) (PEF)-co-PLA and poly(butylene-2,5-furandicarboxylate) (PBF)-*co*-PLA).[192-197] In the field of biomedical applications, block copolymers with hydrophilic and biocompatible materials have attracted attention. Block copolymers with polyethylene oxide have been reported for drug delivery systems and other biomedical uses.[198] The hydrolytic degradability of block copolymers with PCL developed for temporary therapeutic applications (e.g., surgery) has been reported.[199] The copolymerization with flexible and hydrophilic polyethylene glycol has enhanced the shape memory properties of PLA for use in medical materials. PLA-based copolymers are often discussed at low molecular weight.[200] However, the production of high-molecular-weight polymers is necessary for thermoforming and industrialization, and achieving high molecular weight through copolymerization is challenging.[201] Despite these challenges, PLA-based block copolymers represent a promising step toward future application developments.

Outline of This Dissertation

In response to environmental issues such as the mismanagement of plastic waste, which leads to marine pollution, and concerns about the depletion of petroleum resources, PLA, a typical bioplastic, was first developed in 1845 and has since undergone numerous technological innovations. However, compared to global trends, Japanese PLA suppliers have withdrawn from the market, causing delays in domestic PLA supply and a heavy reliance on imports. Technical issues, including brittleness and stiffness, and the difficulty of degradation in marine and soil environments result in the slow adoption of PLA. The IP application status of PLA has already passed its peak, indicating the need for new technological developments. This study contributes to the expansion of the domestic distribution of PLA products by developing composite materials with improved mechanical properties and biodegradability of PLA through block copolymerization, utilizing the PLA production process from wood resources (**Figure 18**).

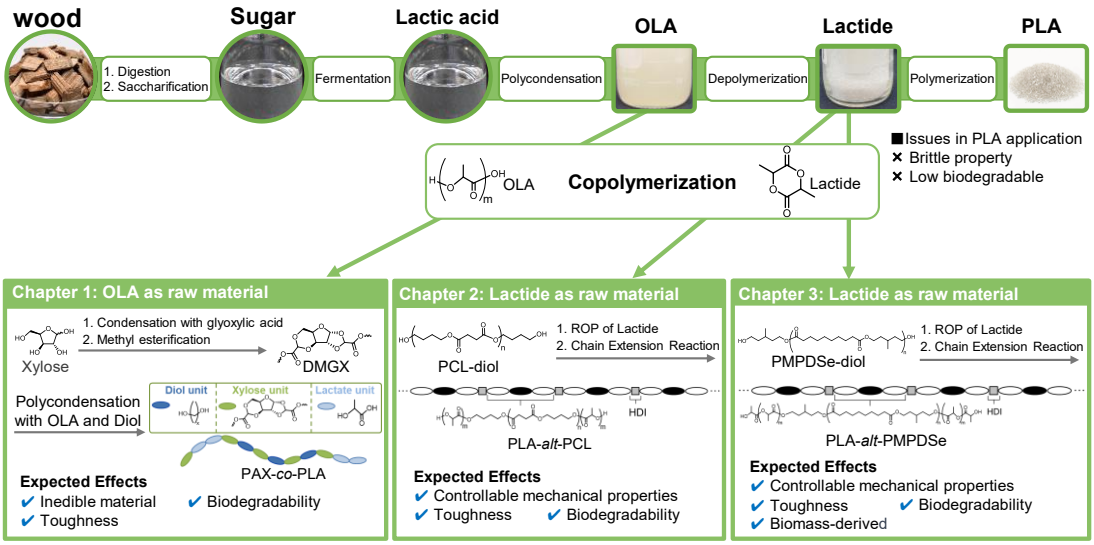

Figure 18. Outline of Chapters 1–3.

Chapter 1 focuses on xylose and lactic acid, which can be obtained from sustainable inedible resources. Poly(alkylene xylosediglyoxylates) (PAX)-*co*-PLA were synthesized using various aliphatic diols (C2–C6) using dimethyl glyoxylate xylose (DMGX), which can be synthesized from xylose, and OLA, which can be synthesized from lactic acid. The thermal and mechanical properties of PAX-*co*-PLA can be tailored by adjusting the copolymer composition. Compared with PLA, poly(hexylene xylosediglyoxylate) (PHX)-*co*-PLA exhibited higher T_g and toughness. Additionally, neat PHX and PHX-*co*-PLA exhibited potential biodegradability in compost and seawater. PHX-*co*-PLA retained its shape and exhibited enhanced water resistance. Given its thermoformability and potential biodegradability, the developed PAX-*co*-PLA can mitigate environmental pollution, particularly microplastic pollution. These materials are expected to have various applications, such as packaging, agricultural use, and marine environments.

In Chapter 2, PLA and PCL-diol are copolymerized *via* ring-opening polymerization of L-lactide, followed by a chain-extension reaction with hexamethylene diisocyanate (HDI) in the same reaction system to synthesize PLA-based PLA–PCL alternating multiblock (PLA-*alt*-PCL) copolymers. The mechanical and thermal properties of PLA-*alt*-PCL copolymers can be controlled by varying the lengths of PLA chains. They exhibited higher toughness and T_g below room temperature compared to random multiblock copolymers and blend composites. This improvement can be attributed to the controlled arrangement of PCL and PLA chains within the alternating multiblock copolymers. Additionally, CO_2 production and biodegradability in compost increased from the beginning of the test, indicating high biodegradability. In seawater, the molecular weight of PLA-*alt*-PCL copolymers was notably lower than that of random copolymers from the initial stage of the test. PLA-*alt*-PCL copolymers exhibited improved initial degradability and were more likely to oligomerize in seawater. This study provides a solution to the problem of plastic waste and can be used in various applications that require high toughness and biodegradability.

In Chapter 3, PLA-based poly(3-methyl-1,5-pentanediol sebacate) (PMPDSe) alternating multiblock (PLA-*alt*-PMPDSe) copolymers were synthesized *via* the copolymerization of PLA and sebacic acid–based PMPDSe, followed by a chain-extension reaction with HDI. The regularly arranged PLA-*alt*-PMPDSe copolymers demonstrated substantially improved mechanical properties compared to the random multiblock copolymers. Improved biodegradability in compost, activated sludge, and marine environments may be attributed to polymer crystallinity, hydrophobicity, and hydrolyzability, as well as the presence of long-chain dicarboxylic acid sebacic acid. In terms of sustainable bioplastics, this study is expected to be applied in various fields that require high toughness and biodegradability, such as packaging, agricultural uses, and marine environments.

References

(1) Plastics Europe. Plastics─the fast Facts 2024. *Plastics Europe* **2024**. https://plasticseurope.org/knowledge-hub/plastics-the-fast-facts-2024/ (accessed May 8, 2025).
(2) OECD. Global Plastics Outlook: Policy Scenarios to 2060. *OECD Publishing*, 2022 https://doi.org/10.1787/aa1edf33-en.
(3) Carafa, R. N.; Foucher, D. A.; Sacripante, G. G. Biobased polymers from lignocellulosic sources. *Green Chem. Lett.Rev.* **2023**. *16* (1). https://doi.org/10.1080/17518253.2022.2153087 .
(4) Jambeck, J. R.; Geyer, R.; Wilcox, C.; Siegler, T.R.; Perryman, M,; Andray, A.; Narayan, R.; Law, K.L. Plastic waste inputs from land into the ocean. *Science* **2015**, *347* (6223), 768–771. https://doi.org/10.1126/science.1260352.
(5) Walker, T. R. Drowning in debris: Solutions for a global pervasive marine pollution problem. Mar. Pollut. Bull. **2018**, *126*, 338. https://doi.org/10.1016/j.marpolbul.2017.11.039.
(6) Rhodes, C. J. Plastic Pollution and Potential Solutions. *Sci. Prog.* **2018**, *101* (3), 207–260. https://doi.org/10.3184/003685018X15294876706211.
(7) United Nations. Kyoto Protocol to the United Nations Framework. *United Nations* **1998**. https://unfccc.int/resource/docs/convkp/kpeng.pdf (accessed June 11, 2025).
(8) European Commission. EU Policy Framework on Biobased, Biodegradable and Compstable Plastics. *European Commission* **2022**. https://environment.ec.europa.eu/document/download/14b709eb-178c-40ea-9787-6a40f5f25948_en?filename=COM_2022_682_1_EN_ACT_part1_v4.pdf (accessed May 8, 2025).
(9) The White House. Bold Goals for U.S. Biotechnology and Biomanufacturing. *The White House* **2023**. https://bidenwhitehouse.archives.gov/wp-content/uploads/2023/03/Bold-Goals-for-U.S.-Biotechnology-and-Biomanufacturing-Harnessing-Research-and-Development-To-Further-Societal-Goals-FINAL.pdf (accessed May 8, 2025).
(10) United States Environmental Protection Agency. National Strategy to Prevent Plastic Pollution. *United States Environmental Protection Agency.* **2024**. https://www.epa.gov/system/files/documents/2024-11/final_national_strategy_to_prevent_plastic_pollution.pdf (accessed June 11, 2025).
(11) Integrated Innovation Strategy Promotion Council Decision. Bioeconomy Strategy. *Cabinet Office (Japan)* **2024**. https://www8.cao.go.jp/cstp/bio/bio_economy_en.pdf (accessed May 8, 2025).
(12) Shibata, N. Realization of an Urban Biorefinery Based on Biomass Saccharification Enzyme Production Technology (doctoral thesis). *Kobe University Repository Kernel.* **2022**. https://hdl.handle.net/20.500.14094/D1008384 (in Japanese).
(13) Gavahian, M.; Munekata, P. E. S.; Eş, I.; Lorenzo, J. M.; Mousavi Khaneghah, A.; Barba, F. J. Emerging techniques in bioethanol production: from distillation to waste valorization. *Green Chem.* **2019**, *21* (6), 1171–1185. https://doi.org/10.1039/c8gc02698j.
(14) Rosegrant, M. W. Biofuels and grain prices: Impacts and policy responses. *International Food Policy Research Institute* **2008**. https://hdl.handle.net/10568/160345.

(15) Manker, L. P.; Jones, M. J.; Bertella, S.; Behaghel de Bueren, J.; Luterbacher, J. S. Current strategies for industrial plastic production from non-edible biomass. *Curr. Opin. Green Sustainable Chem.* **2023**, *41*, 100780 https://doi.org/10.1016/j.cogsc.2023.100780.
(16) Delidovich, I.; Hausoul, P. J. C.; Deng, L.; Pfützenreuter, R.; Rose, M.; Palkovits, R. Alternative Monomers Based on Lignocellulose and Their Use for Polymer Production. *Chem. Rev.* **2016**, *116*(3), 1540–1599. https://doi.org/10.1021/acs.chemrev.5b00354.
(17) Kim-keung, J. H. Formulation of a Systemic PEST Analysis for Strategic Analysis. *Eur. Acad. Res.* **2014**, *2* (5), 6478–6492. https://euacademic.org/UploadArticle/831.pdf (accessed June 11, 2025).
(18) United Nations. The 17 GOALS. *United Nations.* https://sdgs.un.org/goals (accessed June 11, 2025).
(19) Government of Canada. OCEAN PLASTICS CHARTER. *Government of Canada*, **2018**. https://www.canada.ca/content/dam/eccc/documents/pdf/pollution-waste/ocean-plastics/Ocean%20Plastics%20Charter_EN.pdf (accessed June 11, 2025).
(20) European Commission: Directorate-General for Environment. Turning the Tide on Single-Use Plastics. *Publications Office*. **2019**. https://doi.org/10.2779/294711.
(21) United Nations Environment Programme (UNEP). The Basel Convention on the Control of Transboundary. The Basel Convention At A Glance. *UNEP* **1989**. https://www.basel.int/Portals/4/Basel%20Convention/docs/convention/bc_glance.pdf (accessed June 11, 2025).
(22) UNEP. China's trash ban lifts lid on global recycling woes but also offers opportunity. *UNEP.* **2018**. https://www.unep.org/news-and-stories/story/chinas-trash-ban-lifts-lid-global-recycling-woes-also-offers-opportunity (accessed June 11, 2025).
(23) Laville, S. Thailand bans imports of plastic waste to curb toxic pollution. *Guardian News & Media.* **2025**. https://www.theguardian.com/environment/2025/jan/07/thailand-bans-imports-plastic-waste-curb-toxic-pollution (accessed June 11, 2025).
(24) The United States Department of Agriculture (USDA). USDA BIOPREFERRED PROGRAM BRAND AND MARKETING GUIDELINES. The United States Department of Agriculture **2021.** https://www.biopreferred.gov/BPResources/files/BioPreferredBrandGuide.pdf (accessed June 11, 2025).
(25) Ministry of the Environment. The Plastic Resource Circulation Act. *Ministry of the Environment (Japan)* **2021**. https://www.env.go.jp/content/900452895.pdf (accessed June 11, 2025).
(26) USDA's Foreign Agricultural Service. Japan: Introduction of Mandatory Plastic Bag Fee Creates Opportunities for Bioplastic. *USDA's Foreign Agricultural Service* **2020**. https://www.fas.usda.gov/data/japan-introduction-mandatory-plastic-bag-fee-creates-opportunities-bioplastic (accessed April 10, 2025).
(27) Government of Japan. Roadmap for Bioplastics Introduction. *Government of Japan* **2021**. https://www.env.go.jp/recycle/mat21030210_1.pdf (accessed June 11, 2025).
(28) European Bioplastics. Bioplastics market development update 2024. *European Bioplastics.* **2024**. https://www.european-bioplastics.org/market/ (accessed June 11, 2025).
(29) European Bioplastics. ACCOUNTABILITY IS KEY Environmental Communication Guide for Bioplastics. *European Bioplastics* **2017**. https://docs.european-bioplastics.org/2016/publications/EUBP_environmental_communications_guide.pdf (accessed June 11, 2025).
(30) Yamada, K. Trends in ESG Investments in Japan and the World. *Mitsubishi Research Institute* **2022**. https://www.mri.co.jp/knowledge/column/20221125.html (accessed April 11, 2025) (in Japanese).
(31) Aoki, S. Oji Holdings Wields Responsible Management, Utilization of Forest Resources as SDGs Keystones. Nikkei Business Publications, **2024**. https://project.nikkeibp.co.jp/ESG/atcl/eng/sdgf/78/ (accessed June 11, 2025).
(32) Thomson, E. 6 ways Russia's invasion of Ukraine has reshaped the energy world. *World Economic Forum.* **2022**. https://www.weforum.org/stories/2022/11/russia-ukraine-invasion-global-energy-crisis/ (accessed June 11, 2025).
(33) Ministry of Finance. Trade Statistics of Japan. *Ministry of Finance (Japan)*. https://www.customs.go.jp/toukei/info/index_e.htm (accessed June 11, 2025).
(34) Oji Holdings. Oji Group Integrated Report 2024. *Oji Holdings* **2024**. https://www.ojiholdings.co.jp/en/uploads/ir/docs/2024_all_en.pdf (accessed June 11, 2025).

(35) TÜV AUSTRIA. OK Certification. *TÜV AUSTRIA*. https://okcert.tuvaustria.com/ (accessed June 11, 2025).
(36) DIN CERTCO. Environmental Field. *DIN CERTCO*. https://www.dincertco.de/din-certco/en/main-navigation/products-and-services/certification-of-products/environmental-field/overview-environmental-field (accessed June 11, 2025).
(37) NEN. Bio-based content. *NEN*. https://biobasedcontent.eu/ (accessed June 11, 2025).
(38) BPI. Certified Compostable. *BPI* https://bpiworld.org/ (accessed June 11, 2025).
(39) Compostable Materials Certification Scheme. REAL Home Compostable Products Scheme Rules. *REAL 2024.* https://www.compostablematerials.org.uk/upload/real_home_compostable_products_scheme_rules_version_4.pdf (accessed June 11, 2025).
(40) Australasian Bioplastics Association. Home COMPOSTABLE Verification Programme. *Australasian Bioplastics Association.* https://bioplastics.org.au/certification/home-compostable-verification-programme/ (accessed June 11, 2025).
(41) Consorzio Italiano Compostatori. Circular Economy for biowaste in Italy. *Consorzio Italiano Compostatori.* https://www.compost.it/en/ (accessed June 11, 2025).
(42) Ministry of the Environment. Shift to a Sustainable Lifestyle. *Annual Report 2018 on the Environment in Japan* **2018**, *3*, 16–22. https://www.env.go.jp/content/900457436.pdf (accessed June 11, 2025).
(43) JBPA. Overview of bioplastics. *JBPA* **2020**. https://www.env.go.jp/content/900534469.pdf (accessed June 11, 2025) (in Japanese).
(44) JBPA. Identification system. *JBPA.* http://www.jbpaweb.net/identification/index.html (accessed June 11, 2025) (in Japanese).
(45) Mabro, R. The political instability of the Middle East and its impact on oil production and trade. *Energy Stud. Rev.* **1992**, *4* (1), 45-50. https://doi.org/10.15173/esr.v4i1.259.
(46) Cable News Network (CNN). Russia's war in Ukraine sparked a historic food crisis. It's not over. *CNN* **2023**. https://edition.cnn.com/2023/01/15/business/global-food-crisis-davos (accessed June 11, 2025).
(47) Ministry of Agriculture, Monthly Food Security Report, **2024**. https://www.maff.go.jp/j/zyukyu/jki/j_rep/monthly/attach/pdf/r6index-14.pdf (accessed June 11, 2025) (in Japanese).
(48) Japan Organic Resource Association (JORA). Biomass mark. *JORA.* https://www.jora.jp/biomassmark/ (accessed June 11, 2025) (in Japanese).
(49) Hermuth-Kleinschmidt, K. Bioplastic Explained: "How Much 'Bio' Can You Expect in Plastic?" *Eppendorf White Paper 92*, 1–12. https://www.eppendorf.com/product-media/doc/en/10998795/Sustainability_White-Paper_092_Consumables-BioBased_Bioplastic-Explained-How-Much-Bio%E2%80%9D-You-Expect-Plastic%E2%80%9D.pdf.
(50) Japan Paper Association. Statistics on paper, paperboard, and pulpwood. https://www.jpa.gr.jp/en/stats/ (accessed June 11, 2025).
(51) Mitsui Chemicals. Interview with Biodegradable Plastic Developers: From Biodegradability to Biomass. *Mitsui Chemicals.* https://jp.mitsuichemicals.com/jp/sustainability/beplayer-replayer/soso/archive/column/common/2023-0517-01 (accessed June 11, 2025) (in Japanese).
(52) Teixeira, L. V.; Bomtempo, J. V.; Oroski, F. de A.; Coutinho, P. L. de A. The Diffusion of Bioplastics: What Can We Learn from Poly(Lactic Acid)? *Sustainability (Switzerland)* **2023**, *15* (6). https://doi.org/10.3390/su15064699.
(53) Ministry of Economy, Trade and Industry. Biomanufacturing. *Ministry of Economy, Trade and Industry* (Japan). https://www.meti.go.jp/english/policy/mono_info_service/mono/bio/Kennkyuukaihatsu/whitebio/whitebio.html (accessed June 11, 2025).
(54) Robinson, D. K. R.; Nadal, D. Synthetic biology in focus: Policy issues and opportunities in engineering life. *OECD Science, Technology and Industry Working Papers*. **2025**, 1–68 https://doi.org/10.1787/3e6510cf-en.
(55) Bie, F. de.; Sart, G. G. du.; Ravard, M.; Scola, P. La; Veras, R. Stay in the Cycle. Rethinking recycling with PLA bioplastics. *TotalEnergies Corbion White Paper,* **2022**, 1–19. https://tec.leidardev.com/wp-content/uploads/2025/03/Whitepaper-on-the-recyclability-of-Luminy-PLA.pdf.

(56) European Bioplastics. CHEMICAL RECYCLING OF BIO-BASED PLASTICS. **2021,** 1–5. https://docs.european-bioplastics.org/publications/bp/EUBP_BP_Chemical_Recycling.pdf (accessed June 11, 2025).
(57) NatureWorks. Chemical Recycling. *NatureWorks.* https://www.natureworksllc.com/sustainability/end-of-life-opportunities/chemical-recycling (accessed June 11, 2025).
(58) Plastic Waste Management Institute. An Introduction to Plastic Recycling in Japan. *Plastic Waste Management Institute*. **2022**, 1–33. https://www.pwmi.or.jp/ei/plastic_recycling_2022.pdf (accessed June 11, 2025).
(59) Sherwood, J. Closed-Loop Recycling of Polymers Using Solvents. *Johnson Matthey Technology Review* **2020**, *64* (1), 4–15. https://doi.org/10.1595/205651319x15574756736831.
(60) Auras, R.; Harte, B.; Selke, S. An Overview of Polylactides as Packaging Materials. *Macromol. Biosci*. **2004**, 4 (9), 835–864. https://doi.org/10.1002/mabi.200400043.
(61) Karamanlioglu, M.; Preziosi, R.; Robson, G. D. Abiotic and biotic environmental degradation of the bioplastic polymer poly(lactic acid): A review. *Polym. Degrad. Stab.* **2017**, *137*, 122–130. https://doi.org/10.1016/j.polymdegradstab.2017.01.009.
(62) Castro-Aguirre, E.; Iñiguez-Franco, F.; Samsudin, H.; Fang, X.; Auras, R. Poly(lactic acid)—Mass production, processing, industrial applications, and end of life. *Adv. Drug Deliv. Rev.* **2016**, *107*, 333–366. https://doi.org/10.1016/j.addr.2016.03.010.
(63) Ajioka, M.; Enomoto, K.; Suzuki, K.; Yamaguchi, A. The basic properties of poly(lactic acid) produced by the direct condensation polymerization of lactic acid. *J. Environ. Polym. Degrad.* **1995**, *3*, 225-234. https://doi.org/10.1007/BF02068677.
(64) Joint Research Centre: Institute for Prospective Technological Studies; Patel, M.; Angerer, G.; Crank, M.; Schleich, J.; Marscheider-Weidemann, F.; Hüsing, B. Techno-economic feasibility of large-scale production of bio-based polymers in Europe. *Publications Office*, **2005**, https://op.europa.eu/en/publication-detail/-/publication/b4155bd6-b0af-4a3d-9653-511c71ef19e9 (accessed June 11, 2025).
(65) Report Ocean. This Study as Conducted to Gain a Global Overview of the Polylactic Acid Market Size and Demand in 2022. *PR Times* **2023**. https://prtimes.jp/main/html/rd/p/000006003.000067400.html (accessed June 11, 2025) (in Japanese).
(66) Yano Research Institute. Survey on the bioplastics market (2022). *Yano Research Institute* **2022**. https://www.yano.co.jp/press-release/show/press_id/3116 (accessed April 10, 2025) (in Japanese).
(67) Development Bank of Japan. Biodegradable plastics attracting attention in a resource-circulating society. *Development Bank of Japan* **2003**, *53*, 1–47. https://www.dbj.jp/reportshift/report/research/pdf_all/56_all.pdf (accessed April 10, 2025) (in Japanese).
(68) Oji Holdings, FY2021 Demonstration Project for a Plastic Resource Circulation System toward a Decarbonized Society, Demonstration Project for Producing Domestic Biomass Plastic Using Non-Edible Biomass. *Ministry of the Environment* **2021**. https://www.env.go.jp/content/000164284.pdf (accessed April 10, 2025) (in Japanese).
(69) Lunt, J.; Shafer, A. L. Polylactic Acid Polymers from Com. Applications in the Textiles Industry. *J. Ind. Text.* **2000**, *29* (3), 191–205. https://doi.org/10.1177/152808370002900304.
(70) Shen, L.; Haufe, J. I.; Patel, M. K. Product overview and market projection of emerging bio-based plastics. *PRO-BIP 2009: final report* **2009**, 243. https://www.uu.nl/sites/default/files/copernicus_probip2009_final_june_2009_revised_in_november_09.pdf.
(71) Gruber, P. R. Cargill Dow LLC. *J. Ind. Ecol*. **2008**, *7* (3-4) 209–213. https://doi.org/10.1162/108819803323059505.
(72) Gendron, R.; Mihaela Mihai. Extrusion Foaming of Polylactide. In Polymeric Foams, Innovations in Processes, Technologies, and Products, *CRC Press*, **2016**, *5*, 107–157. https://doi.org/10.1201/9781315369365.
(73) Finasucre. 2015/2016 Annual Report. *Finasucre* **2016**. https://www.finasucre.com/medias/upload/files/Rapports/ra_finasucre_2016_en.pdf (accessed April 10, 2025).

(74) Sulzer management. Media Release, Build a PLAnet™ for sustainable bioplastics, Sulzer management **2018**. https://www.sulzer.com/-/media/files/news/news_archive/2018/181206_build_a_planet_for_sustainable_bioplastics.pdf (accessed April 10, 2025).
(75) Jem, K. J.; Tan, B. The development and challenges of poly (lactic acid) and poly (glycolic acid). *Adv. Ind. Eng. Polym. Res.* **2020**, *3* (2), 60–70. https://doi.org/10.1016/j.aiepr.2020.01.002.
(76) Ondrey, G. Teijin's Biofront demonstration plant enters operation. *Chemical Engineering*. **2009**. https://www.chemengonline.com/teijins-biofront-demonstration-plant-enters-operation/ (accessed April 10, 2025).
(77) Nikkei. Teijin Withdraws from Biodegradable Plastic Production. *Nikkei* **2018**. https://www.nikkei.com/nkd/industry/article/?DisplayType=1&n_m_code=023&ng=DGKKZO36572070W8A011C1TJ2000 (accessed April 10, 2025) (in Japanese).
(78) Larson, A.; O'Brien, K.; Anderson, A. Natureworks: Green Chemistry's Contribution to Biotechnology Innovation, Commercialization, and Strategic Positioning. *Darden Business Publishing* **2010**, http://dx.doi.org/10.2139/ssrn.1583304.
(79) TotalEnergies Corbion. Expanding Luminy PLA bioplastics distribution in Japan. *TotalEnergies Corbion* **2024**. https://www.totalenergies-corbion.com/news/expanding-luminy-pla-bioplastics-distribution-in-japan/ (accessed April 10, 2025).
(80) Kobe Fine Chemical. Revode, *Kobe Fine Chemical*. https://kobeseika.co.jp/pdf/revode.pdf (accessed April 10, 2025) (in Japanese).
(81) Oji Holdings. FY2020 Demonstration Project for a Plastic Resource Circulation System toward a Decarbonized Society, Demonstration Project for Producing Domestic Biomass Plastic Using Non-Edible Biomass. *Ministry of the Environment* **2020**. https://www.env.go.jp/content/000166044.pdf (accessed April 10, 2025) (in Japanese).
(82) Zhejiang Hisun Biomaterials. PLA, Plant resources. *Zhejiang Hisun Biomaterials*. https://en.hisunplas.com/ (accessed April 10, 2025).
(83) HighChem. Poly(lactic acid). *Highchem*. https://highchem.co.jp/products/%E3%83%9D%E3%83%AA%E4%B9%B3%E9%85%B8/ (accessed April 10, 2025) (in Japanese).
(84) Avolio, R.; Castaldo, R.; Gentile, G.; Ambrogi, V.; Fiori, S.; Avella, M.; Cocca, M.; Errico, M. E. Plasticization of poly(lactic acid) through blending with oligomers of lactic acid: Effect of the physical aging on properties. *Eur. Polym. J.* **2015**, *66*, 533–542. https://doi.org/10.1016/j.eurpolymj.2015.02.040.
(85) Wang, G. -X.; Huang, D.; Ji, J. -H.; Völker, C.; Wurm, F. R. Seawater-Degradable Polymers—Fighting the Marine Plastic Pollution. *Adv. Sci.* **2021**, *8* (1). 2001121. https://doi.org/10.1002/advs.202001121.
(86) Shah, A. A.; Hasan, F.; Hameed, A.; Ahmed, S. Biological degradation of plastics: A comprehensive review. *Biotechnol. Adv*. **2008**, *26* (3) 246–265. https://doi.org/10.1016/j.biotechadv.2007.12.005.
(87) Min, K.; Cuiffi, J. D.; Mathers, R. T. Ranking environmental degradation trends of plastic marine debris based on physical properties and molecular structure. *Nat. Commun.* **2020**, *11* (1), 727. https://doi.org/10.1038/s41467-020-14538-z.
(88) Mayekar, P. C. ACCELERATING THE BIODEGRADATION OF POLY(LACTIC ACID) AT MESOPHILIC TEMPERATURES (doctoral thesis). Michigan State University Libraries **2024**. https://doi.org/10.25335/2vjm-h186.
(89) Pickett, J. E.; Coyle, D. J. Hydrolysis kinetics of condensation polymers under humidity aging conditions. *Polym. Degrad. Stab.* **2013**, *98* (7), 1311–1320. https://doi.org/10.1016/j.polymdegradstab.2013.04.001.
(90) Rånby, B. Photodegradation and photo-oxidation of synthetic polymers. *J. Anal. Appl. Pyrolysis* **1989**, *15*, 237-247. https://doi.org/10.1016/0165-2370(89)85037-5.
(91) Ter Halle, A.; Ladirat, L.; Gendre, X.; Goudouneche, D.; Pusineri, C.; Routaboul, C.; Tenailleau, C.; Duployer, B.; Perez, E. Understanding the Fragmentation Pattern of Marine Plastic Debris. *Environ. Sci. Technol.* **2016**, *50* (11), 5668–5675. https://doi.org/10.1021/acs.est.6b00594.
(92) Singh, B.; Sharma, N. Mechanistic implications of plastic degradation. *Polym. Degrad. Stab.* **2008**, *93* (3), 561–584. https://doi.org/10.1016/j.polymdegradstab.2007.11.008.
(93) Flemming, H. C.; Wuertz, S. Bacteria and archaea on Earth and their abundance in biofilms. *Nat. Rev. Microbiol.* **2019**, *17* (4), 247–260. https://doi.org/10.1038/s41579-019-0158-9.

(94) Tiso, T.; Winter, B.; Wei, R.; Hee, J.; de Witt, J.; Wierckx, N.; Quicker, P.; Bornscheuer, U. T.; Bardow, A.; Nogales, J.; Blank, L. M. The metabolic potential of plastics as biotechnological carbon sources – Review and targets for the future. *Metab. Eng*. **2022**, *71*, 77–98. https://doi.org/10.1016/j.ymben.2021.12.006.
(95) Woodruff, M. A.; Hutmacher, D. W. The return of a forgotten polymer—Polycaprolactone in the 21st century. *Prog. Polym. Sci.* **2010**, *35* (10) 1217–1256. https://doi.org/10.1016/j.progpolymsci.2010.04.002.
(96) De Hoe, G. X.; Zumstein, M. T.; Getzinger, G. J.; Rüegsegger, I.; Kohler, H. P. E.; Maurer-Jones, M. A.; Sander, M.; Hillmyer, M. A.; McNeill, K. Photochemical Transformation of Poly(Butylene Adipate- *co*-Terephthalate) and Its Effects on Enzymatic Hydrolyzability. *Environ. Sci. Technol.* **2019**, *53* (5), 2472–2481. https://doi.org/10.1021/acs.est.8b06458.
(97) Madigan, M.; Bender, K.; Buckley, D.; Sattley, W.; Stahl, D. Brock Biology of Microorganisms Pearson **2018**. https://api.pageplace.de/preview/DT0400.9781292235196_A31976983/preview-9781292235196_A31976983.pdf (accessed April 10, 2025)
(98) Dhali, S. L.; Parida, D.; Kumar, B.; Bala, K. Recent trends in microbial and enzymatic plastic degradation: a solution for plastic pollution predicaments. *Biotechnol. Sustainable Mater.* **2024**, *1*,11. https://doi.org/10.1186/s44316-024-00011-0.
(99) Rajendran, S. D.; Velu, R. K.; Krishnan, N.; Duraisamy, N.; Kanthaiah, K.; Sekar, C.; Arokiaswamy, R. A. The Role of Microbes in Plastic Degradation. In Environmental Waste Management. *CRC Press*, **2015**, *12*, 341–370. https://doi.org/10.1201/b19243-13.
(100) Haider, T. P.; Völker, C.; Kramm, J.; Landfester, K.; Wurm, F. R. Plastics of the Future? The Impact of Biodegradable Polymers on the Environment and on Society. *Angew. Chem. Int. Ed.* **2019**, *131* (1), 50–63. https://doi.org/10.1002/ange.201805766.
(101) Henton, D.; Gruber, P.; Lunt, J.; Randall, J. Polylactic Acid Technology. In Natural Fibers, Biopolymers, and Biocomposites. *CRC Press*, **2005**, *16*, 528–577. https://doi.org/10.1201/9780203508206.
(102) Souza, P. M. S.; Morales, A. R.; Marin-Morales, M. A.; Mei, L. H. I. PLA and Montmorilonite Nanocomposites: Properties, Biodegradation and Potential Toxicity. *J. Polym. Environ.* **2013**, *21* (3), 738–759. https://doi.org/10.1007/s10924-013-0577-z.
(103) Zaaba, N. F.; Jaafar, M. A review on degradation mechanisms of polylactic acid: Hydrolytic, photodegradative, microbial, and enzymatic degradation. *Polym. Eng. Sci.* **2020**, *60*, 2061–2075. https://doi.org/10.1002/pen.25511.
(104) He, M.; Hsu, Y.-I.; Uyama, H. Superior Sequence-Controlled Poly(L-Lactide)-Based Bioplastic with Tunable Seawater Biodegradation. *J. Hazard Mater* **2024**, *474* 134819. https://doi.org/10.1016/j.jhazmat.2024.134819.
(105) Oliveira, J.; Almeida, P. L.; Sobral, R. G.; Lourenço, N. D.; Gaudêncio, S. P. Marine-Derived Actinomycetes: Biodegradation of Plastics and Formation of PHA Bioplastics—A Circular Bioeconomy Approach. *Mar. Drugs* **2022**, *20* (12) 760. https://doi.org/10.3390/md20120760.
(106) Seok, J. H.; Iwata, T. Effects of Molecular Weight on the Marine Biodegradability of Poly(L-Lactic Acid). *Biomacromolecules* **2024**, *25* (7), 4420–4427. https://doi.org/10.1021/acs.biomac.4c00454.
(107) Chen, X.; Wang, L.; Shi, J.; Shi, H.; Liu, Y. Environmental Degradation of Starch/Poly(Lactic Acid) Composite in Seawater *Polym. Polym. Compos.* **2011**. *19* (7), 559-566. https://doi.org/10.1177/096739111101900705.
(108) Huang, D.; Hu, Z. De; Liu, T. Y.; Lu, B.; Zhen, Z. C.; Wang, G. X.; Ji, J. H. Seawater degradation of PLA accelerated by water-soluble PVA. *e-Polymers* **2020**, *20* (1), 759–772. https://doi.org/10.1515/epoly-2020-0071.
(109) Rheinberger, T.; Wolfs, J.; Paneth, A.; Gojzewski, H.; Paneth, P.; Wurm, F. R. RNA-Inspired and Accelerated Degradation of Polylactide in Seawater. *J. Am. Chem. Soc*. **2021**, *143* (40), 16673–16681. https://doi.org/10.1021/jacs.1c07508.
(110) Gambarini, V.; Pantos, O.; Kingsbury, J. M.; Weaver, L.; Handley, K. M.; Lear, G. PlasticDB: a database of microorganisms and proteins linked to plastic biodegradation. *Database* **2022**, *2022*, baac008. https://doi.org/10.1093/database/baac008.
(111) Akutsu-Shigeno, Y.; Teeraphatpornchai, T.; Teamtisong, K.; Nomura, N.; Uchiyama, H.; Nakahara, T.; Nakajima-Kambe, T. Cloning and Sequencing of a Poly(DL-Lactic Acid) Depolymerase Gene from

Paenibacillus amylolyticus Strain TB-13 and Its Functional Expression in *Escherichia coli*. *Appl. Environ. Microbiol.* **2003**, *69* (5), 2498–2504. https://doi.org/10.1128/AEM.69.5.2498-2504.2003.
(112)Masaki, K.; Kamini, N. R.; Ikeda, H.; Iefuji, H. Cutinase-like Enzyme from the Yeast *Cryptococcus* sp. Strain S-2 Hydrolyzes Polylactic Acid and Other Biodegradable Plastics. *Appl. Environ. Microbiol.* **2005**, *71* (11), 7548–7550. https://doi.org/10.1128/AEM.71.11.7548-7550.2005.
(113)Mayumi, D.; Akutsu-Shigeno, Y.; Uchiyama, H.; Nomura, N.; Nakajima-Kambe, T. Identification and characterization of novel poly(DL-lactic acid) depolymerases from metagenome. *Appl. Microbiol. Biotechnol.* **2008**, *79* (5), 743–750. https://doi.org/10.1007/s00253-008-1477-3.
(114)Kawai, F.; Oda, M.; Tamashiro, T.; Waku, T.; Tanaka, N.; Yamamoto, M.; Mizushima, H.; Miyakawa, T.; Tanokura, M. A Novel Ca^{2+}-activated, thermostabilized polyesterase capable of hydrolyzing polyethylene terephthalate from *Saccharomonospora viridis* AHK190. *Appl. Microbiol. Biotechnol.* **2014**, *98* (24), 10053–10064. https://doi.org/10.1007/s00253-014-5860-y.
(115)Miyakawa, T.; Mizushima, H.; Ohtsuka, J.; Oda, M.; Kawai, F.; Tanokura, M. Structural basis for the Ca^{2+}-enhanced thermostability and activity of PET-degrading cutinase-like enzyme from *Saccharomonospora viridis* AHK190. *Appl. Microbiol. Biotechnol.* **2015**, *99* (10), 4297–4307. https://doi.org/10.1007/s00253-014-6272-8.
(116)Jung, H. W.; Yang, M. K.; Su, R. C. Purification, characterization, and gene cloning of an *Aspergillus fumigatus* polyhydroxybutyrate depolymerase used for degradation of polyhydroxybutyrate, polyethylene succinate, and polybutylene succinate. *Polym. Degrad. Stab.* **2018**, *154*, 186–194. https://doi.org/10.1016/j.polymdegradstab.2018.06.002.
(117)Arena, M.; Abbate, C.; Fukushima, K.; Gennari, M. Degradation of poly (lactic acid) and nanocomposites by *Bacillus licheniformis*. *Environ. Sci. Pollut. Res.* **2011**, *18* (6), 865–870. https://doi.org/10.1007/s11356-011-0443-2.
(118)Zumstein, M. T.; Kohler, H. P. E.; McNeill, K.; Sander, M. Enzymatic Hydrolysis of Polyester Thin Films: Real-Time Analysis of Film Mass Changes and Dissipation Dynamics. *Environ. Sci. Technol.* **2016**, *50* (1), 197–206. https://doi.org/10.1021/acs.est.5b04103.
(119)Liang, T. W.; Jen, S. N.; Nguyen, A. D.; Wang, S. L. Application of Chitinous Materials in Production and Purification of a Poly(L-Lactic Acid) Depolymerase from *Pseudomonas tamsuii* TKU015. *Polymers (Basel)* **2016**, *8* (3), 98. https://doi.org/10.3390/polym8030098.
(120)Jeszeová, L.; Puškárová, A.; Bučková, M.; Kraková, L.; Grivalský, T.; Danko, M.; Mosnáčková, K.; Chmela, Š.; Pangallo, D. Microbial communities responsible for the degradation of poly(lactic acid)/poly(3-hydroxybutyrate) blend mulches in soil burial respirometric tests. *World J. Microbiol. Biotechnol.* **2018**, *34* (7) 101. https://doi.org/10.1007/s11274-018-2483-y.
(121)Pranamuda, H.; Tokiwa, Y. Degradation of poly(L-lactide) by strains belonging to genus *Amycolatopsis*. *Biotechnol. Lett.* **1999**, *21*, 901-905. https://doi.org/10.1023/A:1005547326434.
(122)Jarerat, A.; Pranamuda, H.; Tokiwa, Y. Poly(L-Lactide)-Degrading Activity in Various *Actinomycetes*. *Macromol. Biosci.* **2002**, *2* (9), 420–428. https://doi.org/10.1002/mabi.200290001.
(123)Pranamuda, H.; Tsuchii, A.; Tokiwa, Y. Poly (L-Lactide)-Degrading Enzyme Produced by *Amycolatopsis* sp. *Macromol Biosci* **2001**, *1* (1), 25–29. https://doi.org/10.1002/1616-5195(200101)1:1<25::AID-MABI25>3.0.CO;2-3.
(124)Chomchoei, A.; Pathom-Aree, W.; Yokota, A.; Kanongnuch, C.; Lumyong, S. *Amycolatopsis Thailandensis* sp. nov., a poly(L-lactic acid)-degrading actinomycete, isolated from soil. *Int. J. Syst. Evol. Microbiol.* **2011**, *61* (4), 839–843. https://doi.org/10.1099/ijs.0.023564-0.
(125)Chaisu, K; Charles, A. L; Guu, Y.-K.; Chiu, C.-H. Microbial Degradation of Poly Lactic Acid (PLA) by *Aneurinibacillus aneurinilyticus*. *J. Biobased Mater. Bioenergy* **2013**, *7* (4), 509–511. https://doi.org/10.1166/jbmb.2013.1304.
(126)Torres, A.; Li, S. M.; Roussos, S.; Vert, M. Screening of microorganisms for biodegradation of poly(lactic-acid) and lactic acid-containing polymers. *Appl. Environ. Microbiol.* **1996**, *62* (7), 2393-2397. https://doi.org/10.1128/aem.62.7.2393-2397.1996.
(127)Antipova, T. V.; Zhelifonova, V. P.; Zaitsev, K. V.; Nedorezova, P. M.; Aladyshev, A. M.; Klyamkina, A. N.; Kostyuk, S. V.; Danilogorskaya, A. A.; Kozlovsky, A. G. Biodegradation of Poly-ε-caprolactones and Poly-L-lactides by Fungi. *J. Polym. Environ.* **2018**, *26* (12), 4350–4359. https://doi.org/10.1007/s10924-018-1307-3.
(128)Bonifer, K. S.; Wen, X.; Hasim, S.; Phillips, E. K.; Dunlap, R. N.; Gann, E. R.; DeBruyn, J. M.; Reynolds, T. B. *Bacillus pumilus* B12 Degrades Polylactic Acid and Degradation Is Affected by

Changing Nutrient Conditions. *Front. Microbiol.* **2019**, *10*. 2548. https://doi.org/10.3389/fmicb.2019.02548.
(129)Urbanek, A. K.; Rymowicz, W.; Strzelecki, M. C.; Kociuba, W.; Franczak, Ł.; Mirończuk, A. M. Isolation and characterization of Arctic microorganisms decomposing bioplastics. *AMB Express* **2017**, *7* (1) 148. https://doi.org/10.1186/s13568-017-0448-4.
(130)Tansengco, M. L.; Tokiwa, Y. Thermophilic microbial degradation of polyethylene succinate. *World J. Microbiol. Biotechnol*. **1997**, *14*, 133-138. https://doi.org/10.1023/A:1008897121993.
(131)Kim, M. Y.; Kim, C.; Moon, J.; Heo, J.; Jung, S. P.; Kim, J. R. Polymer Film-Based Screening and Isolation of Polylactic Acid (PLA)-Degrading Microorganisms. *J. Microbiol. Biotechnol.* **2017**, *27* (2), 342–349. https://doi.org/10.4014/jmb.1610.10015.
(132)Kim, M. N.; Park, S. T. Degradation of Poly(L-Lactide) by a mesophilic bacterium. *J. Appl. Polym. Sci.* **2010**, *117* (1), 67–74. https://doi.org/10.1002/app.31950.
(133)Wu, C. S. Renewable resource-based composites of recycled natural fibers and maleated polylactide bioplastic: Characterization and biodegradability. *Polym. Degrad. Stab.* **2009**, *94* (7), 1076–1084. https://doi.org/10.1016/j.polymdegradstab.2009.04.002.
(134)Nair, N. R.; Sekhar, V. C.; Nampoothiri, K. M. Augmentation of a Microbial Consortium for Enhanced Polylactide (PLA) Degradation. *Indian. J. Microbiol.* **2016**, *56* (1), 59–63. https://doi.org/10.1007/s12088-015-0559-z.
(135)Jarerat, A.; Tokiwa, Y.; Tanaka, H. Poly(L-Lactide) degradation by *Kibdelosporangium aridum*. *Biotechnol. Lett.* **2003**, *25*, 2035-2038. https://doi.org/10.1023/B:BILE.0000004398.38799.29.
(136)Nair, N. R.; Nampoothiri, K. M.; Pandey, A. Preparation of Poly(L-lactide) blends and biodegradation by *Lentzea waywayandensis*. *Biotechnol. Lett.* **2012**, *34* (11), 2031–2035. https://doi.org/10.1007/s10529-012-1005-5.
(137)Jarerat, A.; Tokiwa, Y. Degradation of Poly(L-Lactide) by a Fungus. *Macromol. Biosci.* **2001**, *1* (4), 136–140. https://doi.org/10.1002/1616-5195(20010601)1:4<136::AID-MABI136>3.0.CO;2-3.
(138)Pranamuda, H.; Tokiwa, Y.; Tanaka, H. Polylactide Degradation by an Amycolatopsis sp. *Appl. Environ. Microbiol.* **1997**, *63* (4), 1637-1640. https://doi.org/10.1128/aem.63.4.1637-1640.1997.
(139)Stoleru, E.; Hitruc, E. G.; Vasile, C.; Oprică, L. Biodegradation of poly(lactic acid)/chitosan stratified composites in presence of the *Phanerochaete chrysosporium* fungus. *Polym. Degrad. Stab.* **2017**, *143*, 118–129. https://doi.org/10.1016/j.polymdegradstab.2017.06.023.
(140)Wang, Z.; Wang, Y.; Guo, Z.; Li, F.; Chen, S. Purification and characterization of Poly(L-lactic acid) depolymerase from *Pseudomonas* sp. strain DS04-T. *Polym. Eng. Sci.* **2011**, *51* (3), 454–459. https://doi.org/10.1002/pen.21857.
(141)Konkit, M.; Jarerat, A.; Khanongnuch, C.; Lumyong, S.; Pathom-Aree, W. Poly(Lactide) Degradation By *Pseudonocardia alni* AS4.1531^{t}. Chiang Mai J. Sci. **2012**, *39* (1), 128–132. https://www.thaiscience.info/Article%20for%20ThaiScience/Article/62/10032898.pdf (accessed June 15, 2025).
(142)Jarerat, A.; Tokiwa, Y. Poly(L-Lactide) degradation by *Saccharothrix waywayandensis*. *Biotechnol. Lett.* **2003**, *25*, 401-404. https://doi.org/10.1023/A:1022450431193.
(143)Tokiwa, Y.; Jarerai, A. Accelerated Microbial Degradation of Poly(L-Lactide). *Macromol. Symp.* **2005**, 224 (1), 367–376. https://doi.org/10.1002/masy.200550632.
(144)Jeon, H. J.; Kim, M. N. Biodegradation of poly(L-lactide) (PLA) exposed to UV irradiation by a mesophilic bacterium. *Int. Biodeterior. Biodegrad.* **2013**, *85*, 289–293. https://doi.org/10.1016/j.ibiod.2013.08.013.
(145)Lipsa, R.; Tudorachi, N.; Darie-Nita, R. N.; Oprică, L.; Vasile, C.; Chiriac, A. Biodegradation of poly(lactic acid) and some of its based systems with *Trichoderma viride*. *Int. J. Biol. Macromol.* **2016**, *88*, 515–526. https://doi.org/10.1016/j.ijbiomac.2016.04.017.
(146)Sukkhum, S.; Tokuyama, S.; Kitpreechavanich, V. Development of fermentation process for PLA-degrading enzyme production by a new thermophilic *Actinomadura* sp. T16-1. *Biotechnol. Bioprocess Eng.* **2009**, *14* (3), 302–306. https://doi.org/10.1007/s12257-008-0207-0.
(147)Sukkhum, S.; Tokuyama, S.; Tamura, T.; Kitpreechavanich, V. A Novel poly (L-lactide) degrading actinomycetes isolated from Thai forest soil, phylogenic relationship and the enzyme characterization *J. Gen. Appl. Microbiol.* **2009**, *55* (6), 459–467. https://doi.org/10.2323/jgam.55.459.

(148)Sriyapai, P.; Chansiri, K.; Sriyapai, T. Isolation and Characterization of Polyester-Based Plastics-Degrading Bacteria from Compost Soils. *Microbiology (Russian Federation)* **2018**, *87* (2), 290–300. https://doi.org/10.1134/S0026261718020157.
(149)Tomita, K.; Kuroki, Y.; Nagai, K. Isolation of thermophiles degrading poly (L-lactic acid*). J. Biosci. Bioeng.* **1999**, 87 (6), 752–755. https://doi.org/10.1016/S1389-1723(99)80148-0.
(150)Kim, M. N.; Kim, W. G.; Weon, H. Y.; Lee, S. H. Poly(L-lactide)-degrading activity of a newly isolated bacterium. *J. Appl. Polym. Sci.* **2008**, *109* (1), 234–239. https://doi.org/10.1002/app.26658.
(151)Tomita, K.; Tsuji, H.; Nakajima, T.; Kikuchi, Y.; Ikarashi, K.; Ikeda, N. Degradation of Poly(D-Lactic Acid) by a Thermophile. *Polym. Degrad. Stab.* **2003**, *81* (1), 167–171. https://doi.org/10.1016/S0141-3910(03)00086-7.
(152)Tomita, K.; Nakajima, T.; Kikuchi, Y.; Miwa, N. Degradation of poly(L-lactic acid) by a thermophile. *Polym. Degrad. Stab.* **2004**, *84* (3), 433–438. https://doi.org/10.1016/j.polymdegradstab.2003.12.006.
(153)Castro-Aguirre, E.; Auras, R.; Selke, S.; Rubino, M.; Marsh, T. Enhancing the biodegradation rate of poly(lactic acid) films and PLA bio-nanocomposites in simulated composting through bioaugmentation. *Polym. Degrad. Stab.* **2018**, *154*, 46–54. https://doi.org/10.1016/j.polymdegradstab.2018.05.017.
(154)Hanphakphoom, S.; Maneewong, N.; Sukkhum, S.; Tokuyama, S.; Kitpreechavanich, V. Characterization of poly(L-Lactide)- degrading enzyme produced by thermophilic filamentous bacteria *Laceyella sacchari* LP175. *J. Gen. Appl. Microbiol.* **2014**, *60* (1), 13–22. https://doi.org/10.2323/jgam.60.13.
(155)Apinya, T.; Sombatsompop, N.; Prapagdee, B. Selection of a *Pseudonocardia* sp. RM423 that accelerates the biodegradation of poly(lactic) acid in submerged cultures and in soil microcosms. *Int. Biodeterior. Biodegrad.* **2015**, *99*, 23–30. https://doi.org/10.1016/j.ibiod.2015.01.001.
(156)Husárová, L.; Pekařová, S.; Stloukal, P.; Kucharzcyk, P.; Verney, V.; Commereuc, S.; Ramone, A.; Koutny, M. Identification of important abiotic and biotic factors in the biodegradation of poly(L-lactic acid). *Int. J. Biol. Macromol.* **2014**, *71*, 155–162. https://doi.org/10.1016/j.ijbiomac.2014.04.050.
(157)Jarerat, A.; Tokiwa, Y.; Tanaka, H. Production of poly(L-lactide)-degrading enzyme by *Amycolatopsis orientalis* for biological recycling of poly(L-lactide). *Appl. Microbiol. Biotechnol.* **2006**, *72* (4), 726–731. https://doi.org/10.1007/s00253-006-0343-4.
(158)Penkhrue, W.; Kanpiengjai, A.; Khanongnuch, C.; Masaki, K.; Pathom-Aree, W.; Lumyong, S. Effective enhancement of polylactic acid-degrading enzyme production by *Amycolatopsis* sp. strain SCM_MK2-4 using statistical and one-factor-at-a-time approaches. *Prep. Biochem. Biotechnol.* **2017**, *47* (7), 730–738. https://doi.org/10.1080/10826068.2017.1315597.
(159)Nakamura, K.; Tomita, T.; Abe, N.; Kamio, Y. Purification and Characterization of an Extracellular Poly(L-Lactic Acid) Depolymerase from a Soil Isolate, *Amycolatopsis* sp. Strain K104-1. *Appl. Environ. Microbiol.* **2001**, *67* (1), 345–353. https://doi.org/10.1128/AEM.67.1.345-353.2001.
(160)Sakai, K.; Kawano, H.; Iwami, A.; Nakamura, M.; Moriguchi, M. Isolation of a thermophilic poly-L-lactide degrading bacterium from compost and its enzymatic characterization. *J. Biosci. Bioeng.* **2001**; 92 (3), 298-300. https://doi.org/10.1016/S1389-1723(01)80266-8.
(161)Bubpachat, T.; Sombatsompop, N.; Prapagdee, B. Isolation and role of polylactic acid-degrading bacteria on degrading enzymes productions and PLA biodegradability at mesophilic conditions. *Polym. Degrad. Stab.* **2018**, *152*, 75–85. https://doi.org/10.1016/j.polymdegradstab.2018.03.023.
(162)Teeraphatpornchai, T.; Nakajima-Kambe, T.; Shigeno-Akutsu, Y.; Nakayama, M.; Nomura, N.; Nakahara, T.; Uchiyama, H. Isolation and characterization of a bacterium that degrades various polyester-based biodegradable plastics. *Biotechnol. Lett.* **2003**, *25*, 23–28. https://doi.org/10.1023/A:1021713711160.
(163)Akutsu, Y.; Nakajima-Kambe, T.; Nomura, N.; Nakahara, T. Purification and Properties of a Polyester Polyurethane-Degrading Enzyme from *Comamonas acidovorans* TB-35. *Appl. Environ. Microbiol.* **1998**, 64 (1), 62-67. https://doi.org/10.1128/AEM.64.1.62-67.1998.
(164)Ribitsch, D.; Hromic, A.; Zitzenbacher, S.; Zartl, B.; Gamerith, C.; Pellis, A.; Jungbauer, A.; Łyskowski, A.; Steinkellner, G.; Gruber, K.; Tscheliessnig, R.; Acero, E. H.; Guebitz, G. M. Small cause, large effect: Structural characterization of cutinases from *Thermobifida cellulosilytica*. *Biotechnol. Bioeng.* 2**017**, *114*, 2481–2488. https://doi.org/10.1002/bit.26372.

(165)Li, F.; Wang, S.; Liu, W.; Chen, G. Purification and characterization of poly(L-lactic acid)-degrading enzymes from *Amycolatopsis orientalis* ssp. *orientalis*. *FEMS Microbiol. Lett.* **2008**, *282* (1), 52–58. https://doi.org/10.1111/j.1574-6968.2008.01109.x.
(166)Hajighasemi, M.; Nocek, B. P.; Tchigvintsev, A.; Brown, G.; Flick, R.; Xu, X.; Cui, H.; Hai, T.; Joachimiak, A.; Golyshin, P. N.; Savchenko, A.; Edwards, E. A.; Yakunin, A. F.; Biochemical and Structural Insights into Enzymatic Depolymerization of Polylactic Acid and Other Polyesters by Microbial Carboxylesterases. *Biomacromolecules* **2016**, *17* (6), 2027–2039. https://doi.org/10.1021/acs.biomac.6b00223.
(167)Yamashita, K.; Kikkawa, Y.; Kurokawa, K.; Doi, Y. Enzymatic Degradation of Poly(L-lactide) Film by Proteinase K: Quartz Crystal Microbalance and Atomic Force Microscopy Study. *Biomacromolecules* **2005**, *6* (2), 850–857. https://doi.org/10.1021/bm049395v.
(168)Oda, Y.; Yonetsu, A.; Urakami, T.; Tonomura, K. Degradation of Polylactide by Commercial Proteases. *J. Polym. Environ.* **2000**, *8*, 29–32. https://doi.org/10.1023/A:1010120128048.
(169)Tchigvintsev, A.; Tran, H.; Popovic, A.; Kovacic, F.; Brown, G.; Flick, R.; Hajighasemi, M.; Egorova, O.; Somody, J. C.; Tchigvintsev, D.; Khusnutdinova, A.; Chernikova, T. N.; Golyshina, O. V.; Yakimov, M. M.; Savchenko, A.; Golyshin, P. N.; Jaeger, K. E.; Yakunin, A. F. The environment shapes microbial enzymes: five cold-active and salt-resistant carboxylesterases from marine metagenomes. *Appl. Microbiol. Biotechnol.* **2015**, *99* (5), 2165–2178. https://doi.org/10.1007/s00253-014-6038-3.
(170)Nikolaivits, E.; Taxeidis, G.; Gkountela, C.; Vouyiouka, S.; Maslak, V.; Nikodinovic-Runic, J.; Topakas, E. A polyesterase from the Antarctic bacterium *Moraxella* sp. degrades highly crystalline synthetic polymers. *J. Hazard. Mater.* **2022**, *434*, 128900. https://doi.org/10.1016/j.jhazmat.2022.128900.
(171)Mistry, A. N.; Kachenchart, B.; Wongthanaroj, A.; Somwangthanaroj, A.; Luepromchai, E. Rapid biodegradation of high molecular weight semi-crystalline polylactic acid at ambient temperature via enzymatic and alkaline hydrolysis by a defined bacterial consortium. *Polym. Degrad. Stab.* **2022**, *202*. 110051. https://doi.org/10.1016/j.polymdegradstab.2022.110051.
(172)Mohanan, N.; Wong, C. H.; Budisa, N.; Levin, D. B. Characterization of Polymer Degrading Lipases, LIP1 and LIP2 From *Pseudomonas chlororaphis* PA23. *Front. Bioeng. Biotechnol.* **2022**, *10*. https://doi.org/10.3389/fbioe.2022.854298.
(173)Mohanan, N.; Wong, M. C.-H.; Budisa, N.; Levin, D. B. Polymer-Degrading Enzymes of *Pseudomonas chloroaphis* PA23 Display Broad Substrate Preferences. *Int. J. Mol. Sci.* **2023**, *24* (5), 4501. https://doi.org/10.3390/ijms24054501.
(174)Rüthi, J.; Cerri, M.; Brunner, I.; Stierli, B.; Sander, M.; Frey, B. Discovery of plastic-degrading microbial strains isolated from the alpine and Arctic terrestrial plastisphere. *Front. Microbiol.* **2023**, *14*, 1178474. https://doi.org/10.3389/fmicb.2023.1178474.
(175)Wang, Y.; Hu, T.; Zhang, W.; Lin, J.; Wang, Z.; Lyu, S.; Tong, H. Biodegradation of polylactic acid by a mesophilic bacteria *Bacillus safensis*. *Chemosphere* **2023**, *318*, 137991. https://doi.org/10.1016/j.chemosphere.2023.137991.
(176)Wu, F.; Guo, Z.; Cui, K.; Dong, D.; Yang, X.; Li, J.; Wu, Z.; Li, L.; Dai, Y.; Pan, T. Insights into characteristics of white rot fungus during environmental plastics adhesion and degradation mechanism of plastics. *J. Hazard. Mater.* 2023, *448*, 130878. https://doi.org/10.1016/j.jhazmat.2023.130878.
(177)Thomas, G. M.; Quirk, S.; Huard, D. J. E.; Lieberman, R. L. Bioplastic degradation by a polyhydroxybutyrate depolymerase from a thermophilic soil bacterium. *Protein Science* **2022**, *31* (11), e4470. https://doi.org/10.1002/pro.4470.
(178)Yu, J.; Kim, P. Do; Jang, Y.; Kim, S. K.; Han, J.; Min, J. Comparison of polylactic acid biodegradation ability of *Brevibacillus brevis* and *Bacillus amyloliquefaciens* and promotion of PLA biodegradation by soytone. *Biodegradation* **202**2, *33* (5), 477–487. https://doi.org/10.1007/s10532-022-09993-y.
(179)Chuo Kogaku Shuppan, Patent Search Webservice, CKS Webservice. *Chuo Kogaku Shuppan*, https://newcksweb.cks.co.jp/ (accessed April 10, 2025) (in Japanese).
(180)Hitachi, Intellectual Property Database Search Service, Shareresearch. *Hitachi* https://www.hitachi.co.jp/Prod/comp/app/tokkyo/pa/id.html (accessed April 10, 2025) (in Japanese).
(181)Ohara, H.; Sawa, S.; Kawamoto, T.; Polylactic acid production method. Japan Patent JP3301221B2, **1994**. https://patents.google.com/patent/JP3301221B2/en?oq=3301221 (accessed April 10, 2025).

(182)Honma, N.; Ohara, H.; Takenaka, M. Method for producing polylactic acid. Japan Patent JP5674384B2, **2010**. https://patents.google.com/patent/JP5674384B2/en?oq=5674384 (accessed April 10, 2025).
(183)Ikegame, M.; Matsuda, T.; To, S. Polylactic acid fiber and method for producing the same. Japan Patent JP5023065B2, **2007**. https://patents.google.com/patent/JP5023065B2/en?oq=5023065 (accessed April 10, 2025).
(184)Daisen. Teijin and Cargill Form Joint Venture to Produce 140,000 Tons of PLA Polymer. *The Sen-i News*. **2007**. https://www.sen-i-news.co.jp/seninews/view/?article=200199 (accessed April 10, 2025) (in Japanse).
(185)Gondo, A. Polylactic acid long fiber nonwoven fabric. Japan Patent, JP6053289B2, **2012**. https://patents.google.com/patent/JP6053289B2/en?oq=6053289 (accessed April 10, 2025).
(186)Kawamura, K.; Ito, M.; Yamada, K. Method for producing lactic acid. Japan Patent JP6260277B2, **2013**. https://patents.google.com/patent/JP6260277B2/en?oq=6260277 (accessed April 10, 2025).
(187)Dundon, C. A.; Suominen, P.; Aristidou, A.; Rush, B. J.; Koivuranta, K.; Hause, B. M.; McMullin, T. W.; Roberg-Perez, K. Yeast cells having disrupted pathway from dihydroxyacetone phosphate to glycerol. Japan Patent JP5443970B2, **2007**. https://patents.google.com/patent/JP5443970B2/ja (accessed April 10, 2025).
(188)Van Strien, C. J. G.; Merlet, R. B. Method for producing lactic acid. Japan Patent JP2024531891A, **2022**. https://patents.google.com/patent/JP2024531891A/en?oq=2024%EF%BC%8D531891 (accessed April 10, 2025).
(189)Olewnik, E.; Czerwiński, W.; Nowaczyk, J.; Sepulchre, M.-O.; Tessier, M.; Salhi, S.; Fradet, A. Synthesis and structural study of copolymers of L-lactic acid and bis(2-hydroxyethyl terephthalate). *Eur. Polym. J.* **2007**, *43* (3), 1009–1019. https://doi.org/10.1016/j.eurpolymj.2006.11.025.
(190)Li, J.; Jiang, Z.-Q.; Wang, Z. B.; Chen, P.; Li, Y.; Zhou, J.; Liu, J.; Wang, Y.-Z.; Gu, Q. Synthesis, crystallization and hydrolysis of aromatic–aliphatic copolyester: Poly(trimethylene terephthalate)-*co*-poly(L-lactic acid). *Polym. Degrad. Stab*. **2011**, *96* (5), 991–999. https://doi.org/10.1016/j.polymdegradstab.2011.01.023.
(191)Wang, B.-T.; Zhang, Y.; Song, P.-A.; Guo, Z.-H.; Cheng, J.; Fang, Z.-P. Biodegradable aliphatic/aromatic copolyesters based on terephthalic acid and poly(L-lactic acid): Synthesis, characterization and hydrolytic degradation. Chin. *J. Polym. Sci*. **2010**, *28* (3), 405–415. https://doi.org/10.1007/s10118-010-9032-y.
(192)Gandini, A.; Lacerda, T. M.; Carvalho, A. J. F.; Trovatti, E. Progress of Polymers from Renewable Resources: Furans, Vegetable Oils, and Polysaccharides. *Chem. Rev*. **2016**, *116*, 1637–1669. https://doi.org/10.1021/acs.chemrev.5b00264.
(193)Sahu, P.; Thorbole, A.; Gupta, R. K. Polyesters Using Bioderived Furandicarboxylic Acid: Recent Advancement and Challenges toward Green PET. *ACS Sustain. Chem. Eng*. **2024**, *12*, 6811−6826. https://doi.org/10.1021/acssuschemeng.4c01123.
(194)Miah, M. R.; Dong, Y.; Wang, J.; Zhu, J. Recent Progress on Sustainable 2,5-Furandicarboxylate-Based Polyesters: Properties and Applications. *ACS Sustain. Chem. Eng*. **2024**, *12* (8), 2927−2961. https://doi.org/10.1021/acssuschemeng.3c06878.
(195)Matos, M.; Sousa, A. F.; Fonseca, A. C.; Freire, C. S. R.; Coelho, J. F. J.; Silvestre, A. J. D. A New Generation of Furanic Copolyesters with Enhanced Degradability: Poly(ethylene 2,5-furandicarboxylate)-*co*-Poly(lactic acid) Copolyesters. *Macromol. Chem. Phys*. **2014**, *215* (22), 2175–2184. https://doi.org/10.1002/macp.201400175.
(196)Wu, H.; Wen, B.; Zhou, H.; Zhou, J.; Yu, Z.; Cui, L.; Huang, T.; Cao, F. Synthesis and degradability of copolyesters of 2, 5-furandicarboxylic acid, lactic acid, and ethylene glycol. *Polym. Degrad. Stab.* **2015**, *121*, 100–104. https://doi.org/10.1016/j.polymdegradstab.2015.08.009.
(197)Hu, H.; Zhang, R.; Shi, L.; Ying, W. Bin; Wang, J.; Zhu, J. Modification of Poly(butylene 2,5-furandicarboxylate) with Lactic Acid for Biodegradable Copolyesters with Good Mechanical and Barrier Properties. *Ind. Eng. Chem. Res.* **2018**, *57* (32), 11020–11030. https://doi.org/10.1021/acs.iecr.8b02169.
(198)Liu, D.; Lin, Y.; Wang, D.; Jin, Y.; Gong, K.; Investigation of morphology and structure of drug-loaded PLA-*b*-PEO-*b*-PLA polymeric micelle: A dissipative particle dynamics simulations study. *J. Biomed. Mater. Res.* **2024**, *112* (5), e35410. https://doi.org/10.1002/jbm.b.35410.

(199)Huang, M. H.; Li, S.; Vert, M. Synthesis and degradation of PLA–PCL–PLA triblock copolymer prepared by successive polymerization of ε-caprolactone and DL-lactide. *Polymer (Guildf)* **2004**, *45* (26), 8675–8681. https://doi.org/10.1016/j.polymer.2004.10.054.
(200)He, M.; Hsu, Y.-I.; Uyama, H. Design of novel poly(L-lactide)-based shape memory multiblock copolymers for biodegradable esophageal stent application, *Appl. Mater. Today* **2024**, *36*, 102057 https://doi.org/10.1016/j.apmt.2024.102057.
(201)Ali, F. B.; Kang, D. J.; Kim, M. P.; Cho, C.-H.; Kim, B. J. Synthesis of biodegradable and flexible, polylactic acid based, thermoplastic polyurethane with high gas barrier properties. *Polym. Int*. **2014**, *63*, 1620–1626. https://doi.org/10.1002/pi.4662.

Chapter 1. Synthesis of High-Toughness Polyesters Using Xylose and Lactic Acid and Analysis of Their Biodegradability

1.1. Introduction

Plastics have become an integral part of our daily lives and are used in numerous products, most of which are primarily made from petroleum resources. Environmental problems caused by the massive use of fossil resources and the mismanagement of plastic disposal are serious issues.[1,2] Since the 1980s, the availability of fossil resources has reached a critical point, forcing a gradual decline in their industrial use.[3] Plastics derived from fossil resources currently account for 20% of global oil consumption and contribute to GHG emissions. In 2018, 33% of plastics were recycled, 25% were landfilled, and the rest were incinerated.[3] The OECD estimated that total GHG emissions associated with fossil-derived plastics were 1.8×10^9 tons of CO_2 equivalent in 2019, which are predicted to increase to 4.3×10^9 tons of CO_2 equivalent by 2060 due to increased plastic use and disposal.[4] Plastics should continue to contribute to a sustainable society while exhibiting minimal impact on the environment. Therefore, environmentally friendly and sustainable alternative bioresources have gained considerable attention. With increasing global demand, bioplastic production is expected to rise to 7.43 Mt by 2028.[5] Most bioplastics currently in circulation are produced from corn, sugarcane, and sugar beets. The raw materials must be replaced with inedible biomass that does not compete with food to increase the scale of bioplastics.[6] The net CO_2 fixation by land plants is approximately 56×10^9 tons/year, and the worldwide biomass production by land plants is approximately $170–200 \times 10^9$ tons/year.[7,8] Of this biomass, nearly 70% is composed of plant cell walls, which are partially used in the forestry, pulp and paper, and fiber industries. Despite their abundance, humans currently utilize only 2% of this resource. Therefore, the remaining lignocellulosic biomass can be used without competing with food resources.[7] Consequently, inedible biomass represents a sustainable carbon source that can substitute for hydrocarbons in the future.[3,8]

PLA is a promising bioplastic; it ultimately biodegrades into H_2O and CO_2 in a composting environment.[9–11] The synthesis of OLA *via* direct polymerization[12,13] and high-molar-mass PLA *via* ring-opening polymerization of lactide[8] have been studied. In addition, the optimization of lactic acid fermentation from paper sludge[14] and lignocellulosic biomass[15] has been recently examined. Oji Holdings Co. is working on the industrialization of PLA from inedible biomass.[16] PLA exhibits excellent formability and shows promise; however, it is brittle and hard, requiring further improvements to expand its scale.[12,17] Copolymers with polyesters such as PCL[17] and PBS[18] are frequently used to confer biodegradability and controllable mechanical properties. Moreover, the introduction of aromatic components, such as terephthalic acid, into polymers enhances not only their mechanical properties but also their thermal properties, such as T_g. PET-*co*-PLA is synthesized through the polycondensation of BHET, which is readily obtained during PET degradation using lactic acid or OLA.[19,20] Other copolymers synthesized are poly(trimethylene terephthalate)-*co*-PLA,[21] PBT-*co*-PLA,[22] and poly(ethylene-*co*-diethylene

terephthalate)-*co*-PLA.[23] In addition, the chemical conversion of sugars has focused on FDCA[24–26] as a cyclic biobased monomer to replace terephthalic acid. The synthesis and degradability of PEF-*co*-PLA and PBF-*co*-PLA have also been reported.[27–29] Copolymers of hydroxyl-terminated PLA and PPeF-OH with chain extensions were evaluated for their potential as packaging films and biodegradation in compost.[2] Avantium NV successfully produced 40 tons/year of FDCA in 2011[30] and plans to start producing another 5 kt/year of FDCA in 2024.[31,32] However, FDCA production currently relies on edible sugars, and synthesis from inedible sugars requires isomerization to fructose and other steps, making the process complex.[30] Recently, diglyoxylate xylose (DGAX) and its corresponding diester, DMGX, can be directly and scalably synthesized from inedible xylose and lignocellulosic biomass. [33] A DMGX-based class of polyesters, called PAX, has been synthesized and is currently under vigorous development.[33,34] Therefore, not only xylose but also lactic acid can be obtained from inedible raw materials, and the development of copolymerized PAX and PLA materials would be beneficial in this regard.

In this study, PAX-*co*-PLA was synthesized *via* polycondensation using xylose-based PAX and L-lactic acid–based OLA, which can be prepared from sustainable wood resources (**Scheme 1**). The influence of copolymerization was assessed using tensile tests and differential scanning calorimetry (DSC), and the results were compared with those of neat PHX and PLA. Changing the copolymerization composition improved the toughness and T_g. In addition to significant degradation during composting, biochemical oxygen demand (BOD) tests using seawater from Tokyo Bay revealed that PHX and PHX-*co*-PLA were partially biodegradable. Therefore, the development of biodegradable and robust bioplastics from inedible sugars is a crucial strategy.

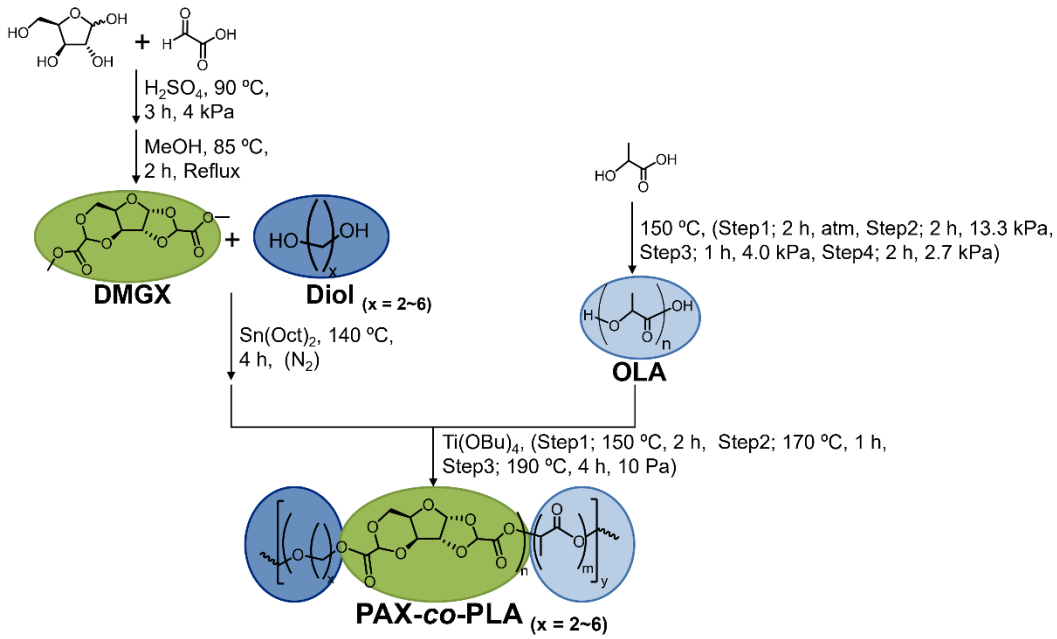

Scheme 1. Synthesis of PAX-*co*-PLA by transesterification and polycondensation reactions.

1.2. Experimental Section

1.2.1. Materials

D-(+)-Xylose was purchased from Sigma-Aldrich Chemical Co. (St. Louis, MO, USA), and chloroform was purchased from Nacalai Tesque Inc. (Kyoto, Japan). Tin (II) 2-ethylhexanoate ($Sn(Oct)_2$), L-lactic acid, glyoxylic acid monohydrate, methanol, diethyl ether, ethylene glycol, 1,3-propanediol, 1,4-butanediol, 1,5-pentanediol, sea sand (425–850 μm), and ammonium chloride were purchased from Fujifilm Wako Pure Chemical Co. (Osaka, Japan). L-lactic acid, L-lactide, 1,6-hexanediol, titanium (IV) tetrabutoxide ($Ti(OBu)_4$), triphenyl phosphite, and potassium dihydrogen phosphate were purchased from Tokyo Chemical Industry (Tokyo, Japan). PLA (Ingeo biopolymer 2003D) [number-average molar mass (M_n) = 92,000 g/mol by size exclusion chromatography (SEC)] was purchased from NatureWorks LLC (Nebraska, USA). All reagents were used as received.

1.2.2. Synthesis of OLA

To synthesize OLA, L-lactic acid (100 g) was placed in a 200-mL three-neck flask and dehydrated at 150°C under atmospheric pressure for 2 h. Subsequently, the reaction system was decompressed to 13.3 kPa for 2 h, then to 4.0 kPa for an additional 1 h, and finally to 2.7 kPa for 2 h.[35] The final product was dissolved in a small amount of chloroform and poured into an excess amount of cold diethyl ether. The precipitate was filtered, washed with diethyl ether, and vacuum-dried to produce a white powder.

1.2.3. Synthesis of DMGX

To obtain DMGX, with reference to previous studies,[33] xylose (100 g) and excess glyoxylic acid monohydrate were melt-heated in the presence of sulfuric acid at a constant temperature of 90°C and low pressure for 3 h and stirred using a mechanical stirrer. Subsequently, the reaction solution was refluxed with methanol at 85°C for 2 h and neutralized with sodium bicarbonate to pH 4–5. The resulting salts were filtered, and the filtrate was concentrated under vacuum and then dissolved in chloroform. The chloroform layer was washed three times with deionized water using a separatory funnel to remove water-soluble impurities and then concentrated. The concentrate was heated to 180°C under low pressure. The distillate containing the previously obtained methyl glyoxylate and residual solvent was discarded. A second fraction of the DMGX product was recovered by maintaining the temperature at 180°C. The product was again dissolved in chloroform, decolorized with activated carbon, filtered, and dried. DMGX was obtained as yellow oil.

1.2.4. Synthesis of PHX, PHX-*co*-PLA, and PAX-*co*-PLA

To synthesize PHX, DMGX (6 g, 1.0 eq.), 1,6-hexanediol (2.93 g, 1.2 eq.), triphenyl phosphite (0.17 mol%), and $Sn(Oct)_2$ (0.008 mol%) were placed in a 100-mL three-neck flask, vacuum-dried at 25°C for 3 h, and then esterified at 140°C for 4 h. The reaction mixture was first cooled to 120°C to avoid bumping

during vacuuming. Subsequently, the reaction mixture was slowly depressurized to 10 Pa to accelerate the polycondensation reaction while distilling away the diol reaction byproducts. The reaction system was heated to 150°C for 2 h, then to 170°C for an additional 1 h, and finally to 190°C for 4 h. The final product was dissolved in a small volume of chloroform and poured into an excess amount of methanol. The precipitate was filtered, washed with methanol, and vacuum-dried to produce the purified product. In the case of the synthesis of (1) PHX-*co*-PLA, this process was performed *via* two-step condensation. First, OLA was obtained by condensing lactic acid, as described in Section 1.2.2. In another flask, DMGX (6 g, 1.0 eq.) and 1,6-hexanediol (4.89 g, 2.0 eq.) were esterified at 140°C for 4 h. Second, OLA and $Ti(OBu)_4$ (0.05 wt%) were added to the flask and dried at 25°C for 2 h to initiate polycondensation. The weight of the added OLA varied according to the ratio of DMGX to OLA. The polycondensation step was performed *via* stepwise heating, similar to the case of PHX. The final product was dissolved in a small amount of chloroform and poured into an excess amount of methanol. The precipitate was filtered, washed with methanol, and vacuum-dried to produce the purified product. The synthesis of PAX-*c*o-PLA followed the same procedure as the previously adjusted polycondensation of PHX-*co*-PLA, including the reaction method, except that the aliphatic diol used was changed. In particular, instead of 1,6-hexanediol, ethylene glycol was used for poly(ethylene xylosediglyoxylate) (PEX)-*co*-PLA, 1,3-propanediol for poly(propylene xylosediglyoxylate) (PPX)-*co*-PLA, 1,4-butanediol for poly(butylene xylosediglyoxylate) (PBX)-*co*-PLA, and 1,5-pentanediol for poly(pentylene xylosediglyoxylate) (PPTX)-*co*-PLA.

1.2.5. Synthesis of the PLA–PHX–PLA by Ring-Opening Polymerization of Lactide

Ring-opening polymerization of lactide was used to synthesize (2) PLA–PHX–PLA. A PHX prepolymer (6 g, M_n = 11,900 g/mol, polydispersity (D) = 1.76) prepared as in the polycondensation procedure described in Section 1.2.4 was used as macroinitiator, except that the amount of 1,6-hexanediol was changed from 1.2 to 2 equivalents. The polycondensation of the PHX prepolymer required 7 h, and the ring-opening polymerization of lactide was performed for 5 h. The PHX prepolymer and L-lactide (3 g) were placed in a 50-mL three-neck flask and vacuum-dried for 3 h at 25°C. A toluene solution of tin (II) 2-ethylhexanoate (1 mol% of the hydroxyl end of the PHX prepolymer) was added to the mixture, which was subsequently vacuum-dried at 25°C for 2 h. Ring-opening polymerization was performed at 150°C for 5 h with stirring (150 rpm) in a nitrogen atmosphere.

1.2.6. Fabrication of Films

To examine the mechanical properties of the prepared polymer samples by tensile tests, polymer samples were heated and compressed using a manual hydraulic heating press (IMC-180C, Imoto Mfg. Co., Ltd., Kyoto, Japan) to produce a film. The sample (5 g) dried under reduced pressure for at least 12 h was sandwiched between aluminum plates set with 0.5 mm spacers. The press was heated at a temperature exceeding 160°C for 5 min. The sample was melted and held at 20 MPa for 10 min to produce a 70.0 × 70.0 × 0.5 mm^3 film. The sample (3 g) was sandwiched between aluminum plates set with 0.1 mm spacers

to investigate its degradability. The press was heated at a temperature exceeding 160°C for 5 min. The sample was melted and held at 20 MPa for 10 min to produce a 70.0 × 70.0 × 0.1 mm^3 film.

1.2.7. Measurements

The molecular structure of the sample (10 mg) was analyzed by proton nuclear magnetic resonance (^{1}H NMR) spectroscopy using chloroform-d (1 mL) as the solvent with JNM-ECS400 (400 MHz) (JEOL Ltd., Tokyo, Japan). The molar masses of the products were determined using SEC (HLC-8420GPC EcoSEC-Elite, Tosoh Co., Yamaguchi, Japan) with a refractive-index detector and TSKgel GMH_{HR} column (Tosoh Co., Yamaguchi, Japan). The SEC test was performed at a flow rate of 1.0 mL/min at 40°C using chloroform as the eluent solvent, and molar masses were calibrated using polystyrene standards (M_n = 1.31 × 10^3 − 3.64 × 10^6 g/mol). The mechanical properties of the prepared sample were determined *via* tensile tests using an Auto Graph Table-TOP universal testing machine (AGS-X, Shimazu Co., Kyoto, Japan) at a cross-head speed of 10 mm/min. Five tensile tests were performed, and the median and pre-/post-values were selected for analysis. T_g of the sample was measured *via* DSC with a thermal analysis system using NEXTA DSC200 (Hitachi High-Tech Science Co., Tokyo, Japan). The sample (approximately 6 mg) was heated from −80°C to 200°C at a heating rate of 10°C/min and then kept at 200°C for 3 min to melt. After heating, the sample was cooled from 200°C to −80°C at a cooling rate of 10°C/min. The temperature was maintained at −80°C for 3 min. Subsequently, the sample was heated again from −80°C to 200°C at a heating rate of 10°C/min. The DSC measurements were performed in a nitrogen atmosphere at a flow rate of 50 mL/min. DSC curves for the first cooling and second heating were obtained from −60°C to 190°C. The thermal degradation temperature (T_d) of the sample was measured via thermogravimetric analysis (TGA) with a thermal analysis system using NEXTA STA200RV (Hitachi High-Tech Science Co., Tokyo, Japan). The samples (approximately 5 mg) were placed in a Pt pan and heated from 50°C to 530°C under a nitrogen atmosphere at a heating rate of 10°C/min. The surface morphology of the resultant samples was observed using scanning electron microscopy (SEM) with SU3500 (Hitachi High-Technologies Co., Tokyo, Japan).

1.2.8. Disintegration Test of Films with Compost

In the disintegration test of films with compost and subsequent experiments, PHX-*co*-PLA, which exhibited the highest toughness among the PAX-*co*-PLA series, was used for evaluation. Films buried in the compost YK-12 from Yawata Bussan Co. were placed in a constant-temperature and -humidity chamber KCL-2000A (EYELA Co., Ltd., Tokyo, Japan) and evaluated visually and by measuring the weight change. Following Japanese Industrial Standard (JIS) K6953-2, after adding dried sea sand (320 g) to the compost (dry mass of 60 g), the moisture content was adjusted to approximately 58% and left for 30 days at a test temperature of 58°C and constant humidity. Square films 2 cm in size were used in the test. The films were sandwiched between a larger nylon mesh (mesh size of 125) and crimped with Polysealer P-200 (Fuji Impulse Co., Ltd., Osaka, Japan) to prevent scattering.

1.2.9. Biodegradation and Disintegration Tests of Films in Seawater

The biodegradability of the films in seawater was evaluated according to ASTMD6691-17 using RESPIROMETRIC Sensor System 6 for Plastic Biodegradability (VELP Scientifica Srl, Usmate, Italy).[36] The seawater used in the BOD test was collected on the morning of January 18, 2024, from Odaiba, Tokyo Bay, on a clear day and filtered through a 77-μm mesh filter. The conditions were adjusted by adding inorganic salts to achieve concentrations of 0.5 g/L ammonium chloride and 0.1 g/L potassium dihydrogen phosphate. Biodegradation tests were conducted under aerobic conditions at 30°C for 1 month. Film samples (approximately 0.5 cm square) were placed in 250 mL of test seawater and stirred at 180 rpm. As a blank, a BOD test was performed with no sample added and the same seawater. The biodegradability of each film was calculated as follows:

$$\text{Biodegradability (\%)} = \frac{\text{BOD (mg/L) of the sample} - \text{BOD (mg/L) of the blank}}{\text{Theoretical oxygen demand of sample (mg/L)}} \times 100. \quad (1)$$

For the disintegration test in seawater, seawater was collected from Odaiba, Tokyo Bay, on the morning of March 14, 2024, and adjusted in the same way as mentioned above. Square films of size 2 cm and 250 mL of the adjusted seawater were placed in a 500 mL bottle and shaken at 30°C and 150 rpm for 3 months using a shaking incubator Bio-Shaker BR-3000 L (Taitec Co., Saitama, Japan). The collected samples were assessed in terms of weight change and visual inspection. As an approximation, the theoretical oxygen demand (ThOD) of PHX-*co*-PLA was calculated considering the integration ratio of ^{1}H NMR ($ThOD^{PLA}$ (mg/mg) = 1.333, $ThOD^{PHX}$ (mg/mg) = 1.423, $ThOD^{PHX\text{-}co\text{-}PLA}$ (mg/mg) = 1.401).

Monomers such as lactic acid and DGAX in the degradation products of seawater were analyzed using a Shimadzu Prominence HPLC system (Shimadzu Co., Kyoto, Japan). This system is equipped with an LC-20AB HPLC pump, a CTO-20AC HPLC column oven, and a refractive-index detector (RID-20A). Samples were desalted using Amberlite™ MB-4 resin (Organo Co., Tokyo, Japan) before injection. Chromatographic separation was performed on a Bio-Rad Aminex HPX-87H column (300 × 7.8 mm) with a Micro-Guard Cation H Refill Cartridges (30 × 4.6 mm) (Bio-Rad Laboratories, CA, USA). The mobile phase consisted of 5 mM H_2SO_4 prepared by diluting H_2SO_4 (Sigma-Aldrich Chemical Co., St. Louis, MO, USA) in MilliQ water. The measurement time was set to 30 min, with a flow rate of 0.6 mL/min, an injection volume of 20 μL, and a column temperature of 60°C.

1.2.10. Evaluation of Water Resistance of Films

Water uptake ratio tests were conducted in fresh water. Dried film specimens (approximately 2 cm square) were immersed in water. After a certain time (10 min, 60 min, 120 min, 240min, 480 min [0.33 days], 1440 min [1 day], 2880 min [2 days], 7200 min [5 days], 14400min [10 days] and 21600 min [15

days]), the swollen samples were gently removed with tweezers, excess water was removed using tissue paper, and the samples were weighed. The water uptake ratio was calculated as follows:

$$\text{Water uptake ratio (\%)} = \frac{W_{ss} - W_{ds}}{W_{ds}} \times 100, \qquad (2)$$

where W_{ds} and W_{ss} are the weights of the dried and swollen samples, respectively.

Hydrolysis tests were performed in distilled water. The evaluation temperature was set to 30°C, the same as that used for seawater tests. Before hydrolysis, all samples were dried under low pressure and weighed to obtain the initial mass (m_0). Subsequently, the samples were immersed in fresh water and shaken. Periodically, the samples were removed, the surface water was wiped off, and the samples were weighed (m_t). The mass retention was calculated as follows:

$$\text{Mass retention (\%)} = \frac{m_t}{m_0} \times 100. \qquad (3)$$

After obtaining weight measurements, the samples were dried under low pressure, and their molar mass was determined using SEC. To evaluate the water durability of the samples, a water contact angle (WCA) test was performed. In the WCA test, the film's hydrophobicity was evaluated contact angle measurements of water droplets deposited on the film surface using the Drop Master DM300 goniometer (Kyowa Interface Science Co. Ltd., Saitama, Japan), equipped with a charge-coupled device camera. The acquired images were analyzed using FAMAS software version 2.3.1 (Kyowa Interface Science Co., Ltd., Saitama, Japan).

1.2.11. Amplicon Sequencing Analysis of Seawater

Total deoxyribonucleic acid (DNA) was extracted from seawater samples that had been tested for 3 months using ISOIL for Beads Beating kit (Nippon Gene Co., Toyama, Japan) and DNeasy PowerClean Pro Cleanup kit (Qiagen Inc., Hilden, Germany). The bacterial and archaeal 16S ribosomal (r) DNA (V3-V4 region) was amplified using a dual-index Pro341F/Pro805R.[37,38] Barcoded amplicons were paired-end sequenced on a 2 × 301-bp cycle using a MiSeq system with a MiSeq Reagent Kit version 3 (600 cycles) chemistry (Illumina Inc., San Diego, CA, USA). The primer sequences on paired-end sequencing reads were trimmed using Cutadapt version 1.18 with default settings.[39] Paired-end sequencing reads were merged using the fastq-join program with default settings.[40] Only joined reads with quality value scores ≥20 for more than 99% of the sequence were extracted using FASTX-Toolkit.[41] The chimeric sequences were deleted using usearch61.[42,43] For the taxonomy of the bacterial and archaeal 16S rDNA (V3-V4 region), the Ribosomal Database Project (RDP) Classifier version 2.13 and TechnoSuruga Lab Microbial Identification database version 16.0 DB-BA (TechnoSuruga Laboratory, Shizuoka, Japan) were used.[44,45] Identification with confidence ≥0.8 and homology ≥97% for the RDP Classifier and DB-BA database,

respectively, was performed using Metagenome@KIN version 2.2.1 analysis software (World Fusion, Tokyo, Japan).

1.3. Results and Discussion

1.3.1. Synthesis of DMGX, PHX, OLA, and PHX-*co*-PLA

The molecular structure of DMGX synthesized in Section 1.2.4 was confirmed by ^{1}H NMR (**Figure 1a**). This spectrum was obtained in DMSO solvent for comparison with the ^{1}H NMR attribution reported in a previous study[33]. The theoretical yield of DMGX from xylose was 30%. The molecular structure of

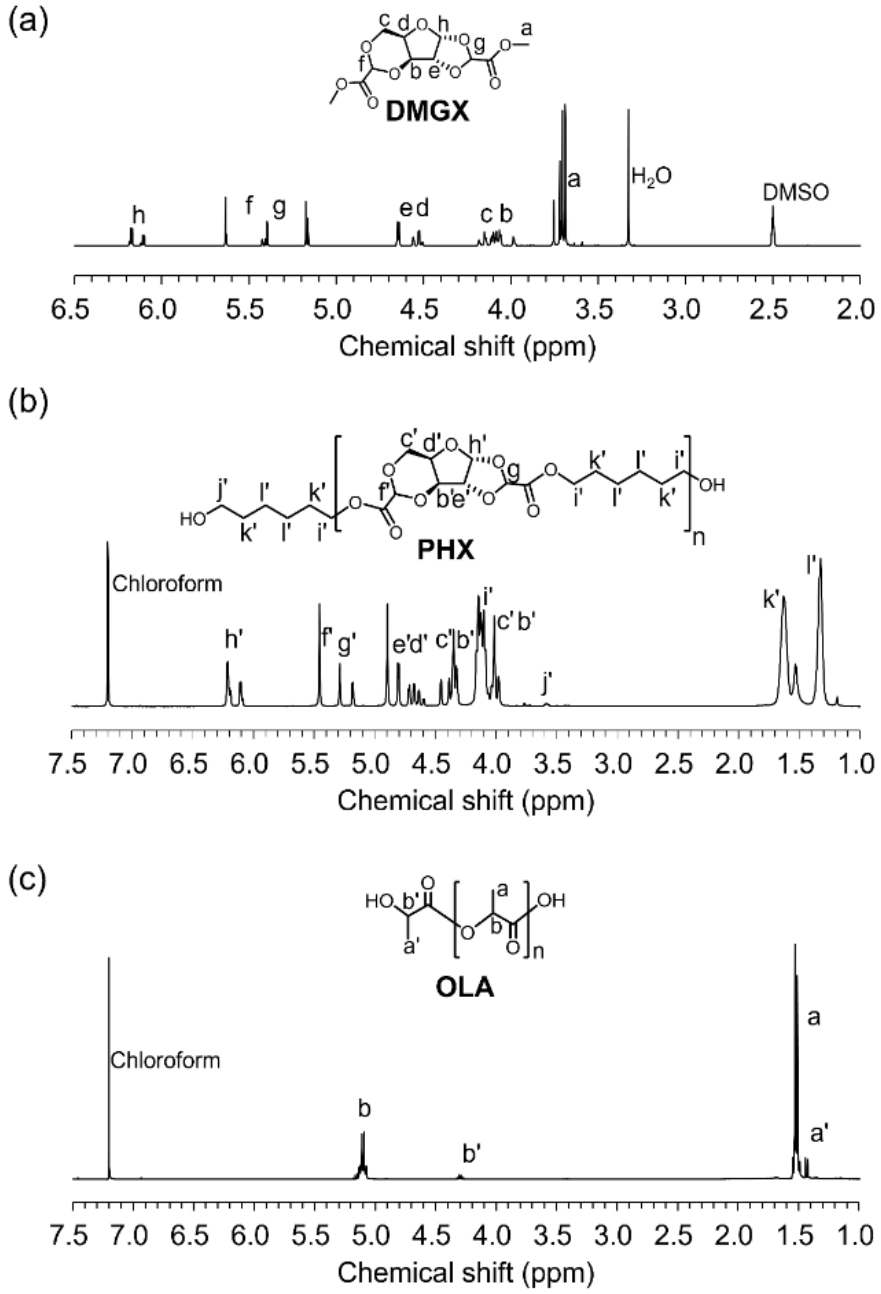

Figure 1. ^{1}H NMR spectra of (a) DMGX, (b) PHX, and (c) OLA.

PHX synthesized in Section 1.2.4 was confirmed by ^{1}H NMR **(Figure 1b**) and compared with the attribution of PHX in the previous study.[33] M_n of PHX calculated from the ratio of the integration value of the signal (h') attributed to the repeating unit to the integration value of the signal at the end (j') by ^{1}H NMR was 22,000 g/mol. The yield of PHX was 44%, and the molar mass and D were determined using SEC (**Table 1**). M_n was 19,200 g/mol, M_w was 88,800 g/mol, and D was 4.63. The molecular structure of the synthesized OLA was confirmed by ^{1}H NMR (**Figure 1c**). M_n of OLA calculated from the ratio of the integration value at (b) due to the lactate repeating units to the integration value at (b') at the lactate terminal by ^{1}H NMR was 800 g/mol. The yield of OLA from lactic acid was 22%, and the molar mass and D were determined by SEC using chloroform as the mobile phase. M_n, M_w, and D were 800 g/mol, 1,400 g/mol, and 1.75, respectively.

Subsequently, we planned to copolymerize PHX and PLA and attempted to make two different copolymers: (1) a classical copolymer PHX-*co*-PLA synthesized by the method described in Section 1.2.5 and (2) a triblock copolymer PLA–PHX–PLA synthesized by the method described in Section 1.2.6. This study described (1) PHX-*co*-PLA using two-step polycondensation with OLA. **Figure 2a** was obtained from ^{1}H NMR of PHX-*co*-PLA in deuterated chloroform solvent. Both PHX and PHX-*co*-PLA exhibited complex peak shifts due to DMGX isomers; however, previous studies have confirmed that the structure of PHX was maintained.[33] Signals derived from 1,6-hexanediol were assigned to o (CH_2, δ = 1.3 ppm), k (CH_2, δ = 1.6 ppm), and i (CH_2, δ = 4.1 ppm). Signals derived from the xylose structure were assigned to b (CH, δ = 4.0 and 4.3–4.4 ppm), c (CH_2, δ = 4.0 and 4.3–4.4 ppm), d (CH, δ = 4.5 and 4.6–4.7 ppm), e (CH, δ = 4.6–4.7 and 4.8 ppm), and h (CH, δ = 6.1–6.3 ppm). Signals derived from glyoxylate were assigned f (CH, δ = 5.3 and 5.5 ppm) and g (CH, δ = 4.9 and 5.2 ppm).

Figure 2c shows the possible structures of the five different segments of PHX-*co*-PLA. In the previously reported PEF-*co*-PLA and PBF-*co*-PLA, conjugative effects from the furan ring structure influenced the signals of adjacent units.[27,29] However, because the five-membered ring structure of xylose had no clear conjugation effect, the strong signals for i overlapped, but the signals derived from lactate were slightly different for p1 and p2 (CH, δ = 5.0–5.2 ppm) and q1 and q2 (CH_3, δ = 1.5–1.6 ppm) (**Figure 2b**). Similar to a previous study,[29] there was little signal for the LA–hexanediol–LA segment, which we did not discuss. The number fractions of the DMGX–hexanediol–DMGX, LA–hexanediol–DMGX, LA–LA, and DMGX–LA segments were determined by the integration value (I) of the ^{1}H NMR peaks and were proportional to $I_{i1}/4$, $I_{i4}/2$, I_{p1}, and I_{p2}, respectively. I_{i3} and I_{i2} were calculated using equations (4)–(5) due to peak overlap:

$$I_{i3} = I_o - (I_{i1} + I_{i2}), \quad (4)$$

$$I_{i3} = I_{i2}. \quad (5)$$

The number-average sequence length (Y_{PLA}, Y_{PHX}) and the degree of randomness (R) were calculated with reference to previous studies[19,29,46] as follows:

$$Y_{\mathrm{PLA}} = \frac{1}{2}\left(\frac{I_{\mathrm{p1}} + \frac{I_{\mathrm{i3}}}{2}}{\frac{I_{\mathrm{i3}}}{2}} + \frac{I_{\mathrm{p1}} + I_{\mathrm{p2}}}{I_{\mathrm{p2}}}\right), \quad (6)$$

$$Y_{\mathrm{PHX}} = \frac{1}{2}\left(\frac{\frac{I_{\mathrm{i1}}}{4} + \frac{I_{\mathrm{i3}}}{2}}{\frac{I_{\mathrm{i3}}}{2}} + \frac{I_{\mathrm{h}}}{I_{\mathrm{p2}}}\right), \quad (7)$$

$$R = \frac{1}{Y_{\mathrm{PLA}}} + \frac{1}{Y_{\mathrm{PHX}}}. \quad (8)$$

Y_{PHX} decreased as the LA unit increased. However, Y_{PLA}, which indicates the probability of finding another LA unit next to the LA unit, increased from 1.34 to 1.53. R decreased as LA units increased; nevertheless, all copolymers exhibited the characteristics of block copolymers ($R < 1$). **Table 1** shows the synthesis results for PHX-*co*-PLA obtained with different OLA preparation ratios, including the ratio of integration values of xylose to lactate units ($I_{\mathrm{h}}/(I_{\mathrm{p1}} + I_{\mathrm{p2}})$) obtained from ^{1}H NMR, as shown in **Figure 2b**. Details of the integration values of typical xylose and lactate units are presented in **Table 2**. As in the PHX synthesis, the copolymer synthesis by $Sn(Oct)_2$ was also possible. However, the combination of $Sn(Oct)_2$ and $Ti(OBu)_4$ slightly promoted polymerization. Polymerization proceeded effectively when 10% OLA was added. As the amount of added OLA increased, the number of lactate units introduced into the polymer increased, and SEC confirmed the formation of copolymers. However, excess OLA reduces the molar mass and may inhibit polymerization (**Table 1**). Reports on increased OLA content are limited in the literature, and some studies have indicated that high OLA content does not result in high molar mass.[27,28] Furthermore,

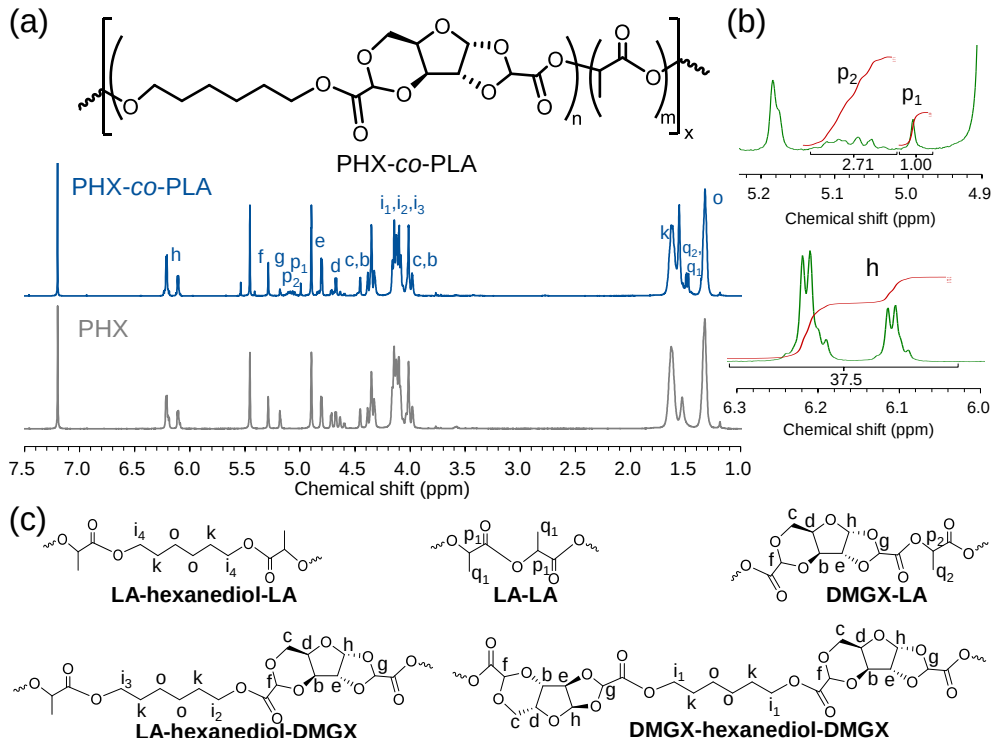

Figure 2. (a) ^{1}H NMR spectra of PHX-*co*-PLA contrasted with PHX and (b) enlarged ^{1}H NMR spectra of PHX-*co*-PLA. Details of the integration values of typical lactate and xylose units are shown in **Table 2**. (c) Segment of PHX-*co*-PLA.

similar results have been reported for copolymerization with PET and other polymers, indicating that the introduction of an appropriate amount of OLA can effectively increase the molar mass.[19,20,22]

Table 1. Synthesis of PHX and PHX-*co*-PLA.

Sample	Catalyst	Composition (wt%)[a]	Xylose/lactate[b]	Y_{PLA}[c]	Y_{PHX}[c]	R[c]	M_n (g/mol)[d]	D[d]	Yields (%)
PHX	$Sn(Oct)_2$	100/-	100/-	-	-	-	19200	4.63	44
PHX	$Sn(Oct)_2/Ti(OBu)_4$	100/-	100/-	-	-	-	26000	4.48	70
PHX-*co*-PLA	$Sn(Oct)_2/Ti(OBu)_4$	95/5	94.5/5.5	1.34	21.2	0.80	41200	3.23	56
PHX-*co*-PLA	$Sn(Oct)_2/Ti(OBu)_4$	90/10	91.0/9.0	1.34	15.8	0.81	30600	5.77	59
PHX-*co*-PLA	$Sn(Oct)_2/Ti(OBu)_4$	80/20	84.8/15.2	1.46	10.0	0.79	16700	2.56	70
PHX-*co*-PLA	$Sn(Oct)_2/Ti(OBu)_4$	60/40	77.3/22.7	1.53	7.3	0.79	20600	2.73	67

[a]Initial DMGX/OLLA mass ratio.
[b]Final molar ratio determined from the ^{1}H NMR spectra ($I_h/(I_{p1} + I_{p2})$).
[c]Calculated from the ^{1}H NMR spectra.
[d]Determined by SEC (in chloroform).

Table 2. Integration and calculated values of typical lactate and xylose units by ^{1}H NMR.

Sample	Composition (wt%)	Typical lactate units				Typical xylose unit	
		δ (ppm)	Integration value (I_{p1})	δ (ppm)	Integration value (I_{p2})	δ (ppm)	Integration value (I_h)
PHX-*co*-PLA	95/5	5.0	1.00	5.1	2.70	6.1–6.3	63.4
PHX-*co*-PLA	90/10	5.0	1.00	5.1	2.71	6.1–6.3	37.5
PHX-*co*-PLA	80/20	5.0	1.00	5.1	2.81	6.1–6.3	21.3
PHX-*co*-PLA	60/40	5.0	1.00	5.1	3.06	6.1–6.3	13.8

1.3.2. Ring-Opening Polymerization of Lactide Using PHX as a Macroinitiator

Of the two copolymers, we adopted (1) PHX-*co*-PLA by polycondensation as described in Section 1.3.1 and abandoned the route of (2) PLA–PHX–PLA. For a detailed description of the synthesis process of PLA–PHX–PLA, please refer to Section 1.2.5. In this section, we discuss the ring-opening polymerization of lactide using the PHX prepolymer as a macroinitiator, which serves as a reason for abandoning PLA–PHX–PLA. Before ring-opening polymerization, the functional groups at the terminal

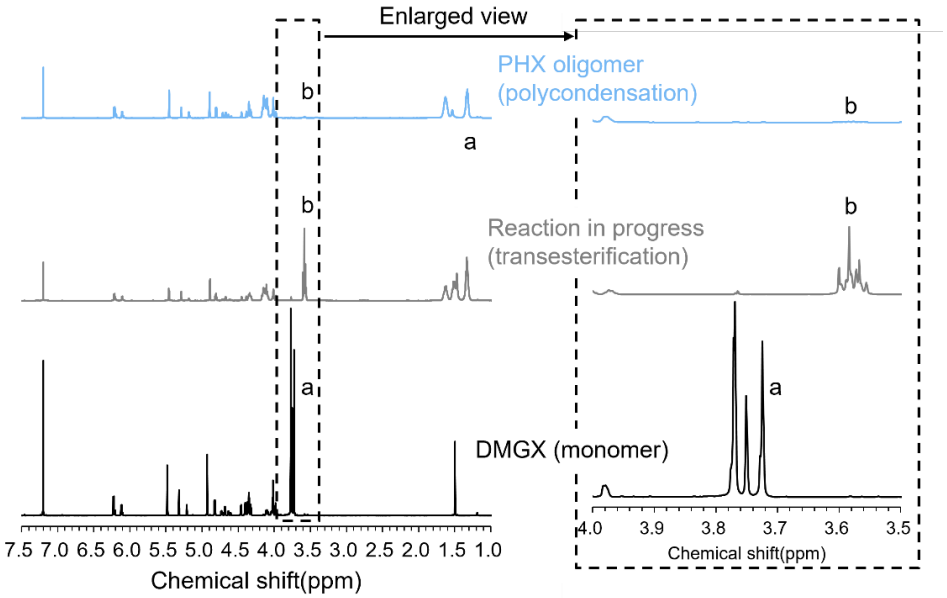

Figure 3. Changes in ^{1}H NMR spectra of DMGX and PHX terminals.

ends of PHX were confirmed by ^{1}H NMR. In **Figure 3,** the CH_3 signal (a) is observed at approximately 3.7 ppm in DMGX. However, after transesterification, the signal (a) disappears, and the terminal CH_2 signal (b) derived from 1,6-hexanediol appears at approximately 3.6 ppm. After the polycondensation reaction, signal (b) was confirmed, indicating that the terminal end of the molecule was hydroxylated. For the ring-opening polymerization of lactide, samples were taken at every reaction time up to 5 h and evaluated by ^{1}H NMR. In **Figure 4**, the lactide-derived signal (c) at approximately 5.0 ppm decreased as the reaction proceeded, whereas the PLA-derived signal (a) at approximately 5.1 ppm increased. The lactide conversion (%) calculated from the ratio of the integration values of signals (c) and (a) reached 90% (**Figure 4**). However, the molar mass of PLA determined from the ratio of the integration value of (a) attributed to the lactate repeating units to the integration value of (a') at the lactate terminal was M_n = 1,260 g/mol at 5 h of reaction, which was lower than the theoretical molar mass of PLA (M_n = 6,000 g/mol) (**Table 3**, **Figure 4**). Additionally, the molar mass of the entire copolymer by SEC decreased to approximately half of the initial molar mass as the reaction proceeded, contrary to the lactide conversion. The molar mass was presumed to result from side reactions (**Table 3**, **Figure 4**). In the synthesis of PET-*co*-PLA, the ring-opening polymerization of lactide led to immediate thermal degradation during the reaction and could only be synthesized through polycondensation.[19] The phenomenon observed in this study, specifically the decrease in molar mass, is also assumed to result from thermal decomposition during ring-opening polymerization. As no improvement in molar mass was expected, we abandoned (2) PLA–PHX–PLA and adopted (1) PHX-*co*-PLA *via* polycondensation and expanded to evaluate PHX-*co*-PLA and synthesize PAX-*co*-PLA using other diols.

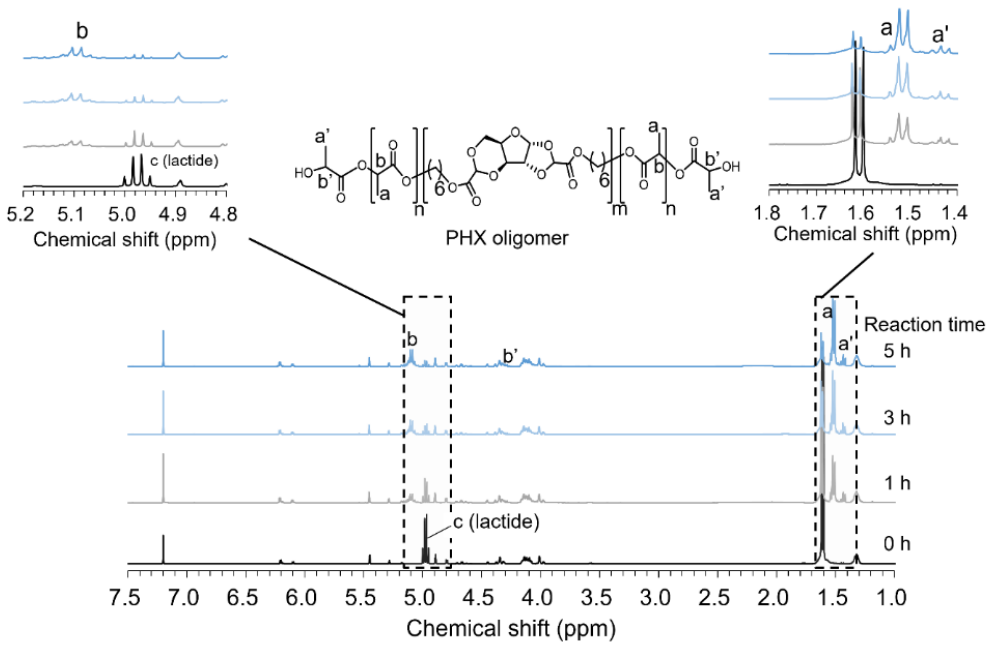

Figure 4. ^{1}H NMR spectra of PLA–PHX–PLA. Changes in the ring-opening polymerization reaction of lactide using PHX as a macroinitiator up to 5 h.

Table 3. Synthesis of triblock copolymer PLA–PHX–PLA.

Sample	Reaction time (h)[a]	Lactide conversion (%)[b]	M_n^{PLA} (Theo.)[c]	M_n^{PLA} (g/mol)[b]	M_n (g/mol)[d]	D[d]
PLA–PHX–PLA	0	0	-	0	11,900	1.76
PLA–PHX–PLA	1	44.8	-	800	10,000	1.78
PLA–PHX–PLA	3	79.3	-	1,200	7,400	1.89
PLA–PHX–PLA	5	89.7	6,000	1,260	5,500	2.09

[a]Reaction time for ring-opening polymerization of lactide with PHX as macroinitiator.
[b]Calculated from the ^{1}H NMR spectra (**Figure 4**).
[c]Theoretical molar mass of PLA synthesized by ring-opening polymerization.
[d]Determined by SEC (in chloroform).

1.3.3. Thermophysical Properties of Polymers

Figure 5 shows the DSC charts of the copolymers obtained *via* polycondensation with OLA, and **Table 4** presents a summary of the thermal analysis results, including TGA results. The DSC charts of the copolymers obtained by varying the feed ratio of OLA to DMGX, from 5% to 40%, exhibit no observable melting temperature (T_m), similar to the case of neat PHX, confirming that the polymers are amorphous. The DSC charts of the copolymers obtained by varying the feed ratio of OLA to DMGX from 5% to 40%

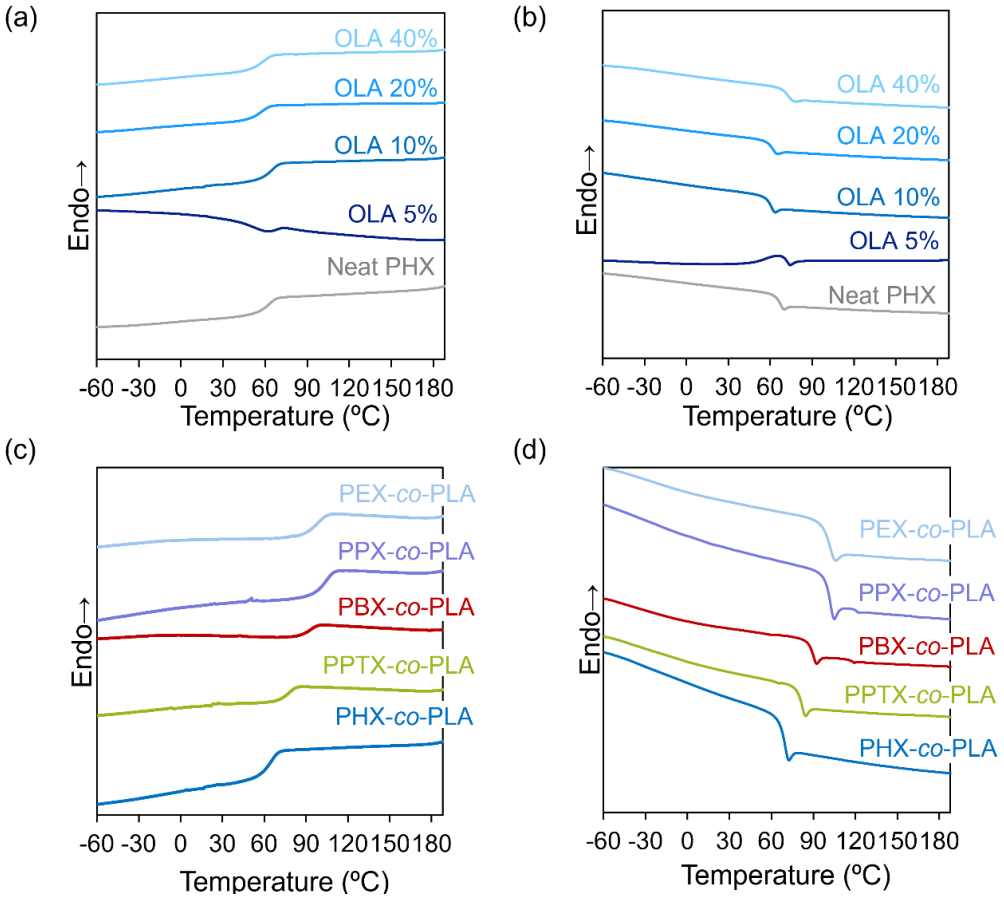

Figure 5. Thermal parameters of polymers. DSC (a) first cooling and (b) second heating curves of neat PHX and PHX-*co*-PLA with OLA feed ratios of 5, 10, 20, and 40%. DSC (c) first cooling and (d) second heating curves of PEX-*co*-PLA using ethylene glycol, PPX-*co*-PLA using 1,3-propanediol, PBX-*co*-PLA using 1,4-butanediol, PPTX-*co*-PLA using 1,5-pentanediol, and PHX-*co*-PLA using 1,6-hexanediol.

show the complete disappearance of the melting temperature (T_m), similar to the case of neat PHX, confirming that the polymer is amorphous. In **Figure 5a**, T_g of neat PHX is 71 °C; however, it tends to decrease with increasing OLA addition: at 5%, T_g = 71 °C; at 10%, T_g = 70 °C; at 20%, T_g = 64 °C; and at 40%, T_g = 63 °C. Similarly, **Figure 5b** shows a decrease in T_g with the introduction of OLA, indicating that PHX-*co*-PLA exhibits higher heat resistance than neat PLA. As shown in **Table 1**, a reduction in T_g is expected due to the plasticizing effect of OLA and the difficulty in achieving higher molar masses as the feed ratio of OLA increases. The TGA results in **Table 4** reveal that T_d of neat PHX is 386 °C, indicating that the addition of OLA lowers T_d by 1 °C–2 °C. Nevertheless, this value is higher than T_d of PLA (367 °C), indicating that the thermostable structure based on PHX is maintained.

Subsequently, the feed ratio of OLA was fixed at 10%, and the diols were changed to ethylene glycol, 1,3-propanediol, 1,4-butanediol, 1,5-pentanediol, and 1,6-hexanediol for polycondensation. For a detailed description of the synthesis process of PAX-*co*-PLA using various diols, please refer to Section 1.2.4. The ^{1}H NMR results of the obtained copolymers are summarized in **Figure 6,** and the synthesis results and thermal analysis results of the various copolymers, including TGA results, are summarized in **Table 5**. The DSC charts are presented in **Figure 3c** and **3d**, where T_m of all copolymers disappear, indicating that the polymers are amorphous. PEX-*co*-PLA, PPX-*co*-PLA, PBX-*co*-PLA, and PPTX-*co*-PLA exhibited T_g of 106°C, 109°C, 98°C, and 83°C, respectively, all higher than those of PHX-*co*-PLA and PLA. The use of shorter diols is assumed to have reduced the degrees of freedom between the polymer chains, resulting in stronger intermolecular interactions and higher T_g. This observation is consistent with those of previous

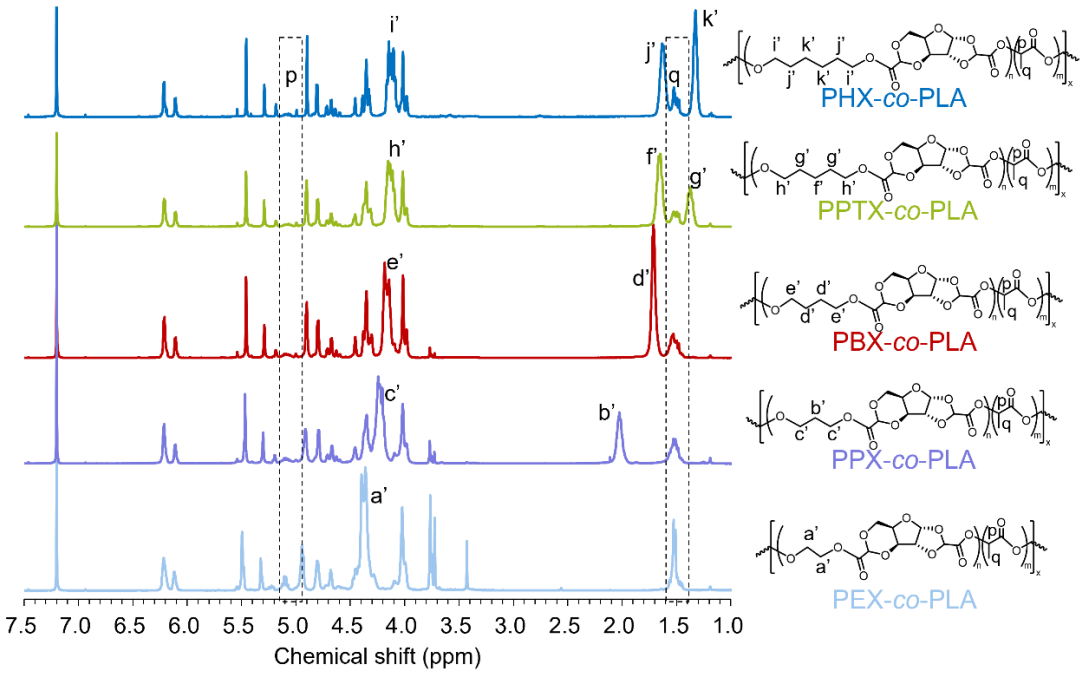

Figure 6. ^{1}H NMR results of the obtained PAX-*co*-PLA using various diols, such as ethylene glycol (light blue), 1,3-propanediol (purple), 1,4-butanediol (red), 1,5-pentanediol (light green), and 1,6-hexanediol (blue).

studies.[33] With the use of ethylene glycol or 1,3-propanediol, increasing the molar mass becomes difficult. In the case of ethylene glycol, T_g of neat PEX is 137°C. In contrast, PEX-*co*-PLA only polymerizes up to M_n = 1,300 and is relatively susceptible to the lactic acid unit, which is estimated to cause T_g to drop to 107 °C. Regarding T_d presented in **Table 5**, each copolymer shows values between 377 °C and 385 °C, which are higher than that of PLA without any significant decrease due to the introduction of OLA. Manker *et al*. reported that increasing the molar mass of PEX and PBX through optimized polymerization methods could enable the use of their high T_g values in the future.[33] Similarly, when using ethylene glycol and 1,3-propanediol, high-molar-mass PAX-*co*-PLA could be developed using polymerization methods that consider the conformation of DMGX and the boiling points of the diols.

Table 4. Thermal parameters of PHX-*co*-PLA with different OLA preparation ratios.

	Composition (wt%)[a]	T_g DSC 1st cooling (°C)[b]	T_g DSC 2nd heating (°C)[b]	T_d TGA Max (°C)[c]
Neat PHX	100/-	71	66	386
PHX-*co*-PLA	95/5	71	66	383
PHX-*co*-PLA	90/10	70	65	385
PHX-*co*-PLA	80/20	64	57	385
PHX-*co*-PLA	60/40	63	58	384
Neat PLA	0/100[b]	56	55	367

[a]Initial DMGX/OLA mass ratio. For neat PLA, the ratio of PLA instead of OLA is shown.
[b]Determined using DSC.
[c]Determined using TGA.

Table 5. Thermal parameters of PAX-*co*-PLA using various diols.

	Composition (wt%)[a]	M_n (g/mol)[b]	D[b]	T_g DSC 1st Cooling (°C)[c]	T_d TGA Max (°C)[d]	Ref.
Neat PEX	100/-	2,500	4.92	137	374	(33)
PEX-*co*-PLA	90/10	1,300	2.69	106	377	This work
Neat PPX	100/-	9,500	3.58	117	379	(33)
PPX-*co*-PLA	90/10	7,500	1.65	109	379	This work
Neat PBX	100/-	31,300	2.49	100	369	(33)
PBX-*co*-PLA	90/10	18,500	2.43	98	376	This work
Neat PPTX	100/-	35,060	2.00	84	383	(33)
PPTX-*co*-PLA	90/10	29,900	4.29	83	382	This work
Neat PHX	100/-	26,000	4.48	70	386	This work
PHX-*co*-PLA	90/10	30,600	5.77	70	385	This work

[a]Initial DMGX/OLLA mass ratio.
[b]Determined using SEC.
[c]Determined using DSC.
[d]Determined using TGA.

1.3.4. Mechanical Properties

Figure 7 presents the results of the tensile tests performed to evaluate the mechanical properties of the heat-pressed film. **Figure 7a** shows the stress–strain curves of PHX-*co*-PLA obtained by varying the OLA feed ratio from 5% to 40%. **Figure 7b** summarizes the toughness and compares it with that of neat PHX and neat PLA. The maximum stress and Young's modulus were improved in copolymers with 5%,

10%, and 20% OLA compared to neat PHX. However, they decreased rapidly with higher additions. Compared to neat PLA with brittle properties, the addition of 5% and 10% considerably increased the elongation at break, which decreased rapidly with further addition. The use of two different catalysts could be a contributing factor, with the addition of a small amount of OLA resulting in the highest increase in toughness because of its higher molar mass compared to neat PHX. When more than 20% OLA was added, thermoforming became possible. However, polymerization was inhibited, resulting in lower molar mass and inferior mechanical properties. The addition of 5% or 10% was assumed to efficiently introduce low-molecular-weight lactic acid oligomers into the polymer (**Table 1**), resulting in a moderate increase in molar mass and improved mechanical properties. **Table 6** summarizes the mechanical properties of neat PLA, neat PHX, and PHX-*co*-PLA at different OLA feed ratios.

Figure 7c shows the stress–strain curves of PBX-*co*-PLA, PPTX-*co*-PLA, and PHX-*co*-PLA synthesized using different diols with OLA feed ratios fixed at 10%, except for PEX-*co*-PLA and PPTX-*co*-PLA, which have low molar mass and are brittle. **Figure 7d** shows a comparison of toughness with that of neat PLA. A comparison of the results for PBX-*co*-PLA, PPTX-*co*-PLA, and PHX-*co*-PLA reveals that Young's modulus and the maximum stress increased upon decreasing the length of the diol, whereas the

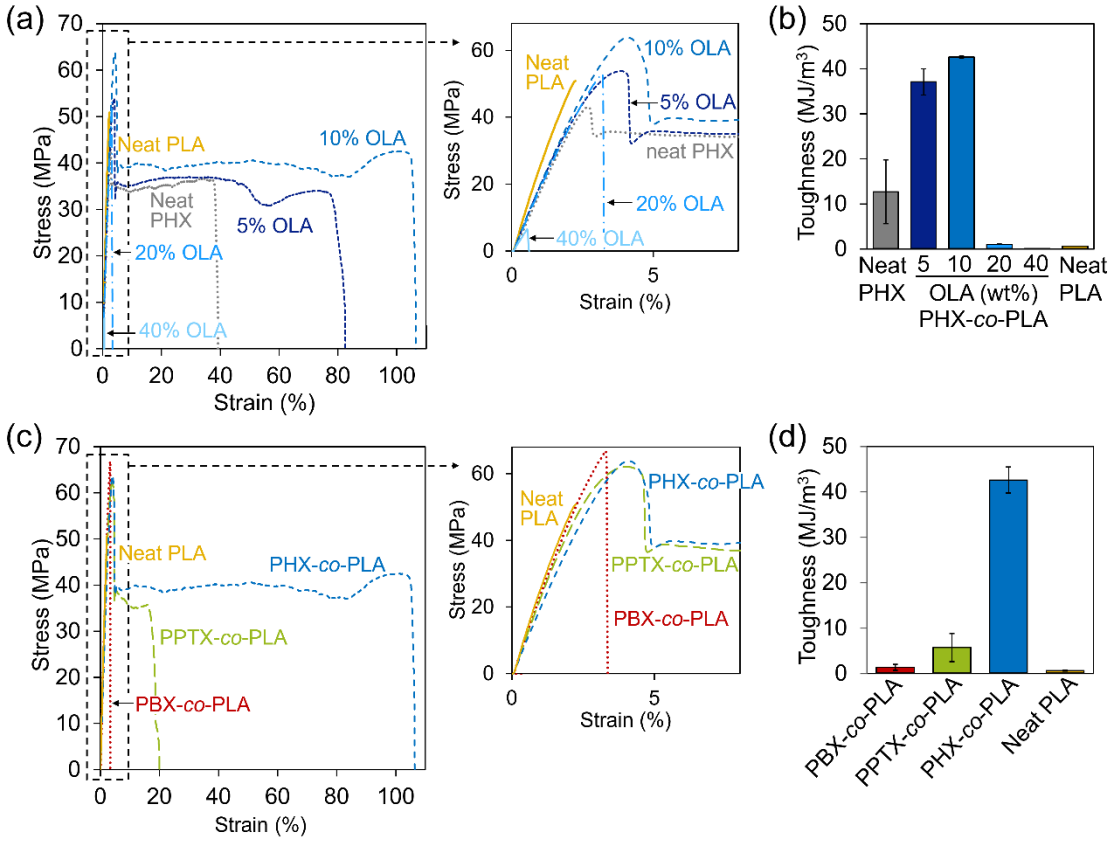

Figure 7. (a) Stress–strain curves and (b) toughness obtained from tensile tests of hot-pressed films of PHX-*co*-PLA with different OLA feed ratios (average of three replicates). (c) Stress–strain curves and (d) toughness obtained from tensile tests of hot-pressed films of PBX-*co*-PLA using 1,4-butanediol (red), PPTX-*co*-PLA using 1,5-pentanediol (light green), and PHX-*co*-PLA using 1,6-hexanediol (average of three replicates).

elongation at break improved upon increasing the length of the diol. This observation is consistent with that reported previously.[33] Manker *et al*. reported that PBX, PPTX, and PHX can form films. However, neat PEX and PPX are too brittle to form films, which is consistent with the behavior observed in the copolymers in this study, along with changes in the mechanical properties with diol length.[33] Changes in mechanical properties and in T_g (**Table 5**) may result from the reduced degrees of freedom between polymer chains and enhanced intermolecular interactions due to the use of shorter diols. Compared to neat PLA, Young's modulus of the three copolymers decreased. However, the maximum stress and elongation at break increased, with PHX-*co*-PLA, in particular, exhibiting the highest toughness. **Table 7** presents a summary of the mechanical properties of PBX-*co*-PLA, PPTX-*co*-PLA, PHX-*co*-PLA, and neat PLA.

Table 6. Mechanical properties of PHX-*co*-PLA with different OLA preparation ratios.

		Mechanical properties (tensile test)			
	Composition (%)[a]	Young's modulus (MPa)	Maximum stress (MPa)	Elongation at break (%)	Toughness (MJ/m^3)
Neat PHX	100/-	2,050 ± 190	49.0 ± 9.1	43.8 ± 8.7	12.7 ± 7.9
PHX-*co*-PLA	95/5	2,210 ± 67	53.1 ± 2.9	97.0 ± 18.5	37.1 ± 7.1
PHX-*co*-PLA	90/10	2,220 ± 61	59.6 ± 5.2	106 ± 4	42.6 ± 2.9
PHX-*co*-PLA	80/20	2,180 ± 100	54.0 ± 7.3	3.23 ± 0.40	1.06 ± 0.30
PHX-*co*-PLA	60/40	1,530 ± 110	5.41 ± 1.12	1.12 ± 0.44	0.04 ± 0.02
Neat PLA	-/100	2,880 ± 30	49.9 ± 3.2	2.26 ± 0.09	0.61 ± 0.06

[a]Initial DMGX/OLA mass ratio. For neat PLA, the ratio of PLA instead of OLA is shown.

Table 7. Mechanical properties of PAX-*co*-PLA using 1,4-butanediol, 1,5-pentanediol, and 1,6-hexanediol.

		Mechanical properties (tensile test)			
	Composition (%)[a]	Young's modulus (MPa)	Maximum stress (MPa)	Elongation at break (%)	Toughness (MJ/m^3)
PBX-*co*-PLA	90/10	2,550 ± 60	62.8 ± 12.9	3.34 ± 1.02	1.36 ± 0.65
PPTX-*co*-PLA	90/10	2,540 ± 46	60.9 ± 2.5	15.4 ± 7.2	5.71 ± 3.10
PHX-*co*-PLA	90/10	2,220 ± 61	59.6 ± 5.2	106 ± 4	42.6 ± 2.9
Neat PLA	100/-	2,880 ± 30	49.9 ± 3.2	2.26 ± 0.09	0.61 ± 0.06

[a]Initial DMGX/OLA mass ratio. For neat PLA, the ratio of PLA instead of OLA is shown.

1.3.5. Disintegration Test of Films in Compost

Experiments were conducted to evaluate the biodegradability and water resistance of PHX-*co*-PLA, which exhibited the highest toughness. As a simple way to test whether the films disintegrate, **Figure 8** shows the change in the appearance of PHX, PHX-*co*-PLA, and PLA films after 1 month of composting. Relatively similar to neat PHX and PHX-*co*-PLA, each film began to break brittle after 5 days in compost. They disintegrated finely after 10 days and exhibited no visible remnants after 20 days. Neat PLA began to disintegrate between 10 and 20 days, and disintegration progressed further when the test was extended. Previous studies have reported that neat PHX is highly hydrolyzable and can be chemically recycled in water.[33] Owing to their higher hydrolyzability, neat PHX and PHX-*co*-PLA with sugar structures are expected to degrade more rapidly than neat PLA when exposed to an active microbial environment in compost under high temperatures and humidity.

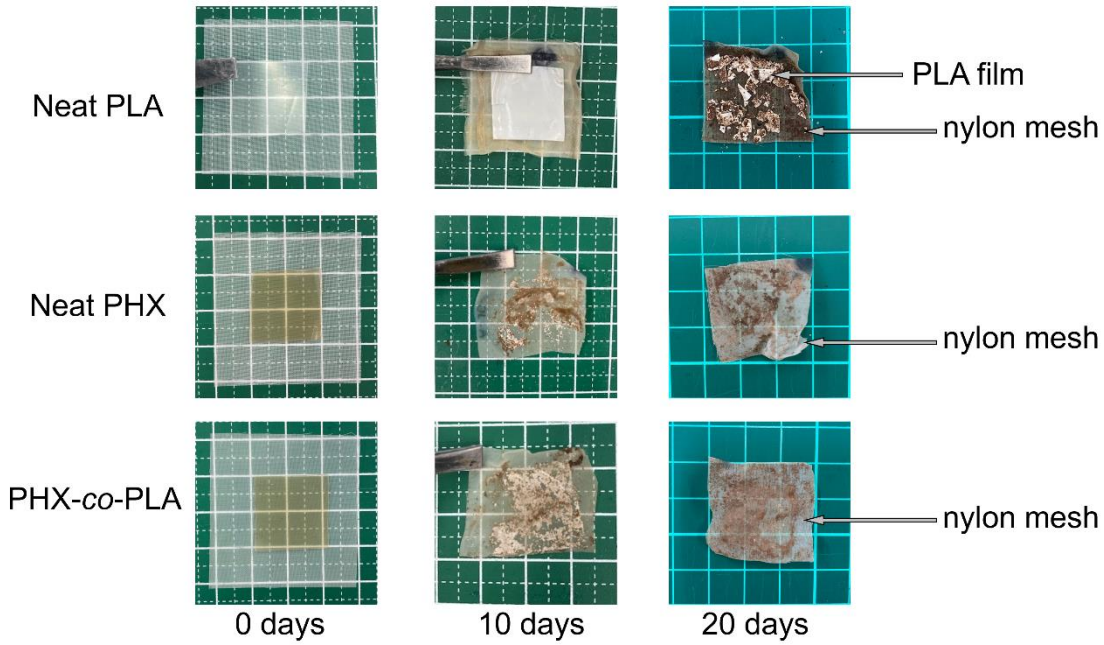

Figure 8. 20-day compost disintegration test of films of PHX, PHX-*co*-PLA, and PLA.

1.3.6. Marine Biodegradability and Water Resistance Evaluation of Films

Figure 9 presents the behaviors of neat PHX and PHX-*co*-PLA and neat PLA films in seawater at Odaiba, Tokyo Bay. Neat PHX and PHX-*co*-PLA exhibited more pronounced microbial flocs drifting in the test seawater than neat PLA. The neat PLA films maintain their shape in seawater for three months, whereas neat PHX and PHX-*co*-PLA lose their shape after 1 month, similar to the changes in compost that were conducted as an initial evaluation (**Figure 9a)**. Additionally, neat PLA exhibited no weight loss in seawater, whereas neat PHX and PHX-*co*-PLA showed significant weight loss of 94% and 88%, respectively, at 1 month, and the films were even smaller at 3 months. These observations are consistent with previous studies that reported minimal degradation of PLA in seawater.[47,48] Weight loss and biodegradability by BOD in seawater have been reported for other biodegradable polymers in several studies. For example, poly(3-hydroxybutyrate) (P(3HB)) exhibited 9% weight loss over 10 weeks[49] and 41% weight loss and 27% biodegradability within 1 month.[50] PCL showed 25% weight loss over 10 weeks[49] and 100% weight loss and 79% biodegradability in 1 month.[50] PBS exhibited 2% weight loss over 6 weeks[51] and 2% weight loss and 1% biodegradability in 1 month.[50] The weight losses of PHX and PHX-*co*-PLA were comparable to or higher than those of the other biodegradable polymers. Further investigation of molar mass and biodegradability is required. As shown in **Figure 9b**, M_n of neat PLA does not change; however, both neat PHX (M_n = 24,100 g/mol) and PHX-*co*-PLA (M_n = 25,900 g/mol) show a marked decrease in molar mass, degrading to M_n = 685 g/mol and M_n = 1,160 g/mol, respectively, after 1 month. HPLC analysis was performed on the seawater samples after 3 months. The results confirmed the presence of DGAX and lactic acid in seawater as a result of the progressive degradation of PHX-*co*-PLA (**Figure 10**). The pH of seawater

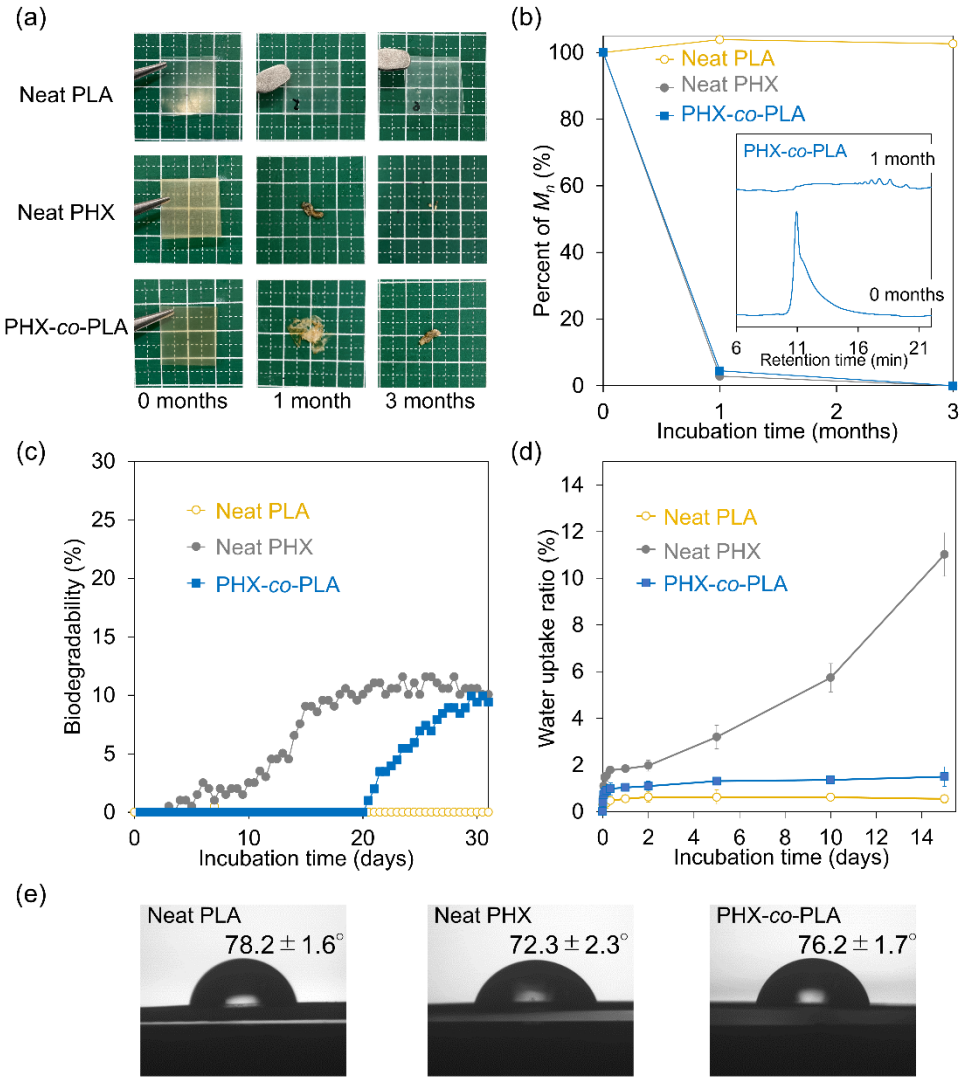

Figure 9. (a), (b), and (c) Biodegradability test of film in seawater. (d) and (e) Water resistance test using fresh water. (a) Appearance of neat PHX, PHX-*co*-PLA, and neat PLA films during the 3-month seawater disintegration test (average, two replicates). (b) Number average molar mass (M_n) of neat PHX, PHX-*co*-PLA, and neat PLA films during the 3-month seawater disintegration test. A single peak is considered undetectable if it can no longer be identified by SEC. (c) Biodegradability test by BOD in seawater for 1 month. (d) Water resistance test for films. Water absorption of neat PHX, PHX-*co*-PLA, and neat PLA films at 20°C using fresh water (average of 3 replicates). (e) WCA of films of neat PHX, PHX-*co*-PLA, and neat PLA (average of 3 replicates).

decreased from an initial value of approximately 7.6 to approximately 2.8 after 3 months for neat PHX and PHX-*co*-PLA. This decrease in pH most likely results from microbial effects or the effect of the carboxy groups of DGAX and lactic acid due to hydrolysis to the monomer level. **Figure 11** presents the SEM observation results of the surface of PHX-*co*-PLA films after the test. Traces of what appear to be microorganisms are observed, although they cannot be identified at this stage.

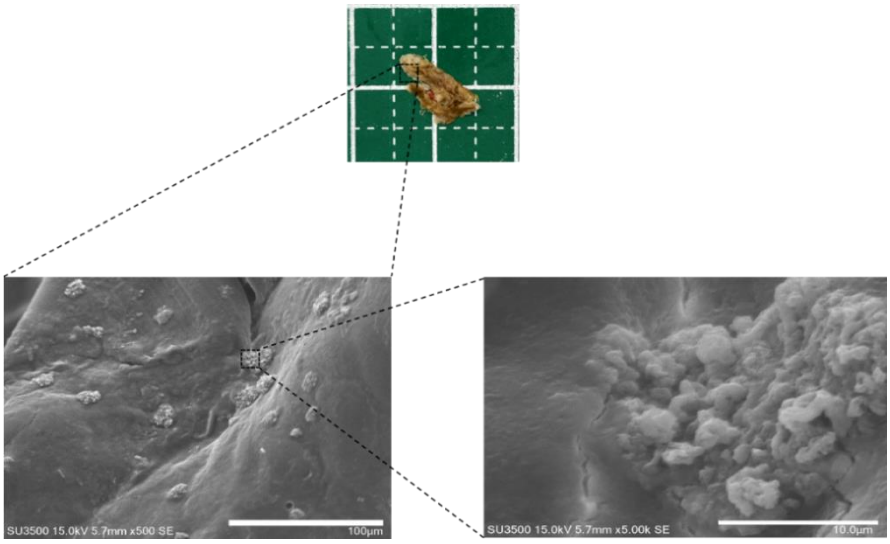

Figure 11. SEM observation of the film surface of PHX-*co*-PLA after seawater disintegration test.

In **Figure 9d**, the water absorption of the films is examined at 20°C to evaluate the water resistance of each sample. Initially, the water absorption of neat PHX and PHX-*co*-PLA gradually increases in sequence with the soaking time. However, as the soaking time increases, the water absorption of PHX-*co*-PLA and neat PLA appears to stabilize at approximately 1.5% and 0.6%, respectively. Although neat PHX appears to be stable, it exhibits a rapid increase in water absorption after 48 h **(Figure 9d)**. **Figure 12a** presents the evaluation of mass retention at 30°C in fresh water, and **Figure 12b** shows the evaluation of the molar mass change under the same conditions. Neat PLA does not show any change in shape or a significant decrease in molar mass. After water absorption, neat PHX is less water-resistant and retains its shape for up to 7 days. However, it loses its shape and weight at 14 days and shows a marked decrease in molar mass. PHX-*co*-PLA is slightly more water-resistant than neat PHX. It absorbs water at a slower rate

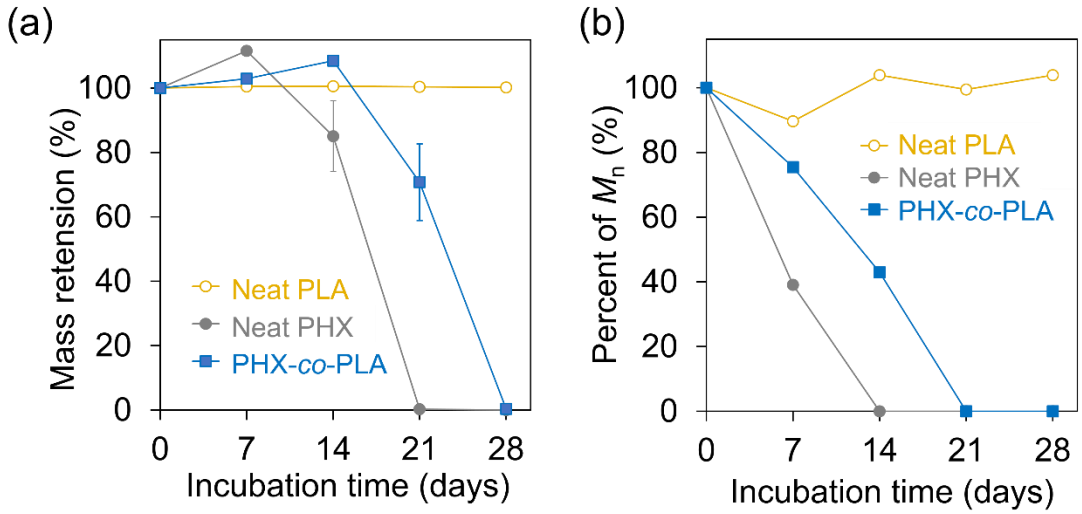

Figure 12. (a) Mass retention (average of three replicates) and (b) M_n of neat PHX, PHX-*co*-PLA, and neat PLA in water at 30°C. A single peak is considered undetectable if it can no longer be identified by SEC.

and retains its shape for up to 14 days. Nevertheless, it starts to lose its shape and weight at 21 days. Eventually, both dissolved almost completely in water and became visually undetectable. The WCA measurement results in **Figure 9e** show no penetration of water droplets, indicating that the film functions well. The WCA of neat PLA is 78°, whereas that of neat PHX is 72°, reflecting a slightly higher affinity for water. The WCA of PHX-*co*-PLA is 76°, which is slightly better than that of neat PHX, indicating its hydrophobicity. Accordingly, the lactic acid groups introduced into PHX-*co*-PLA play a role in controlling the hydrolysis rate and improving the hydrolysis stability, which presents a challenge.

Figure 9c shows the results of the biodegradability test conducted in seawater using the BOD method. PLA did not increase the BOD; however, PHX increased the BOD and biodegraded to 14%, with PHX-*co*-PLA reaching 13% slightly later **(Figure 9c)**. This delay could result from the increased hydrophobicity due to copolymerization with PLA, as shown in the WCA results in **Figure 9e**. BOD measurements were also performed for neat PHX and PHX-*co*-PLA in fresh water without microorganisms. No increase in BOD was observed in this case, indicating that the increase in BOD in seawater resulted from biodegradation by microorganisms in seawater. However, there is a gap between the weight loss and BOD in seawater, which can be attributed to the significant decrease in M_n of neat PHX and PHX-*co*-PLA in seawater (**Figure 9b**). Because hydrolysis proceeds faster than mineralization, the monomer was assumed to lower the pH of seawater and inhibit microbial activity.[52] Amplicon sequencing analysis was used to evaluate the relative abundance of the bacterial family in seawater samples (**Figure 13**, Section 1.2.11). When unclassified bacteria were included, blank and PHX-*co*-PLA seawater samples exhibited similar taxon counts (>11,000). However, when comparing the relative abundance of bacteria, the PHX-*co*-PLA

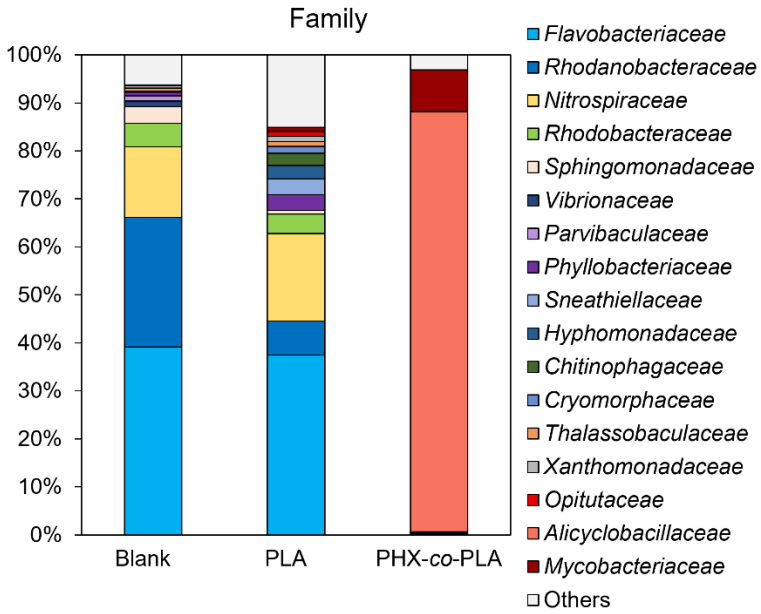

Figure 13. Relative abundances of the family of bacteria in the seawater samples containing a biofilm obtained by the 3-month marine disintegration test. Including unclassified bacteria, the taxon counts were 11,979 for blanks, 15,088 for PLA, and 11,538 for PHX-*co*-PLA. However, bacteria with abundances <1% or unattributed are labeled as "Others." See Section 1.2.11 for details of the experiment.

samples showed a higher abundance of *Alicyclobacillaceae*, which prefers acidic conditions,[53] indicating a particular environment (acidic environment) that would be expected to occur only at the lab scale. In actual natural environments, including field tests, the effect of pH is small and does not inhibit biodegradation. Therefore, the polymer is eventually hydrolyzed to a low molar mass and biodegraded by microorganisms to mineralize into CO_2 and H_2O. In this study, PHX-*co*-PLA appeared to be a promising alternative material that can be prepared from inedible resources, exhibiting a certain degree of water resistance and partial biodegradability, which may contribute to reducing microplastics. However, complete mineralization has not been determined, and further investigation is required to thoroughly understand its long-term environmental impact.

1.4. Conclusion

This study focused on xylose and lactic acid, which can be obtained from inedible resources. By using DMGX, which can be synthesized from xylose, and OLA, which can be synthesized from lactic acid, the PAX-*co*-PLA series was synthesized using various diols. The thermal and mechanical properties were evaluated after adjusting the OLA feed ratio and using various diols. PAX-*co*-PLA exhibited higher toughness and T_g than neat PLA. Among PAX-*co*-PLA, we focused on PHX-*co*-PLA, which demonstrated the highest mechanical properties, and then evaluated its biodegradability. Evaluation of film disintegration in compost showed marked disintegration of neat PHX and PHX-*co*-PLA. PHX-*co*-PLA exhibited a slight increase in hydrophobicity and retained its shape longer in water. In WCA tests, the water droplets did not penetrate immediately, and the contact angle of PHX-*co*-PLA was comparable to that of neat PLA, indicating that it functioned well as a film. PHX-*co*-PLA was found to disintegrate in seawater, and partial mineralization to CO_2 and H_2O was confirmed at the laboratory level. However, tests at a level closer to the actual environment have not been conducted, and further studies should explore the possibility of complete mineralization. The copolymers obtained in this study can be prepared from sustainable inedible biomass; they exhibit good film properties, including high toughness, water resistance, and partial marine biodegradability. PAX-*co*-PLA can be prepared using renewable, inedible biomass and can be deployed in various applications requiring high toughness and biodegradability, including packaging, agricultural applications, and marine environments. These materials can contribute to solving the plastic waste problem.

1.5. References

(1) Evode, N.; Qamar, S. A.; Bilal, M.; Barceló, D.; Iqbal, H. M. N. Plastic waste and its management strategies for environmental sustainability. *Case Stud. Chem. Environ. Eng.* **2021**, *4*, 100142. https://doi.org/10.1016/j.cscee.2021.100142.

(2) Bianchi, E.; Guidotti, G.; Soccio, M.; Siracusa, V.; Gazzano, M.; Salatelli, E.; Lotti, N. Biobased and Compostable Multiblock Copolymer of Poly(L-lactic acid) Containing 2,5-Furandicarboxylic Acid for Sustainable Food Packaging: The Role of Parent Homopolymers in the Composting Kinetics and Mechanism. *Biomacromolecules* **2023**, *24* (5), 2356–2368. https://doi.org/10.1021/acs.biomac.3c00216.

(3) Carafa, R. N.; Foucher, D. A.; Sacripante, G. G. Biobased Polymers from Lignocellulosic Sources. Green Chem. Lett. Rev. 2023, 16 (1). https://doi.org/10.1080/17518253.2022.2153087.

(4) OECD. Global Plastics Outlook: Policy Scenarios to 2060. *OECD Publishing*, **2022** https://doi.org/10.1787/aa1edf33-en.
(5) European Bioplastics. Bioplastics market development update 2023. *European Bioplastics* **2023**. https://www.european-bioplastics.org/market/ (accessed Mar 21, 2024).
(6) Manker, L. P.; Jones, M. J.; Bertella, S.; Behaghel de Bueren, J.; Luterbacher, J. S. Current strategies for industrial plastic production from non-edible biomass. *Curr. Opin. Green Sustainable Chem.* **2023**, *41*, 100780. https://doi.org/10.1016/j.cogsc.2023.100780.
(7) Pauly, M.; Keegstra, K. Cell-wall carbohydrates and their modification as a resource for biofuels. *Plant J.* **2008**, *54* (4), 559–568. https://doi.org/10.1111/j.1365-313X.2008.03463.x.
(8) Delidovich, I.; Hausoul, P. J. C.; Deng, L.; Pfützenreuter, R.; Rose, M.; Palkovits, R. Alternative Monomers Based on Lignocellulose and Their Use for Polymer Production. *Chem. Rev.* **2016**, *116* (3), 1540–1599. https://doi.org/10.1021/acs.chemrev.5b00354.
(9) Auras, R.; Harte, B.; Selke, S. An Overview of Polylactides as Packaging Materials. *Macromol. Biosci*. **2004**, *4 (9)*, 835–864. https://doi.org/10.1002/mabi.200400043.
(10) Pluta, M.; Murariu, M.; Alexandre, M.; Galeski, A.; Dubois, P. Polylactide compositions. The influence of ageing on the structure, thermal and viscoelastic properties of PLA/calcium sulfate composites. *Polym. Degrad. Stab.* **2008**, *93* (5), 925–931. https://doi.org/10.1016/j.polymdegradstab.2008.02.001.
(11) Zhang, N.; Yu, X.; Duan, J.; Yang, J.-H.; Huang, T.; Qi, X.-D.; Wang, Y. Comparison study of hydrolytic degradation behaviors between α′- and α-poly(L-lactide). *Polym. Degrad. Stab.* **2018**, *148*, 1–9. https://doi.org/10.1016/j.polymdegradstab.2017.12.014
(12) Avolio, R.; Castaldo, R.; Gentile, G.; Ambrogi, V.; Fiori, S.; Avella, M.; Cocca, M.; Errico, M. E. Plasticization of poly(lactic acid) through blending with oligomers of lactic acid: Effect of the physical aging on properties. *Eur. Polym. J*. **2015**, *66*, 533–542. https://doi.org/10.1016/j.eurpolymj.2015.02.040.
(13) Alijanian, S.; Zohuriaan-Mehr, M. J.; Esmaeilzadeh, M.; Salimi, A.; Razavi-Nouri, M. Glycerol-oligo(lactic acid) bioresins as fully biobased modifiers for poly(Lactic acid): synthesis, green chemistry metrics, and the modified PLA film Properties. *J. Polym. Environ*. **2023**. *32*, 641-657. https://doi.org/10.1007/s10924-023-02987-8.
(14) Marques, S.; Santos, J. A. L.; Gírio, F. M.; Roseiro, J. C. Lactic acid production from recycled paper sludge by simultaneous saccharification and fermentation. *Biochem. Eng. J*. **2008**, *41* (3), 210–216. https://doi.org/10.1016/j.bej.2008.04.018.
(15) Esquivel-Hernández, D. A.; García-Pérez, J. S.; López-Pacheco, I. Y.; Iqbal, H. M. N.; Parra-Saldívar, R. Resource recovery of lignocellulosic biomass waste into lactic acid - Trends to sustain cleaner production. *J. Environ. Manage*. **2022**, *301*, 113925. https://doi.org/10.1016/j.jenvman.2021.113925.
(16) Yataka Y.; Development of Biomass Plastics Derived from Wood Pulp. *Jpn. Tappi J.* **2023**, *77* (5), 428-431. https://doi.org/10.2524/jtappij.77.428.
(17) Takagi, A.; Hsu, Y.-I.; Uyama, H. Biodegradable poly(lactic acid) and polycaprolactone alternating multiblock copolymers with controllable mechanical properties. *Polym. Degrad. Stab.* **2023**, *218*, 110564. https://doi.org/10.1016/j.polymdegradstab.2023.110564.
(18) Supthanyakul, R.; Kaabbuathong, N.; Chirachanchai, S. Random poly(butylene succinate-*co*-lactic acid) as a multi-functional additive for miscibility, toughness, and clarity of PLA/PBS blends. *Polymer (Guildf)* **2016**, *105*, 1–9. https://doi.org/10.1016/j.polymer.2016.10.006.
(19) Olewnik, E.; Czerwiński, W.; Nowaczyk, J.; Sepulchre, M.-O.; Tessier, M.; Salhi, S.; Fradet, A. Synthesis and structural study of copolymers of L- lactic acid and bis(2-hydroxyethyl terephthalate). *Eur. Polym. J.* **2007**, *43* (3), 1009–1019. https://doi.org/10.1016/j.eurpolymj.2006.11.025.
(20) Olewnik, E.; Czerwiński, W.; Nowaczyk, J. Hydrolytic degradation of copolymers based on L-lactic acid and bis-2-hydroxyethyl terephthalate. *Polym. Degrad. Stab.* **2007**, *92* (1), 24–31. https://doi.org/10.1016/j.polymdegradstab.2006.10.003.
(21) Li, J.; Jiang, Z.-Q.; Wang, Z. B.; Chen, P.; Li, Y.; Zhou, J.; Liu, J.; Wang, Y.-Z.; Gu, Q. Synthesis, crystallization and hydrolysis of aromatic–aliphatic copolyester: Poly(trimethylene terephthalate)-*co*-poly(L-lactic acid). *Polym. Degrad. Stab*. **2011**, *96* (5), 991–999. https://doi.org/10.1016/j.polymdegradstab.2011.01.023.
(22) Wang, B.-T.; Zhang, Y.; Song, P.-A.; Guo, Z.-H.; Cheng, J.; Fang, Z.-P. Biodegradable aliphatic/aromatic copolyesters based on terephthalic acid and poly(L-lactic acid): Synthesis,

characterization and hydrolytic degradation. Chin. *J. Polym. Sci*. **2010**, *28* (3), 405–415. https://doi.org/10.1007/s10118-010-9032-y.
(23) Li, J.; Jiang, Z.-Q.; Zhou, J.; Liu, J.; Shi, W.-Tgu, Q.; Wang, Y.-Z. A Novel Aromatic-Aliphatic Copolyester of Poly(ethylene-*co*-diethylene terephthalate)-*co*-Poly(L-lactic acid): Synthesis and Characterization. *Ind. Eng. Chem. Res*. **2010**, *49* (20), 9803–9810. https://doi.org/10.1021/ie100915y.
(24) Gandini, A.; Lacerda, T. M.; Carvalho, A. J. F.; Trovatti, E. Progress of Polymers from Renewable Resources: Furans, Vegetable Oils, and Polysaccharides. *Chem. Rev*. **2016**, *116*, 1637–1669. https://doi.org/10.1021/acs.chemrev.5b00264.
(25) Sahu, P.; Thorbole, A.; Gupta, R. K. Polyesters Using Bioderived Furandicarboxylic Acid: Recent Advancement and Challenges toward Green PET. *ACS Sustain. Chem. Eng*. **2024**, *12*, 6811−6826. https://doi.org/10.1021/acssuschemeng.4c01123.
(26) Miah, M. R.; Dong, Y.; Wang, J.; Zhu, J. Recent Progress on Sustainable 2,5-Furandicarboxylate-Based Polyesters: Properties and Applications. *ACS Sustain. Chem. Eng*. **2024**, *12* (8), 2927−2961. https://doi.org/10.1021/acssuschemeng.3c06878.
(27) Matos, M.; Sousa, A. F.; Fonseca, A. C.; Freire, C. S. R.; Coelho, J. F. J.; Silvestre, A. J. D. A New Generation of Furanic Copolyesters with Enhanced Degradability: Poly(ethylene 2,5-furandicarboxylate)-*co*-poly(lactic acid) Copolyesters. *Macromol. Chem. Phys*. **2014**, *215* (22), 2175–2184. https://doi.org/10.1002/macp.201400175.
(28) Wu, H.; Wen, B.; Zhou, H.; Zhou, J.; Yu, Z.; Cui, L.; Huang, T.; Cao, F. Synthesis and degradability of copolyesters of 2, 5-furandicarboxylic acid, lactic acid, and ethylene glycol. *Polym. Degrad. Stab.* **2015**, *121*, 100–104. https://doi.org/10.1016/j.polymdegradstab.2015.08.009.
(29) Hu, H.; Zhang, R.; Shi, L.; Ying, W. Bin; Wang, J.; Zhu, J. Modification of Poly(butylene 2,5-furandicarboxylate) with Lactic Acid for Biodegradable Copolyesters with Good Mechanical and Barrier Properties. *Ind. Eng. Chem. Res.* **2018**, *57* (32), 11020–11030. https://doi.org/10.1021/acs.iecr.8b02169.
(30) Sajid, M.; Zhao, X.; Liu, D. Production of 2,5-furandicarboxylic acid (FDCA) from 5-hydroxymethylfurfural (HMF): recent progress focusing on the chemical-catalytic routes. *Green Chem*. **2018**, *20* (24), 5427–5453. https://doi.org/10.1039/c8gc02680g.
(31) Avantium Press Release, Avantium celebrates the First Piling Ceremony for its FDCA Flagship Plant. *Avantium* **2022**. https://www.avantium.com/wp-content/uploads/2022/04/20220420-Avantium-celebrates-First-Piling-Ceremony-of-its-FDCA-Flagship-Plant_final.pdf. (accessed Mar 21, 2024).
(32) Stadler, B. M.; Wulf, C.; Werner, T.; Tin, S.; De Vries, J. G. Catalytic Approaches to Monomers for Polymers Based on Renewables. *ACS Catal*. **2019**, *9*, 8012–8067. https://doi.org/10.1021/acscatal.9b01665.
(33) Manker, L. P.; Dick, G. R.; Demongeot, A.; Hedou, M. A.; Rayroud, C.; Rambert, T.; Jones, M. J.; Sulaeva, I.; Vieli, M.; Leterrier, Y.; Potthast, A.; Maréchal, F.; Michaud, V.; Klok, H.-A.; Luterbacher, J. S. Sustainable polyesters via direct functionalization of lignocellulosic sugars. *Nat. Chem*. **2022**, *14*, 976-984. https://doi.org/10.1038/s41557-022-00974-5.
(34) Vieli, M.; Hedou, M. A.; Scholten, P. B. V.; Demongeot, A.; Manker, L. P.; Buser, R.; Luterbacher, J. S.; Michaud, V.; Héroguel, F. Tuning the Mechanical Properties of Poly(butylene xylosediglyoxylate) via Compounding Strategies. *ACS Appl. Polym. Mater.* **2023**, *5* (12), 9732–9741. https://doi.org/10.1021/acsapm.3c01219.
(35) Hsu, Y.-I.; Yamaoka, T. Visualization and quantification of the bioactive molecules immobilized at the outmost surface of PLLA-based biomaterials. *Polym. Degrad. Stab*. **2018**, *156*, 66–74. https://doi.org/10.1016/j.polymdegradstab.2018.08.001.
(36) Standard Test Method for Determining Aerobic Biodegradation of Plastic Materials in the Marine Environment by a Defined Microbial Consortium or Natural Sea Water Inoculum. ASTM D6691-17. https://doi.org/10.1520/D6691-17 (accessed Mar 21, 2024).
(37) Takahashi, S.; Tomita, J.; Nishioka, K.; Hisada, T.; Nishijima, M. Development of a Prokaryotic Universal Primer for Simultaneous Analysis of *Bacteria* and *Archaea* Using Next-Generation Sequencing. *PLoS One* **2014,** *9* (8). https://doi.org/10.1371/journal.pone.0105592.
(38) Hisada, T.; Endoh, K.; Kuriki, K. Inter- and intra-individual variations in seasonal and daily stabilities of the human gut microbiota in Japanese. *Arch. Microbiol.* **2015**, *197* (7), 919–934. https://doi.org/10.1007/s00203-015-1125-0.

(39) Martin, M. Cutadapt Removes Adapter Sequences from High-Throughput Sequencing Reads. *EMBnet. J.* **2011**, *17* (1). https://doi.org/10.14806/ej.17.1.200.
(40) Aronesty, E. Comparison of Sequencing Utility Programs, *The Open Bioinf. J.* **2013**, *7*, 1–8, https://doi.org/10.2174/1875036201307010001.
(41) Gordon, A.; Hannon, G.J., FASTX-Toolkit FASTQ/A short-reads preprocessing tools (unpublished) **2010**. http://hannonlab. cshl. edu/fastx_toolkit.
(42) Caporaso, J. G.; Kuczynski, J.; Stombaugh, J.; Bittinger, K.; Bushman, F. D.; Costello, E. K.; Fierer, N.; Pĕa, A. G.; Goodrich, J. K.; Gordon, J. I.; Huttley, G. A.; Kelley, S. T.; Knights, D.; Koenig, J. E.; Ley, R. E.; Lozupone, C. A.; McDonald, D.; Muegge, B. D.; Pirrung, M.; Reeder, J.; Sevinsky, J. R.; Turnbaugh, P. J.; Walters, W. A.; Widmann, J.; Yatsunenko, T.; Zaneveld, J.; Knight, R. QIIME allows analysis of high-throughput community sequencing data. *Nat. Method*. **2010**, *7*, 335–336. https://doi.org/10.1038/nmeth.f.303.
(43) Edgar, R. C.; Haas, B. J.; Clemente, J. C.; Quince, C.; Knight, R. UCHIME improves sensitivity and speed of chimera detection. *Bioinformatics* **2011**, *27* (16), 2194–2200. https://doi.org/10.1093/bioinformatics/btr381.
(44) Wang, Q.; Garrity, G. M.; Tiedje, J. M.; Cole, J. R. Naïve Bayesian Classifier for Rapid Assignment of rRNA Sequences into the New Bacterial Taxonomy. *Appl. Environ. Microbiol.* **2007**, *73* (16), 5261–5267. https://doi.org/10.1128/AEM.00062-07.
(45) Kasai, C.; Sugimoto, K.; Moritani, I.; Tanaka, J.; Oya, Y.; Inoue, H.; Tameda, M.; Shiraki, K.; Ito, M.; Takei, Y.; Takase, K. Comparison of the gut microbiota composition between obese and non-obese individuals in a Japanese population, as analyzed by terminal restriction fragment length polymorphism and next-generation sequencing. *BMC Gastroenterol.* **2015**, *15*, 100. https://doi.org/10.1186/s12876-015-0330-2.
(46) Feng, Y.; Wang, C.; Yang, J.; Tan, T.; Yang, J. Poly(ethylene succinate-*co*-lactic acid) as a Multifunctional Additive for Modulating the Miscibility, Crystallization, and Mechanical Properties of Poly(lactic acid). *ACS Omega* **2024**, *9 (6)*, 6578–6587. https://doi.org/10.1021/acsomega.3c07489.
(47) Deroiné, M.; Le Duigou, A.; Corre, Y.-M.; Le Gac, P.- Y.; Davies, P.; César, G.; Bruzaud, S. ageing of polylactide in aqueous environments: Comparative study between distilled water and seawater. *Polym. Degrad. Stab*. **2014**, *108*, 319–329. https://doi.org/10.1016/j.polymdegradstab.2014.01.020.
(48) Bagheri, A. R.; Laforsch, C.; Greiner, A.; Agarwal, S. Fate of So‐Called Biodegradable Polymers in Seawater and Freshwater. *Global Challenges* **2017**, *1* (4), 1700048. https://doi.org/10.1002/gch2.201700048.
(49) Tsuji, H.; Suzuyoshi, K. Environmental degradation of biodegradable polyesters 1. Poly(ε-Caprolactone), Poly[(R)-3-hydroxybutyrate], and poly (L-lactide) films in controlled static seawater. *Polym. Degrad. Stab.* **2002**, *75*, 347-355. https://doi.org/10.1016/S0141-3910(01)00240-3.
(50) Kasuya, K.; Takagi, K."; Ishiwatari, S.; Yoshida, Y.; Doi, Y. Biodegradabilities of various aliphatic polyesters in natural waters. *Polym. Degrad. Stab.* **1998**, *59*, 327-332. https://doi.org/10.1016/S0141-3910(97)00155-9.
(51) Nakayama, A.; Yamano, N.; Kawasaki, N. Biodegradation in seawater of aliphatic polyesters. *Polym. Degrad. Stab*. **2019**, *166*, 290–299. https://doi.org/10.1016/j.polymdegradstab.2019.06.006.
(52) Wang, Y.; Davey, C. J. E.; Van der Maas, K.; Van Putten, R.-J.; Tietema, A.; Parsons, J. R.; Gruter, G.-J. M. Biodegradability of novel high T_g poly(isosorbide-*co*-1,6-hexanediol) oxalate polyester in soil and marine environments. *Sci. Total Environ.* **2022**, *815*, 152781. https://doi.org/10.1016/j.scitotenv.2021.152781.
(53) de Souza Sant'Ana, A.; Alvarenga, V. O.; Oteiza, J. M.; Peña, W. E. L. *Alicyclobacillus*. *Encyclopedia of Food Microbiology* (2nd Ed.) (Academic Press), **2014**, 42–53. https://doi.org/10.1016/B978-0-12-384730-0.00380-3.

Chapter 2. Biodegradable Poly(lactic acid) and Polycaprolactone Alternating Multiblock Copolymers with Controllable Mechanical Properties

2.1. Introduction

Plastics are used in numerous products and have become an integral part of our daily life. The production of plastics is increasing globally, increasing from 2 Mt in 1950 to 380 Mt in 2015 and 460 Mt in 2019. Between 2015 and 2016, the packaging industry generated 141 Mt of plastic waste.[1,2] Various issues related to plastics have been identified, including the increased demand for disposable plastics due to the pandemic, which further complicates plastic waste management.[3] Notably, 50% of the plastic produced is discarded after a single use.[4] Among the 275 Mt of plastic waste in 2010, 4.8–12.7 Mt entered the oceans.[5] Although marine pollution by plastics has been reported since the early 1970s, the accumulation of plastics in oceans has recently emerged as a global challenge.[5,6] Plastic waste, not only in the marine environment but also across every corner of the world's landmass, poses a significant concern due to its impact on ecosystems.[2] Researchers, industrialists, and environmentalists have considered the development of biobased or biodegradable plastics promising for reducing environmental pollution and dependence on petroleum resources.[1,7] Typical biodegradable polymers include PLA, PCL, PBS, PBAT, and PHA. The global production capacity of biobased or biodegradable plastics is 2.42 Mt, which is small compared to the total production of plastics.[8]

The biodegradation process of biodegradable plastics is not a simple reduction in molecular weight; complete mineralization is also essential.[9,10] Numerous biodegradable plastics are mineralized by bacterial attack on the polymer itself.[11] In contrast, microorganisms producing the degradative enzyme proteinase K are scarce in the environment,[12] and PLA is mineralized by a two-step degradation mechanism that differs slightly from that of other biodegradable plastics.[7,11,13] Therefore, the degradation behavior of PLA is unlikely to occur in seawater.[14] Optimal biodegradability can only be obtained in a controlled environment, such as a composting environment,[10] in which PLA is hydrolyzed to oligomers with a molecular weight of 10,000–20,000 in the first stage—the rate-limiting stage.[13] In the second stage, oligomers with lower molecular weights begin to be assimilated by microorganisms and are finally biodegraded to CO_2 and H_2O.[13,15] At higher temperatures in compost tests, the chains in the amorphous region of PLA become more flexible, allowing more water between the chains and faster hydrolysis.[10,13] One factor hindering the smooth degradation of PLA in seawater is that its T_g higher than the ambient temperature, preventing the first step of oligomerization.[10,13,16]

Although PLA is difficult to biodegrade in seawater, it is promising for industrial applications because it has excellent processability and transparency and is produced from environmentally friendly raw materials, such as corn-based starch.[17] However, PLA is brittle and has several drawbacks that limit its use,

including an elongation at break <10%.[18] Numerous studies have been conducted on PLA/PCL composites, in which the disadvantages of PLA are complemented and reinforced with PCL, which exhibits high toughness.[19] PLA/PCL blends have been examined to enhance their mechanical properties.[19,20] The synthesis of block copolymers by chemical bonding has also been investigated. Block copolymers have been used as compatibilizers[21] and medical materials reinforced with ABA triblock copolymer structures containing PLA as a side block.[22] The hydrolytic degradability of ABA triblock copolymers developed for temporary therapeutic applications (e.g., surgery) has been reported.[23] Although the production of high-molecular-weight polymers is necessary for thermoforming and industrialization, PLA-based copolymers are often discussed at low molecular weight, and achieving high molecular weight through copolymerization is challenging.[24] Chain extension with HDI simplifies the development of PLA-based thermoplastic polyurethanes (TPUs) with high molecular weight. PCL/PLA thermoplastic elastomers were synthesized to develop tough, flexible, and biodegradable polymers for clinical applications and were evaluated for *in vitro* degradation.[25] However, few studies have compared the mechanical strength of different PLA/PCL composites or conducted mineralization tests using compost of highly toughened PLA-based copolymers.

In this study, PLA was copolymerized with PCL-diol, followed by a chain-extension reaction with HDI to synthesize PLA–PCL alternating multiblock (PLA-*alt*-PCL) copolymers based on PLA. Copolymers with different PLA chain lengths were prepared *via* ring-opening polymerization. Regularly arranged copolymer (a) films were evaluated using tensile tests to compare their mechanical properties to those of PLA–PCL random multiblock (PLA-*ran*-PCL) copolymers (b) and blend composites (c) (**Figure 1**). The thermal properties were evaluated using DSC. The mechanical properties could be controlled by varying the lengths of PLA chains; thus, PLA-*alt*-PCL copolymers with high toughness could be obtained. The CO_2 production and biodegradability of the copolymers in compost increased from the start of the test, indicating that the copolymers are highly biodegradable. The change in the molecular weight of the

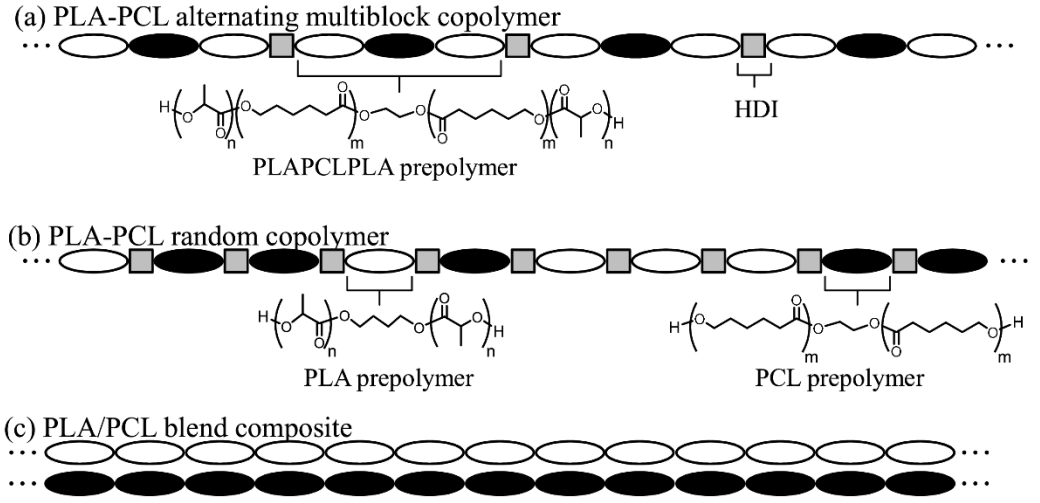

Figure 1. Model structures of the (a) PLA-*alt*-PCL copolymers, (b) PLA-*ran*-PCL copolymers, and (c) PLA/PCL blend composite.

copolymer films was evaluated using seawater collected from Tokyo Bay. Although biodegradability in the marine environment could not be confirmed, the copolymer's regularly arranged structure and low T_g might have contributed to its low molecular weight in seawater, which is considered one of the bottlenecks for PLA biodegradation.

2.2. Experimental Section

2.2.1. Materials

PCL (M_n = 80,000 g/mol) was purchased from Sigma-Aldrich Chemical Co. (St. Louis, MO, USA). PCL-diol (M_n = 2,000 g/mol) (Placcel 220N) was purchased from Daicel Co. (Osaka, Japan). Chloroform was purchased from Nacalai Tesque Inc. (Kyoto, Japan). In addition, Tin (II) 2-ethylhexanoate, methanol, diethyl ether, sea sand (425–850 μm), and ammonium chloride were purchased from Fujifilm Wako Pure Chemical Co. (Osaka, Japan). L-Lactide, 1,4-butanediol, HDI, and potassium dihydrogen phosphate were purchased from Tokyo Chem. Ind. (Tokyo, Japan), and PLA (Ingeo biopolymer 2003D) (M_n = 92,000 g/mol by SEC) was purchased from NatureWorks LLC (Nebraska, USA). All reagents were used as received.

2.2.2. Synthesis of PLA–PCL Alternating Multiblock (PLA-*alt*-PCL) Copolymers

PCL-diol (3 g) and L-lactide (12 g) were placed in a 50-mL three-neck flask and vacuum-dried at room temperature for 3 h to synthesize PLA–PCL–PLA. The amount of L-lactide was changed to synthesize copolymers with different PLA chain lengths. Subsequently, a toluene solution of tin(II) 2-ethylhexanoate (1 mol% of the hydroxyl end of PCL-diol) was added to the mixture, which was vacuum-dried at room temperature for 2 h. Ring-opening polymerization was performed at 180 °C for 3 h with stirring (150 rpm) under a nitrogen atmosphere. Subsequently, HDI was added to the mixture at an NCO/OH molar ratio of 2 mol mol^{-1}. The chain-extension reaction was performed at 180°C for 0.5 h with stirring (100 rpm) under a nitrogen atmosphere. The final product was dissolved in chloroform and poured into an excess volume of methanol for reprecipitation. The precipitates were filtered, washed with methanol, and vacuum-dried to obtain PLA-*alt*-PCL copolymers as white powders.

2.2.3. Synthesis of PLA–PCL Random Multiblock (PLA-*ran*-PCL) Copolymers

PLA-diol was synthesized by the ring-opening polymerization of L-lactide (20 g), as described in Section 2.2.2, using 1,4-butanediol (0.9 g) as an initiator. The synthesized mixture was dissolved in chloroform and poured into an excess volume of diethyl ether for reprecipitation. The precipitate was filtered, washed with diethyl ether, and vacuum-dried to obtain PLA-diol. PLA-diol (5.3 g) and PCL-diol (0.9 g) were placed in a flask; HDI was added to the flask at an NCO/OH molar ratio of 2 mol mol^{-1}. The mixture was heated at 180°C for 0.5 h with stirring (100 rpm) under a nitrogen atmosphere. The final product was dissolved in chloroform and poured into an excess volume of methanol for reprecipitation. The precipitate was filtered, washed with methanol, and vacuum-dried to obtain PLA-*ran*-PCL copolymers.

2.2.4. Kneading of Each Sample

The PLA and PCL pellets were dried in a vacuum oven at 50°C for 4 h to remove absorbed moisture. The dried pellets were mixed and extruded using Labo Plastomill (4C150-01, Toyo Seiki Seisakusho, Co., Ltd., Tokyo, Japan) to fabricate neat samples and composites. PLA (85 g) and PCL (15 g) were melted at 170°C and 70 rpm for 5 min. Kneading was performed at 170°C and 70 rpm for 10 min.

2.2.5. Fabrication of Films

For the fabrication methods applied in this section, please refer to Section 1.2.6 in Chapter 1.

2.2.6. Measurement

For ^{1}H NMR, SEC, and tensile testing applied in this section, refer to Section 1.2.7 in Chapter 1. For the WCA test and TGA methods applied in this section, refer to Section 1.2.10 in Chapter 1. T_g and melting temperature (T_m) of the sample were measured by DSC using a DSC6220 thermal analysis system (Hitachi High-Tech Science Co., Tokyo, Japan). The sample (approximately 6 mg) was heated from −80 °C to 200 °C at a heating rate of 10 °C/min and then maintained at 200°C for 3 min to melt. After heating, the sample was cooled from 200 °C to −80°C at a cooling rate of 10 °C/min. The temperature was maintained at −80°C for 3 min. The sample was heated again from −80°C to 200 °C at a heating rate of 10 °C/min. The DSC measurements were conducted under a nitrogen atmosphere at a flow rate of 50 mL/min. Films were prepared (drying conditions: 70 °C overnight), and XRD analysis was performed using an X-ray diffractometer (XRD) (RINT-Ultima, Rigaku Co., Ltd., Tokyo, Japan) operated at 40 kV and 40 mA. Data were collected within the range of scattering angles (2θ) of 5°–30° at a rate of 1°/min.

2.2.7. Biodegradation Test of a Powder and Disintegration Test of Films with a Compost

The biodegradation of polymers in compost was evaluated according to JIS K6953-2 based on the amount of carbon dioxide generated using a microbial oxidative degradation evaluation system (MODA-CS, Yawata Bussan Co., Shizuoka, Japan). The YK-12 compost from Yawata Bussan Co. was used for evaluation. After the addition of the dried sea sand (320 g) to the compost (dry mass of 60 g), the moisture content was adjusted to approximately 58%. For evaluation, samples (10 g) were frozen and ground into a powder using a freezing and grinding machine (JFC-2000, Japan Analytical Industry Co., Tokyo, Japan). The test was conducted for 45 days at a temperature of 58°C and moisture content of 58% with weekly agitation. Containers without samples, only with the compost, were used as blanks. The biodegradability (%) of the compost test was calculated as follows:

$$\text{Biodegradability (\%)} = \frac{\text{CO}_2 \text{ production (g) by the sample} - \text{CO}_2 \text{ production (g) by the blank}}{\text{Theoretical CO}_2 \text{ production (g) by the sample}} \times 100\ (\%).$$

The net CO_2 production from the sample in the experiment was calculated by subtracting CO_2 production (g) in the blank container from that (g) in the container containing the sample. The theoretical amount of CO_2 production (g) is the total amount of CO_2 production (g) that would have been generated when the sample is completely decomposed. The theoretical amount of CO_2 production (g) was calculated as follows:

$$\text{Theoretical amount of } CO_2 \text{ production (g)} = \frac{\text{Dry weight of the sample (g)} \times \text{carbon content of the sample (\%)}}{100} \times \frac{44}{12},$$

where the dry weight of the sample is the amount of sample in the container, 44 is the molecular weight of CO_2, and 12 is the atomic weight of carbon. The carbon content (%) of the samples was analyzed using the CHN measurement mode of an organic element analyzer (Vario EL Cube, Elementar Ltd., Hanau, Germany). For the disintegration test of films in compost applied in this section, please refer to Section 1.3.4 in Chapter 1.

2.2.8. Molecular Weight Change of Polymers in Seawater

The molecular weight change of polymers in seawater was evaluated using a shaking incubator (Bio-Shaker BR-3000L, TAITEC Co., Saitama, Japan) according to the disintegration of OK biodegradable MARINE. On the morning of May 17, 2022, seawater was sampled in Odaiba, Tokyo Bay, under light rain. The collected seawater was filtered through a 77-μm mesh filter, and inorganic salts were added to the adjusted seawater to obtain 0.5 g/L ammonium chloride and 0.1 g/L potassium dihydrogen phosphate according to the American Society for Testing and Materials (ASTM) D6691-17.[26] The test was performed by placing two 2-cm square films with adjusted seawater (250 mL) in a 500-mL bottle and stirring at 150 rpm and 30°C.

2.2.9. Amplicon Sequencing Analysis of Seawater

For the film fabrication methods applied in this section, please refer to Section 1.2.11 in Chapter 1.

2.3. Results and Discussion

2.3.1. Synthesis of PLA–PCL Alternating Multiblock (PLA-*alt*-PCL) Copolymers

PLA–PCL–PCL triblock copolymers were synthesized by ring-opening polymerization of L-lactide using PCL-diol as an initiator. Subsequently, PLA-*alt*-PCL copolymers were synthesized *via* a chain-extension reaction. **Figure 2** shows representative NMR spectra.

After ring-opening polymerization, typical signals from PLA–PCL–PCL triblock copolymers were observed in the PLA and PCL units **(Figure 2a)**. The CH_3 and CH signals of the PLA chain appeared at 5.1 (A) and 1.5 (B) ppm, respectively, whereas the CH_2 signal for the PCL chain was assigned at 4.0 (C), 2.3

(G), 1.6 (D, F), and 1.4 (E) ppm. For PLA-*alt*-PCL copolymers (**Figure 2b**), the typical signals (a, b, c, d, e, f, and g) of the PLA and PCL chains were assigned (**Figure 2a**). The CH_2OCONH signal adjacent to the urethane group was assigned to 3.1 ppm (h), whereas the peak at the lactate terminus corresponding to B' was infinitesimally small. **Table 1** presents a summary of the synthesis of copolymers. The lactide conversion (%) of PLA–PCL–PLA triblock copolymers in the ring-open polymerization is calculated by the integral ratio at 5.1 ppm (A) due to the lactate units (5.0 ppm [I]) in **Figure 2a**. All lactide conversions exceeded 95%, indicating that the ring-open polymerization was successful. The molecular weight of the PLA segment was determined by ^{1}H NMR based on the ratio of the integral at 5.1 ppm (A) due to the lactate repeating units to the integral at 4.3 ppm (A') at the lactate terminus. Furthermore, the molecular weight of the PCL segment was determined by ^{1}H NMR based on the ratio of the 4.0-ppm integral (C) attributed to the repeating unit to the 4.3-ppm integral (J) of the initiator. The molecular weight of the entire PLA–PCL–PLA triblock copolymers was calculated by ^{1}H NMR based on the sum of PLA and PCL. The PLA content in polymers [PLA (%)] in **Table 1** was calculated by the ratio of the molecular weight of the entire PLA–PCL–PLA triblock copolymers obtained by ^{1}H NMR to the molecular weight of PLA segments obtained by ^{1}H NMR. Copolymers with different lengths of PLA chains were synthesized by varying the amount of L-lactide. The PLA (%) in polymers was adjusted to 50%, 66%, 84%, and 91%. After the synthesis of each PLA–PCL–PLA triblock copolymer with different chain lengths, the NCO/OH molar ratio was added to reach 2 mol mol^{-1} without stopping the reaction in a one-pot reaction system.

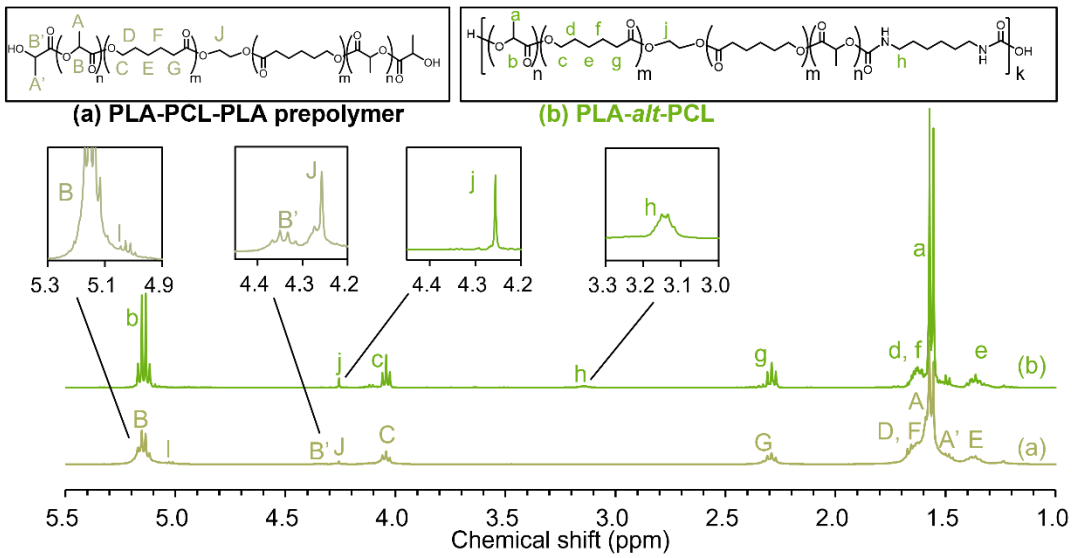

Figure 2. ^{1}H NMR spectra of (a) PLA–PCL–PLA and (b) PLA-*alt*-PCL copolymers.

Table 1. Synthesis of the PLA–PCL–PLA mixture by ring-opening polymerization and chain-extension reaction with HDI.

Copolymers	Ring-opening polymerization[a]								Chain extension[b]				
	PLA[c] (NMR) (%)	Oligomer[d] (Theo.) (g/mol)	Lactide conversion (NMR) (%)	M_n[e] (PLA) (NMR) (g/mol)	M_n[e] (NMR) (g/mol)	M_n[f] (SEC) (g/mol)	M_w[f] (SEC) (g/mol)]	D[f]	[OH]/[NCO][g] (mol/mol)	M_n[f] (SEC) (g/mol)	M_w[f] (SEC) (g/mol)	D[f]	Yield[h] [%]
PLA-*alt*-PCL	50	4,000	95.5	2,200	4,300	5,500	6,700	1.23	2	48,300	133,200	2.76	89
	66	6,000	98.6	3,720	5,600	7,300	9,500	1.29	2	51,200	117,600	2.30	89
	84	10,000	97.2	10,600	12,600	12,600	18,100	1.43	2	49,700	112,100	2.25	97
	90	180,000	96.7	16,000	18,000	18,000	24,900	1.38	2	54,900	114,300	2.08	94
PLA-*ran*-PCL	85[i]	10,000	96.9	11,400	-	13,000	21,800	1.68	2	27,100	61,900	2.23	85

[a]At 180°C for 3 h.
[b]At 180°C for 0.5 h.
[c]PLA (%) = PLA (determined by ^{1}H NMR)/overall (determined by ^{1}H NMR) × 100.
[d]Theoretical molecular weight of PLA synthesized by L-lactide ring-opening polymerization.
[e]Determined by ^{1}H NMR.
[f]Determined by SEC (in chloroform).
[g]Preparation ratio of diols and HDI.
[h]For the final copolymer mixture.
[i]Preparation ratio of PLA-diol and PCL-diol.

2.3.2. Mechanical Properties of Hot-Pressed Films

The mechanical properties of the hot-pressed films were evaluated by tensile testing, as shown in **Figure 3**. **Figure 3a** shows the stress–strain curves of PLA-*alt*-PCL copolymers containing 50%–90% PLA. **Figure 3b–d** present a comparison of the mechanical properties of PLA-*alt*-PCL copolymers to those of neat PLA, neat PCL, PLA-*ran*-PCL copolymers, and PLA/PCL blend composites. The tensile testing results of PLA-*alt*-PCL copolymers, PLA-*ran*-PCL copolymers, PLA/PCL blend composites, neat PLA, and neat PCL are summarized in **Table 2**. Unlike the other samples, we used commercially available high-molecular-weight PLA and PCL. The other samples were also of relatively high molecular weight and should not notably affect the comparison of their mechanical properties. Young's modulus of the PLA-*alt*-PCL copolymers increased with the PLA content and approached the value of neat PLA. Conversely, the elongation at break increased with the decrease in the PLA content and approached the value of neat PCL. The toughness was the highest for the PLA-*alt*-PCL copolymers containing 84% PLA. **Figure 3d** shows a comparison of stress–strain curves for PLA–PCL composites containing the same amount of PLA. The PLA-*alt*-PCL copolymers exhibited improved elongation at break and higher toughness than the PLA-*ran*-PCL copolymers and PLA/PCL blend composites. These results reveal that even with a small amount of PCL segments, PLA-*alt*-PCL copolymers function more effectively and have better mechanical properties than PLA-*ran*-PCL copolymers or blend composites.

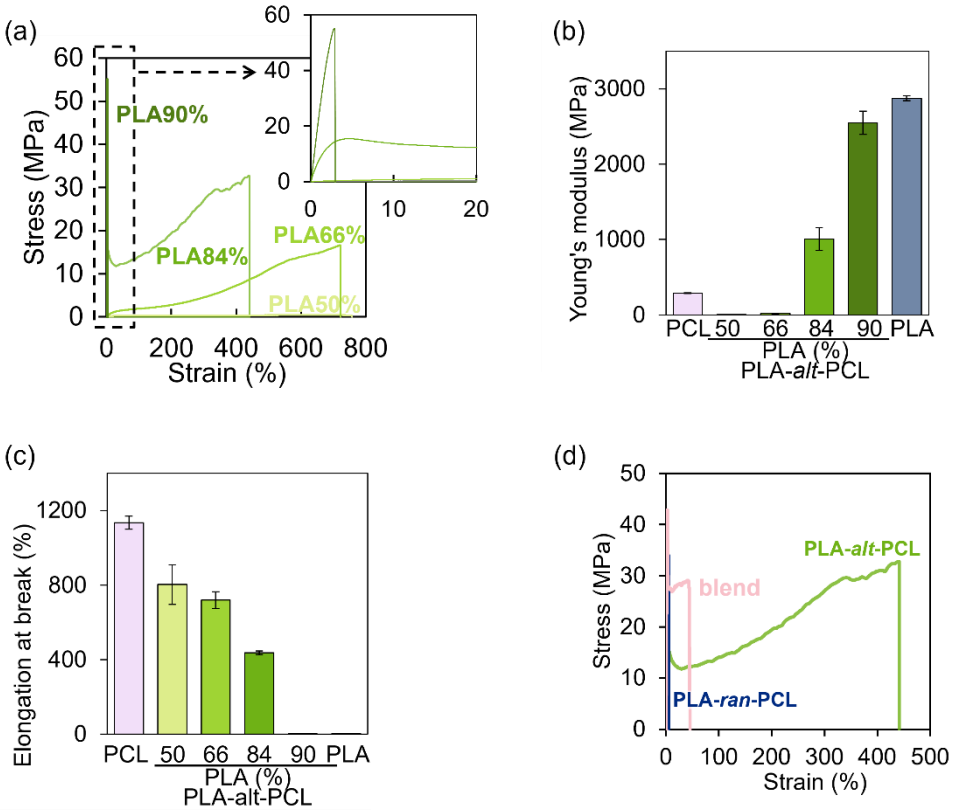

Figure 3. (a) Stress–strain curves obtained by tensile tests of hot-pressed films of PLA-*alt*-PCL copolymers. (b) Young's modulus, (c) elongation at break, and (d) toughness obtained by a tensile test (average, three replicates).

Table 2. Mechanical properties of each sample.

		Mechanical properties (tensile test)			
	PLA (%)	Young's modulus (MPa)	Maximum stress (MPa)	Elongation at break (%)	Toughness (MJ/m^3)
PLA-*alt*-PCL	50	5.13 ± 1.14	0.44 ± 0.06	803 ± 106	1.18 ± 0.19
	66	18.3 ± 1.1	17.8 ± 1.1	720 ± 44	15.1 ± 1.1
	84	1,010 ± 150	31.7 ± 0.9	437 ± 10	83.4 ± 4.8
	90	2,550 ± 160	55.8 ± 1.9	2.91 ± 0.18	0.95 ± 0.11
PLA-*ran*-PCL	85	1,540 ± 120	33.9 ± 0.7	5.10 ± 0.56	1.22 ± 0.20
PLA/PCL blend	85	2,520 ± 40	42.6 ± 2.0	54.0 ± 21.3	16.9 ± 8.6
Neat PLA	100	2,880 ± 30	49.9 ± 3.2	2.26 ± 0.09	0.61 ± 0.06
Neat PCL	0	287 ± 4	41.5 ± 2.2	1,140 ± 40	298 ± 5

2.3.3. Thermal Parameters of Each Sample

Figure 4 shows the results of thermophysical properties evaluated by DSC. The DSC curve shows that T_m and T_g increase with PLA content in the PLA-*alt*-PCL copolymers, whereas T_m and T_g decrease with decreasing PLA content (**Figure 4a**). The DSC results of the PLA-*alt*-PCL copolymers, PLA-*ran*-PCL copolymers, PLA/PCL blend composites, neat PLA, and neat PCL are summarized in **Table 3**. T_g of the PLA-*alt*-PCL copolymers with a PLA content of 84% was 16°C, whereas that of the PLA-*ran*-PCL copolymers containing the same amount of PLA was 23°C (**Figure 4b**). T_g values of PLA-*alt*-PCL and PLA-*ran*-PCL copolymers were lower than room temperature and T_g of PLA (55°C), indicating that the function of the PCL segments is expressed by copolymerization. The PLA/PCL blend composite exhibited T_g values of −76°C and 59°C derived from PLA and PCL, respectively. The PLA-*alt*-PCL copolymers and PLA-*ran*-PCL copolymers exhibited T_m exceeding 150°C, as well as the neat PLA, when the PLA content was >84%. In addition, T_m of the PLA-*alt*-PCL copolymers decreased with decreasing the PLA content. T_m disappeared, and the copolymers became amorphous at 50%. The PLA/PCL blend composites exhibited two melting points at 55°C and 152°C derived from PLA and PCL, respectively.

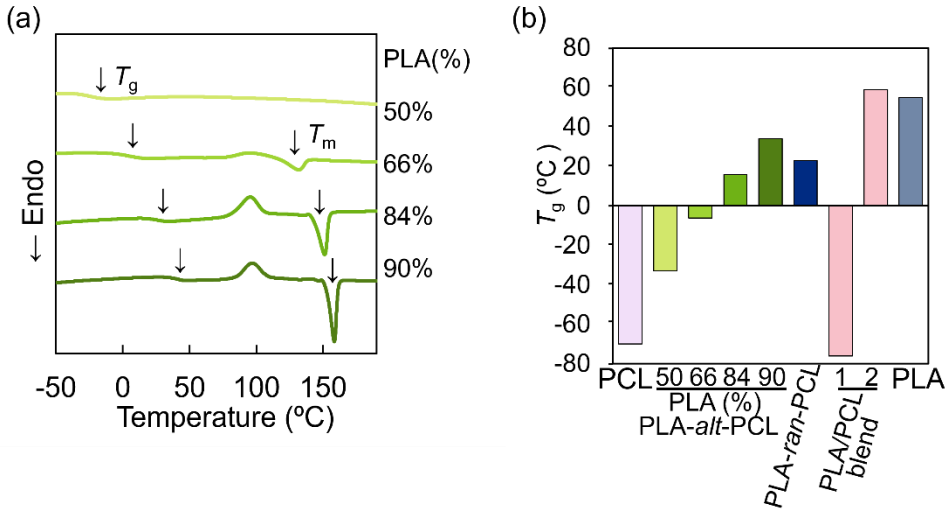

Figure 4. Thermal parameters of each sample. (a) DSC curves of PLA-*alt*-PCL copolymers and (b) T_g of each sample.

Table 3. Thermal parameters of each sample.

		Thermal parameters (DSC)	
	PLA (%)	T_g (°C)	T_m (°C)
PLA-*alt*-PCL	50	−33	-
	66	−6	132
	84	16	151
	90	34	158
PLA-*ran*-PCL	85	23	155
PLA/PCL blend	85	−76, 59	55, 152
Neat PLA	100	55	150
Neat PCL	0	−70	55

2.3.4. Biodegradation Test of a Powder and Disintegration Test of Films with a Compost

The results of the 1-month compost disintegration test for each film of PLA and PLA-*alt*-PCL copolymers are shown in **Figure 5**. Each film became brittle and broken 10 days after burial in compost and disappeared and collapsed without trace after 30 days. Further extension of the test would result in further disappearance. The results of the compost biodegradation test are shown in **Figure 6**. After incubation for 45 days, compared with the CO_2 production (10 g) and biodegradability (70%) of cellulose, the PLA-*alt*-PCL copolymers and PLA exhibited higher CO_2 production (>16 g) and biodegradability (96%). These results indicate that PLA-*alt*-PCL copolymers with a PLA content of 84% were mineralized and biodegraded in compost as well as in PLA. Furthermore, the PLA-*alt*-PCL copolymers outperformed PLA in CO_2 production and biodegradability for the first 22 days of the test, indicating that it was more biodegradable than PLA in the initial stages. This outcome may result from the lower T_g (**Figure 4**, **Table 3**) and lower crystallinity of the PLA-*alt*-PCL copolymers. This was attributed to the increased flexibility of the amorphous regions of the polymer chains in the compost, which made them more easily degradable.

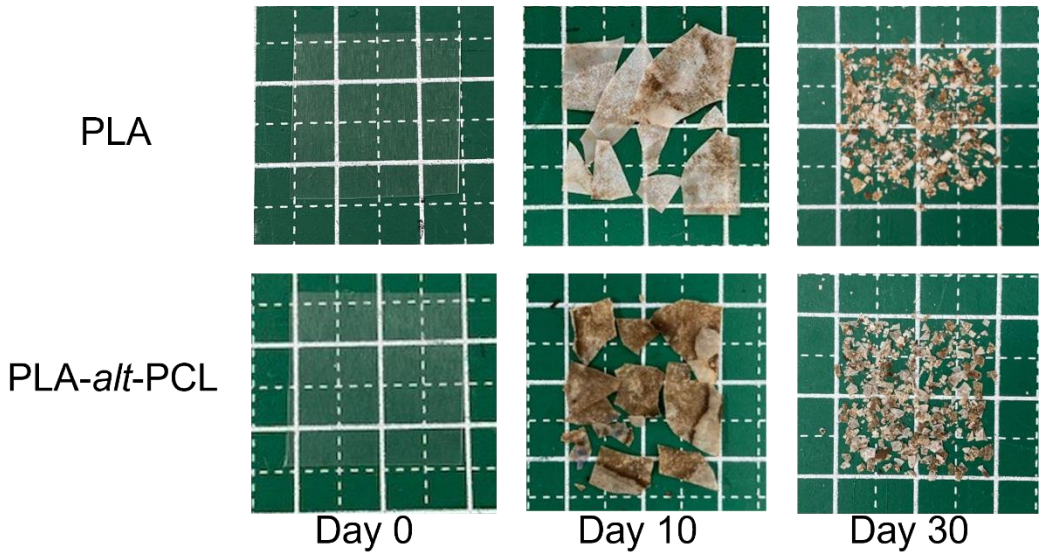

Figure 5. One-month compost disintegration test of each film of PLA and PLA-*alt*-PCL copolymers.

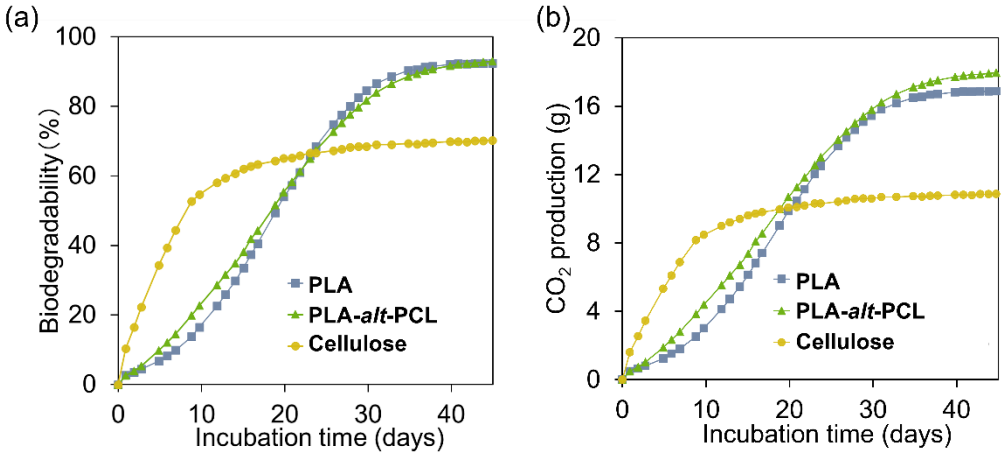

Figure 6. (a) Biodegradability and (b) CO_2 production of PLA and PLA-*alt*-PCL copolymer (84% PLA). and cellulose microcrystalline (control) by compost test. (average two replicates).

2.3.5. Molecular Weight Change of Films in Seawater

Changes in the molecular weight of each film in seawater are shown in **Figure 7a**. The molecular weight of PLA-*alt*-PCL copolymers, as measured by SEC, decreased from the initial value at the beginning of the test from M_n = 52,300 g/mol and M_w = 105,000 g/mol to M_n = 5,500 g/mol and M_w = 14,400 g/mol. It was observed to decrease to 11% of its initial value after 6 months. Although the molecular weight of PLA decreased from M_n = 44,000 g/mol and M_w = 94,000 g/mol to M_n = 31,300 g/mol and M_w = 78,700 g/mol, it maintained 71% of the initial value. The molecular weight of PLA-*ran*-PCL copolymers decreased from M_n = 22,000 g/mol and M_w = 49,000 g/mol to M_n = 8,200 g/mol and M_w = 18,900 g/mol, maintaining 38% of the initial value. **Figure 7b**–**d** show changes in the molecular weight distribution curve of each sample. The SEC curve of the PLA-*alt*-PCL copolymers shows an increase in polydispersity and a peak shift from the high- to the low-molecular-weight side (**Figure 7b**). The polydispersity increased for PLA; however, no significant peak shift was observed from the high- to the low-molecular-weight side (**Figure 7c**). Although no increase in polydispersity was observed for the PLA-*ran*-PCL copolymers, a slight peak shift to the low-molecular-weight side was observed (**Figure 7d**). For PLA to be mineralized and biodegraded, several bonds must be cleaved in the initial stages of degradation and reduced to an oligomer size that can be absorbed by a microbe.[13] The PLA-*alt*-PCL copolymers have low T_g (**Figure 4**, **Table 3**) and crystallinity; therefore, their molecular weight is likely to decrease in seawater as well as in compost. Furthermore, PCL chains are irregularly arranged in the PLA-*ran*-PCL copolymers. Conversely, in the PLA-*alt*-PCL copolymers, PCL chains are regularly arranged between PLA chains, which is assumed to be an influence, resulting in efficient degradation in the initial stages and low molecular weight. Accordingly, biodegradability in seawater is expected to improve; however, mineralization tests and further studies in seawater are necessary to prove this hypothesis.

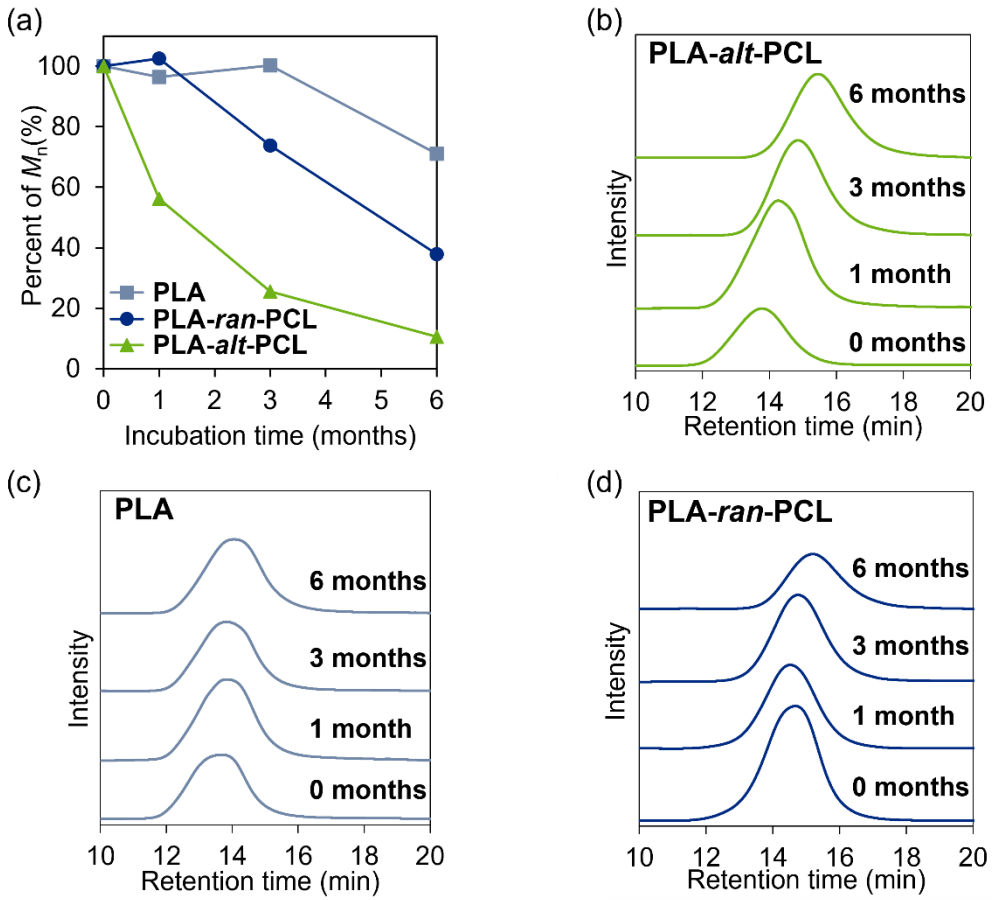

Figure 7. (a) M_n change of polymers in seawater over 6 months. Molecular weight shifts of (b) PLA-*alt*-PCL copolymer (84% PLA), (c) PLA, and (d) PLA-*ran*-PCL copolymer and cellulose microcrystalline (control) by compost test (average two replicates).

2.3.6. Relative Abundance of Bacteria in Seawater and Biofilm

Figure 8 shows the appearance of each film removed from seawater after 6 months. The PLA film maintained its shape and remained transparent (**Figure 8b**). In contrast, the PLA-*alt*-PCL films became brittle and turbid and were notably covered with biofilm (**Figure 8a**). The PLA-*ran*-PCL copolymer films became brittle and turbid and were slightly covered with biofilm (**Figure 8c**). Although biofilms could form on the surface of non-biodegradable commodity plastics, such as PE and PS,[27] and thus do not suggest marine biodegradability, the DNA concentration extracted from the test seawater and the biofilm in the PLA-*alt*-PCL copolymers was approximately 1.8 times higher than that in the PLA, indicating that microorganisms were activated and grew (**Table 4**). Therefore, amplicon sequencing analysis was conducted to evaluate the relative abundance of bacterial phyla, classes, and orders in the biofilm and test seawater (**Figure 9**). Bhagwat et al. stated that the *Proteobacteria* phylum is most observed in marine plastic debris.[28] As shown in **Figure 9a**, the abundance of the phylum Proteobacteria in the PLA-*alt*-PCL copolymers (92%) and PLA (75%) increased compared with the blank (58%). Furthermore, the class *Alphaproteobacteria*, which is vital for the initial formation of biofilms and attaches to film surfaces,[29] was

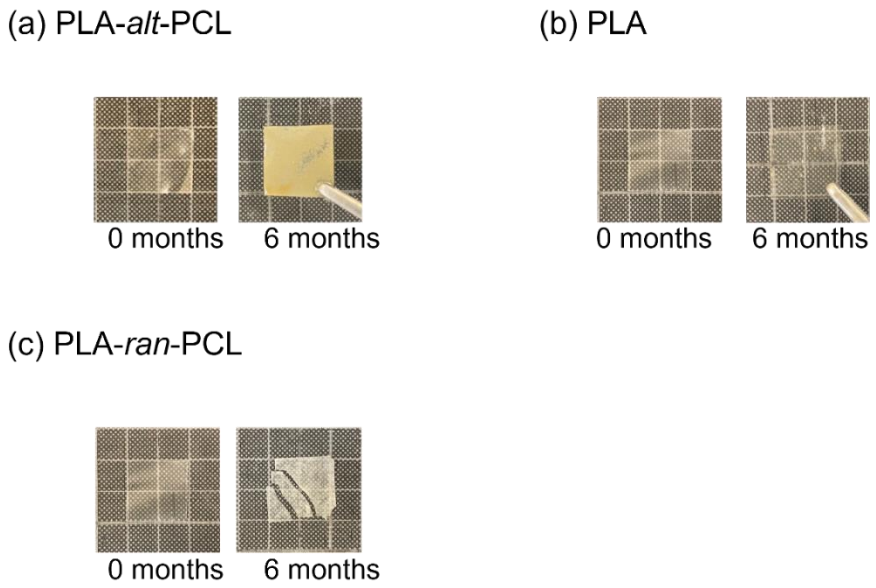

Figure 8. Appearances of the (a) PLA-*alt*-PCL copolymer (84% PLA), (b) PLA, and (c) PLA-*ran*-PCL copolymer films recovered from seawater.

observed in each film (**Figure 9b**). As shown in **Figure 9c**, the order *Rhodobacterales* was present in both samples. This order is a key metric for biofilm formation, and the exopolysaccharides produced by this order promote the establishment of other microbes.[30] The order *Xanthomonadales* was abundant in both samples, particularly in the PLA-*alt*-PCL copolymers, in the order *Sneathiellales* (22%), *Sphingomonadales* (19%), and *Rhizobiales* (12%). Several species of *Xanthomonadales* have been reported to produce PLA-degrading enzymes,[31,32] which are expected to exhibit activity against relatively high-molecular-weight PLA during the initial stages of degradation. Additionally, several species of *Rhizobiales* have been reported to produce enzymes that show degrading activity against PCL and relatively low-molecular-weight PLA,[33,34] which are expected to be effective in low-molecular-weight PLA after degradation has progressed or in copolymers containing low-molecular-weight PLA segments. Biofilm formation may have facilitated the establishment of microorganisms and created an environment suitable for biodegradation. However, further studies, such as mineralization and enzyme activity tests, are required to confirm that PLA-*alt*-PCL copolymers exhibit marine biodegradability under the influence of the above enzymes.

Table 4. DNA concentrations and A260/A280 in 250 mL of test seawater. They were measured using a spectrophotometer (NanoDrop ND8000, Thermo Fisher Scientific, MA, USA).

	DNA concentrations (ng/μL)	A260/280
Blank	3.2	1.73
PLA-*alt*-PCL	5.7	1.99
PLA	3.1	1.69

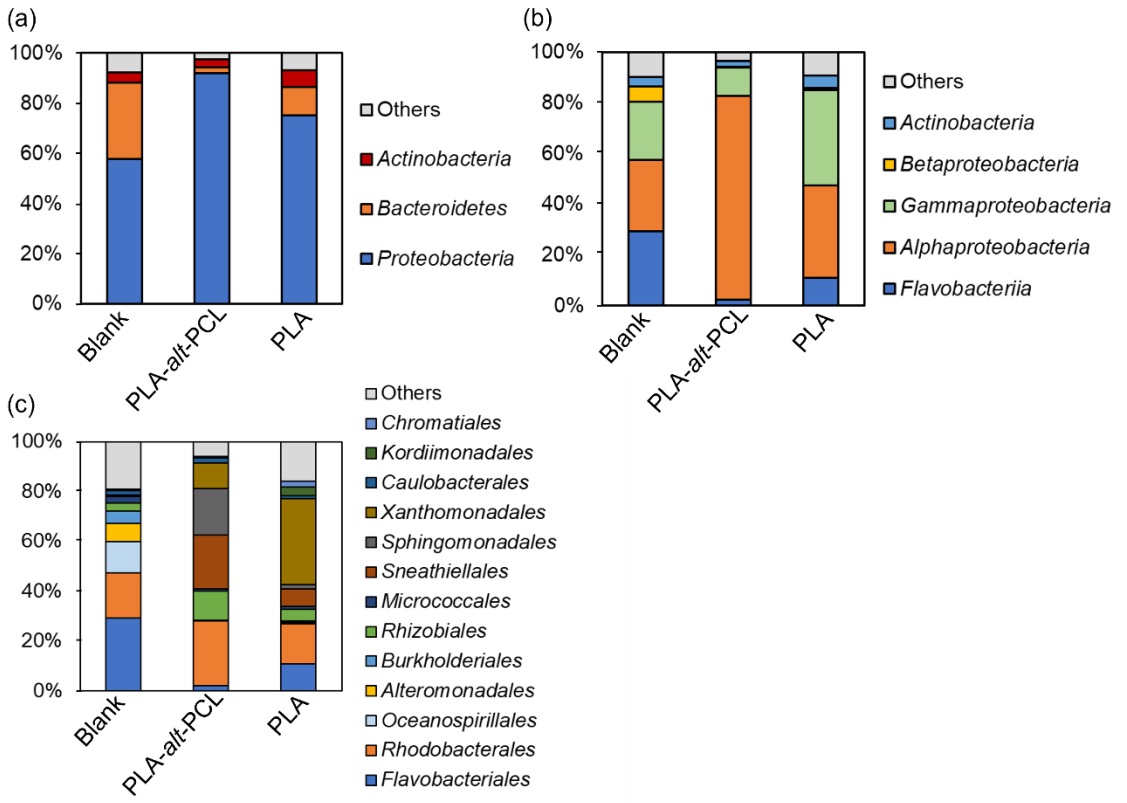

Figure 9. Relative abundances of (a) phylum, (b) class, and (c) order of bacteria in the test seawater containing a biofilm obtained over the 6-month marine disintegration test. Various bacteria classified into 161 families and unattributed bacteria were identified from the test seawater, and bacteria with abundances <2% or unattributed are labeled as "Others."

2.4. Conclusion

The demand for biodegradable plastics and bioplastics is increasing because of environmental pollution issues and the need to reduce dependence on petroleum resources. These materials must demonstrate environmental friendliness and have high mechanical properties. This study synthesized a tough biodegradable plastic based on PLA and evaluated its biodegradability. The triblock copolymers PLA–PCL–PLA with PLA composition ratios of 50%–90% were synthesized by ring-opening polymerization of L-lactide using PCL-diol as an initiator, which was then chain-extended to easily synthesize PLA-*alt*-PCL copolymers in the same reaction system. The PLA-*alt*-PCL copolymers exhibited controllable mechanical properties by changing the PLA chain lengths, higher toughness, and T_g below room temperature compared with other composites. This outcome may result from the effective function of the regularly arranged PCL chains, which improved the properties. In compost, it showed significant disintegration and biodegraded as completely as PLA. In the initial stages of testing, CO_2 production and biodegradability were higher than PLA. The above results indicate that the lower T_g of PLA-*alt*-PCL copolymers than PLA increased the flexibility of the amorphous regions of the polymer chains, thereby affecting their degradability in compost. The observed change in molecular weight in seawater

demonstrated that the PLA-*alt*-PCL copolymers had a substantially lower molecular weight than the PLA-*ran*-PCL copolymers from the initial stage of the test. PCL chains can be regularly arranged between PLA chains in alternating multiblock copolymerization, whereas the introduction of PCL chains cannot be controlled in random copolymerization. PLA-*alt*-PCL copolymers exhibited improved initial degradability and were more likely to oligomerize in seawater. Additional studies are required to confirm their marine biodegradability. This study may provide a solution to the plastic waste problem and is expected to be deployed in various applications requiring high toughness and biodegradability.

2.5. References

(1) Geyer, R.; Jambeck, J. R.; Law, K. L. Production, use, and fate of all plastics ever made. *Sci. Adv*. **2017**, *3* (7) 25-29. https://doi.org/10.1126/sciadv.1700782.

(2) Ritchie, H.; Roser, M. Plastic Pollution. *Our World in Data* (updated in 2022-04). https://ourworldindata.org/plastic-pollution.

(3) Vanapalli, K. R.; Sharma, H. B.; Ranjan, V. P.; Samal, B.; Bhattacharya, J.; Dubey, B. K.; Goel, S. Challenges and strategies for effective plastic waste management during and post COVID-19 pandemic. *Sci. Total Environ.* **2021**, 750. https://doi.org/10.1016/j.scitotenv.2020.141514.

(4) Mathalon, A.; Hill, P. Microplastic fibers in the intertidal ecosystem surrounding Halifax Harbor, Nova Scotia. *Mar. Pollut. Bull*. **2014**, *81* (1), 69–79. https://doi.org/10.1016/j.marpolbul.2014.02.018.

(5) Jambeck, J. R.; Geyer, R.; Wilcox, C.; Siegler, T.R.; Perryman, M,; Andray, A.; Narayan, R.; Law, K.L. Marine Pollution. Plastic waste inputs from land into the ocean. *Science* **2015**, *347* (6223), 768–771. https://doi.org/10.1126/science.1260352.

(6) Walker, T. R. Drowning in debris: Solutions for a global pervasive marine pollution problem. *Mar. Pollut. Bull.* **2018**, *126*, 338. https://doi.org/10.1016/j.marpolbul.2017.11.039.

(7) Palai, B.; Mohanty, S.; Nayak, S. K. A Comparison on Biodegradation Behaviour of Polylactic Acid (PLA) Based Blown Films by Incorporating Thermoplasticized Starch (TPS) and Poly (Butylene Succinate-co-Adipate) (PBSA) Biopolymer in Soil. *J. Polym. Environ.* **2021**, *29*, 2772. https://doi.org/10.1007/s10924-021-02055-z.

(8) European Bioplastics. BIOPLASTICS facts and figures. *European bioplastics* **2021**. https://docs.european-bioplastics.org/publications/EUBP_Facts_and_figures.pdf.

(9) Lucas, N.; Bienaime, C.; Belloy, C.; Queneudec, M.; Silvestre, F.; Nava-Saucedo, J. E. Polymer biodegradation: Mechanisms and estimation techniques – A review. *Chemosphere* **2008**, *73*, 429–442. https://doi.org/10.1016/j.chemosphere.2008.06.064.

(10) Haider, T. P.; Völker, C.; Kramm, J.; Landfester, K.; Wurm, F. R. Plastics of the Future? The Impact of Biodegradable Polymers on the Environment and on Society. *Angewandte Chemie* **2019**, *131* (1), 50–63. https://doi.org/10.1002/ange.201805766.

(11) Lunt, J. Large-scale production, properties and commercial applications of polylactic acid polymers. *Polym. Degrad. Stab.* **1998**, *59*, 145-152. https://doi.org/10.1016/S0141-3910(97)00148-1.

(12) Tokiwa, Y.; Jarerat, A. Biodegradation of poly(L-lactide) . *Biotechnol. Lett.* **2004**, *26*, 771–777. https://doi.org/10.1023/B:BILE.0000025927.31028.e3.

(13) Souza, P. M. S.; Morales, A. R.; Marin-Morales, M. A.; Mei, L. H. I. PLA and Montmorilonite Nanocomposites: Properties, Biodegradation and Potential Toxicity. *J. Polym. Environ.* **2013**, *21* (3), 738–759. https://doi.org/10.1007/s10924-013-0577-z.

(14) Wang, G.-X.; Huang, D.; Ji, J. H.; Völker, C.; Wurm, F. R. Seawater-Degradable Polymers—Fighting the Marine Plastic Pollution. *Adv. Sci*. **2021**, *8*, 2001121 https://doi.org/10.1002/advs.202001121.

(15) Stloukal, P.; Pekařová, S.; Kalendova, A.; Mattausch, H.; Laske, S.; Holzer, C.; Chitu, L.; Bodner, S.; Maier, G.; Slouf, M.; Koutny, M. Kinetics and mechanism of the biodegradation of PLA/clay nanocomposites during thermophilic phase of composting process. *Waste Management* **2015**, *42*, 31–40. https://doi.org/10.1016/j.wasman.2015.04.006.

(16) Karamanlioglu, M.; Preziosi, R.; Robson, G. D. Abiotic and biotic environmental degradation of the bioplastic polymer poly(lactic acid): A review. *Polym. Degrad. Stab*. **2017**, *137*, 122–130. https://doi.org/10.1016/j.polymdegradstab.2017.01.009.

(17) Arrieta, M. P.; Samper, M. D.; Aldas, M.; López, J. On the Use of PLA-PHB Blends for Sustainable Food Packaging Applications. *Materials* **2017**, 10. https://doi.org/10.3390/ma10091008.
(18) Pluta, M.; Murariu, M.; Alexandre, M.; Galeski, A.; Dubois, P. Polylactide compositions. The influence of ageing on the structure, thermal and viscoelastic properties of PLA/calcium sulfate composites. *Polym. Degrad. Stab.* **2008**, *93* (5), 925–931. https://doi.org/10.1016/j.polymdegradstab.2008.02.001.
(19) Fortelny, I.; Ujcic, A.; Fambri, L.; Slouf, M. Phase Structure, Compatibility, and Toughness of PLA/PCL Blends: A Review. *Front. Mater.* **2019**, *6*, 206. https://doi.org/10.3389/fmats.2019.00206.
(20) Carmona, V. B.; Corrêa, A. C.; Marconcini, J. M.; Mattoso, L. H. C. Properties of a Biodegradable Ternary Blend of Thermoplastic Starch (TPS), Poly(ε-Caprolactone) (PCL) and Poly(Lactic Acid) (PLA). *J. Polym. Environ.* **2015,** *23* (1), 83–89. https://doi.org/10.1007/s10924-014-0666-7.
(21) Choi, N. S.; Kim, C. H.; Cho, K. Y.; Park, J. K. Morphology and hydrolysis of PCL/PLLA blends compatibilized with P(LLA-*co*-ϵCL) or P(LLA-*b*-ϵCL). *J. Appl. Polym. Sci.* **2002**, *86* (8), 1892–1898. https://doi.org/10.1002/app.11134.
(22) Mulchandani, N.; Masutani, K.; Kumar, S.; Yamane, H.; Sakurai, S.; Kimura, Y.; Katiyar, V. Toughened PLA-*b*-PCL-*b*-PLA triblock copolymer based biomaterials: effect of self-assembled nanostructure and stereocomplexation on the mechanical properties. *Polym. Chem*. **2021**, *12* (26), 3806–3824. https://doi.org/10.1039/d1py00429h.
(23) Huang, M. H.; Li, S.; Vert, M. Synthesis and degradation of PLA-PCL-PLA triblock copolymer prepared by successive polymerization of ε-caprolactone and DL-lactide. *Polymer (Guildf)* **2004**, *45* (26), 8675–8681. https://doi.org/10.1016/j.polymer.2004.10.054.
(24) Ali, F. B.; Kang, D. J.; Kim, M. P.; Cho, C.-H.; Kim, B. J. Synthesis of biodegradable and flexible, polylactic acid based, thermoplastic polyurethane with high gas barrier properties. *Polym. Int*. **2014**, *63*, 1620–1626. https://doi.org/10.1002/pi.4662.
(25) Cohn, D.; Hotovely Salomon, A. Designing biodegradable multiblock PCL/PLA thermoplastic elastomers. **2005**, *26* (15), 2297–2305. https://doi.org/10.1016/j.biomaterials.2004.07.052.
(26) ASTM D6691-17, Standard Test Method for Determining Aerobic Biodegradation of Plastic Materials in the Marine Environment by a Defined Microbial Consortium or Natural Sea Water Inoculum. ASTM International (2018 updated). https://doi.org/10.1520/D6691-17.
(27) Zettler, E. R.;Mincer, T. J.; Amaral-Zettler, L. A. Life in the "Plastisphere"_ Microbial Communities on Plastic Marine Debris _ Environmental Science & Technology. *Environ. Sci. Technol*. **2013**, 7137–7146. https://doi.org/https://doi.org/10.1021/acs.est.0c07952.
(28) Bhagwat, G.; Zhu, Q.; O'Connor, W.; Subashchandrabose, S.; Grainge, I.; Knight, R.; Palanisami, T. Exploring the Composition and Functions of Plastic Microbiome Using Whole-Genome Sequencing. *Environ. Sci. Technol.* **2021**, *55* (8), 4899–4913. https://doi.org/10.1021/acs.est.0c07952.
(29) De Tender, C. A.; Devriese, L. I.; Haegeman, A.; Maes, S.; Ruttink, T.; Dawyndt, P. Bacterial Community Profiling of Plastic Litter in the Belgian Part of the North Sea. *Environ. Sci. Technol.* **2015**, *49* (16), 9629–9638. https://doi.org/10.1021/acs.est.5b01093.
(30) Amaral-Zettler, L. A.; Zettler, E. R.; Mincer, T. J. Ecology of the plastisphere. *Nat. Rev. Microbiol.* **2020**, *18*, 139–151. https://doi.org/10.1038/s41579-019-0308-0.
(31) Hajighasemi, M.; Nocek, B. P.; Tchigvintsev, A.; Brown, G.; Flick, R.; Xu, X.; Cui, H.; Hai, T.; Joachimiak, A.; Golyshin, P. N.; Savchenko, A.; Edwards, E. A.; Yakunin, A. F. Biochemical and Structural Insights into Enzymatic Depolymerization of Polylactic Acid and Other Polyesters by Microbial Carboxylesterases. *Biomacromolecules* **2016**, *17*, 2027–2039. https://doi.org/10.1021/acs.biomac.6b00223.
(32) Tournier, V.; Duquesne, S.; Guillamot, F.; Cramail, H.; Taton, D.; Marty, A.; André, I. Enzymes' Power for Plastics Degradation. *Chem. Rev.*, **2023**, *123*, 5612–5701. https://doi.org/10.1021/acs.chemrev.2c00644.
(33) Yagi, H.; Ninomiya, F.; Funabashi, M.; Kunioka, M. Mesophilic anaerobic biodegradation test and analysis of eubacteria and archaea involved in anaerobic biodegradation of four specified biodegradable polyesters. *Polym. Degrad. Stab.* **2014**, *110*, 278–283. https://doi.org/10.1016/j.polymdegradstab.2014.08.031.
(34) Bubpachat, T.; Sombatsompop, N.; Prapagdee, B. Isolation and role of polylactic acid-degrading bacteria on degrading enzymes productions and PLA biodegradability at mesophilic conditions. *Polym. Degrad. Stab*. **2018**, *152*, 75–85. https://doi.org/10.1016/j.polymdegradstab.2018.03.023.

Chapter 3. Biomass-Derived Poly(lactic acid) and Poly(3-methyl-1,5-pentanediol sebacate) Alternating Multiblock Copolymers with Improved Marine Biodegradability and Mechanical Properties

3.1. Introduction

Plastics have become an indispensable part of our daily life, with production increasing rapidly since 1950 and reaching 460 Mt in 2019.[1] However, reliance on fossil resources[2,3] and the mismanagement of plastic disposal[4] have caused serious environmental problems. In the 1980s, the use of fossil resources reached a critical level, necessitating a gradual reduction in industrial applications.[3] Since then, attention has shifted to sustainable bioresources, with bioplastic production projected to increase to 7.43 Mt by 2028.[5] Marine pollution caused by plastics, reported since the early 1970s, remains a global problem.[6,7] By 2060, 11.6 Mt of improperly managed plastics is estimated to be discharged into aquatic environments, of which 4 Mt will be discharged into the ocean.[1] Discarded fishing gear can have a serious impact on marine organisms,[8,9] and microplastics can accumulate throughout the food chain, potentially affecting human health.[10,11] Therefore, biodegradable plastics should be developed from sustainable bioresources. PLA is an attractive biobased and biodegradable material with desirable properties, including ease of manufacture, zero toxicity, biocompatibility, high mechanical strength, thermoplasticity, and compostability.[12–14] Accordingly, PLA is a major candidate for industrial applications, accounting for 31% of bioplastic production at 0.68 Mt in 2023, which is expected to grow to 43.6% or 3.24 Mt in the next 5 years.[5] It is ultimately decomposed into H_2O and CO_2,[13,15] hydrolyzed into low-molecular-weight oligomers in the compost, and mineralized by microorganisms.[15,16] However, PLA biodegradation is limited to composting environments;[17,18] it is poorly biodegradable in seawater owing to the lack of microorganisms.[19] Notably, T_g of PLA is higher than the ambient temperature, which prevents its conversion to a lower molecular weight.[13,17] Given the presence of complicated and uncontrollable external factors, researchers have focused on the intrinsic degradation factors of polymers in marine environments, such as their crystallinity, T_g, and hydrophobicity.[20,21] Recently, PLA oligomers have demonstrated potential marine biodegradability in marine environments,[22] and the possibility of microorganisms suggesting marine biodegradation of PLA chains in marine environments has been discussed.[23,24] Melt blending or copolymerization with biodegradable materials is a practical approach for improving the potential marine biodegradability of PLA. Blends with water-soluble, degradable thermoplastic starch[25] or polyvinyl alcohol[26] take advantage of the readily degradable nature of the material, with the biodegradable domains being degraded primarily by the incorporated material. However, PLA remains stable. Inspired by the intramolecular transesterification mechanism of RNA, which rapidly hydrolyzes due to its phosphate ester linkages, an attempt has been made to improve degradability in seawater by introducing synthetic phosphate linkages as breaking points into PLA through copolymerization.[27] Additionally, the introduction of biodegradable units into PLA through copolymerization compensates for the brittleness of PLA.[14,24] Copolyesters with long-chain

dicarboxylic acids introduced into polyethylene succinate and PBS backbones exhibit high marine biodegradability.[28] Accordingly, the introduction of long-chain dicarboxylic acids into PLA-based polymers would generate numerous degradation points and improve their marine biodegradability. Sebacic acid is produced by the alkaline pyrolysis of castor oil[29] and has attracted considerable attention as a raw material for bioplastics.[30] Promising results have been obtained in biodegradation tests of polymers based on this finding.[31,32] Kuraray Co., Ltd. developed PMPDSe-diol, which uses sebacic acid as the dicarboxylic acid and 3-methyl-1,5-pentanediol (MPD) as the diol.[33] Currently, MPD is made from petroleum; however, Kuraray Co., Ltd. is producing partially biobased products in some of its plants certified under the ISCC PLUS sustainable product certification system.[34] Other studies have been conducted to convert MPD into fully biobased products.[35,36] Visolis Inc. is developing biobased products.[37,38] To the best of our knowledge, the synthesis and evaluation of the versatility and biodegradability of PLA-based copolymers using sebacic acid as the biodegradable unit have not been extensively discussed. For example, studies on synthesis have reported the formation of relatively low-molecular-weight PLA–poly(sebacic acid) triblock copolymers, which have been investigated for their degradation and drug release properties in drug delivery applications.[39,40] Additionally, poly(alditol sebacate)–PLA copolymers have been synthesized and studied for their wettability and hydrolytic degradation properties in water.[41] Therefore, this study focuses on the synthesis and evaluation of high-molecular-weight PLA-based copolymers using sebacic acid units as the biodegradable unit to control the mechanical properties and improve biodegradability.

In this study, PLA-based PLA–PMPDSe alternating multiblock (PLA-*alt*-PMPDSe) copolymers were synthesized *via* the copolymerization of PLA and sebacic acid–based prepolymers, followed by a chain-extension reaction with HDI. Copolymers with different PLA chain lengths were prepared *via* ring-opening polymerization. Regularly arranged PLA-*alt*-PMPDSe copolymer (a) films were compared to PLA–PMPDSe random multiblock (PLA-*ran*-PMPDSe) copolymer (b) films. Their thermal and mechanical properties and biodegradability were evaluated (**Figure 1**). To contribute to the development of sustainable bioplastics with high biomass content materials, this study aimed to control the thermal and mechanical properties of PLA by changing its chain length and to enhance the biodegradability of the copolymers.

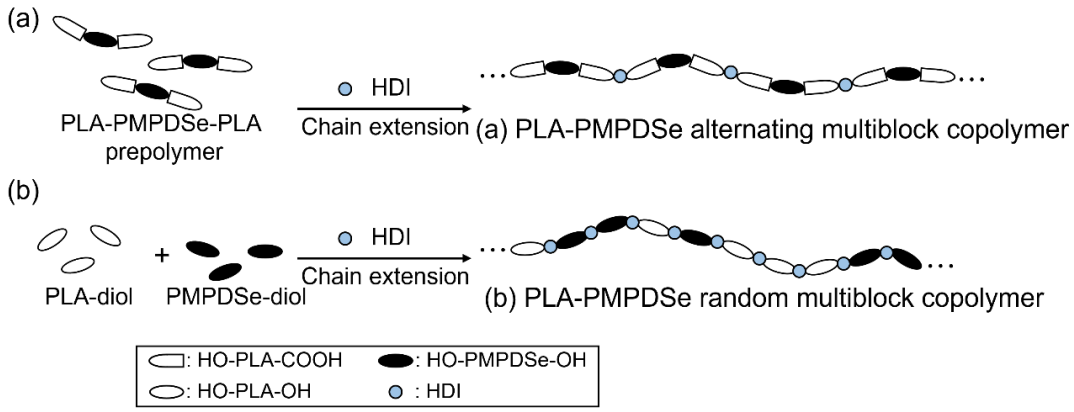

Figure 1. Model structures of (a) PLA-*alt*-PMPDSe and (b) PLA-*ran*-PMPDSe copolymerization. The OH group side of the segment is rounded, and the COOH group side is flat.

3.2. Experimental Section

3.2.1. Materials

PMPDSe-diol (M_n = 2,000) (Kuraray Polyol P-2050) was supplied by Kuraray Co., Ltd. (Tokyo, Japan). Chloroform was purchased from Nacalai Tesque, Inc. (Kyoto, Japan). Tin(II) 2-ethylhexanoate, methanol, diethyl ether, sea sand (425–850 μm), ammonium chloride, and soda lime were purchased from Fujifilm Wako Pure Chemical Co. (Osaka, Japan). L-lactide, 1,4-butanediol, HDI, and potassium dihydrogen phosphate were purchased from Tokyo Chem. Inc. (Tokyo, Japan). PLA (Ingeo Biopolymer 2003D) was purchased from NatureWorks LLC (Nebraska, USA). All the reagents were used as received.

3.2.2. Synthesis of PLA–PMPDSe Alternating Multiblock (PLA-*alt*-PMPDSe) Copolymers

To synthesize PLA–PMPDSe–PLA, PMPDSe-diol and L-lactide were placed in a 50-mL three-neck flask and vacuum-dried at room temperature for 3 h. To synthesize copolymers with different PLA chain lengths, the amount of L-lactide was adjusted with PMPDSe-diol/L-lactide ratios of 5/5, 3/6, 2/8, or 1/8 g. A solution of tin(II) 2-ethylhexanoate (1.0 mol% of the hydroxyl end of the PMPDSe-diol) was added to the mixture, which was vacuum-dried at room temperature for 2 h. The ring-opening polymerization was performed at 180°C for 3 h with stirring (150 rpm) under a nitrogen atmosphere. Subsequently, HDI was added to the mixture at an NCO/OH molar ratio of 1.5 mol mol^{-1}. The chain-extension reaction was conducted at 180°C for 0.5 h with stirring (100 rpm) under a nitrogen atmosphere. The final product was dissolved in chloroform and poured into excess methanol for reprecipitation. The precipitate was filtered, washed with methanol, and vacuum-dried to obtain PLA-*alt*-PMPDSe copolymers as white solids.

3.2.3. Synthesis of PLA–PMPDSe Random Multiblock (PLA-*ran*-PMPDSe) Copolymers

PLA-diol was synthesized by the ring-opening polymerization of L-lactide using 1,4-butanediol as the initiator (Section 3.2.2). To synthesize PLA-diol with different PLA chain lengths, the amount of L-lactide was adjusted, with 1,4-butanediol/L-lactide ratios of 0.63/14, 0.45/20, 0.23/20, or 0.11/20 g. The synthesized mixture was dissolved in chloroform and poured into excess diethyl ether for reprecipitation. The precipitate was filtered, washed with diethyl ether, and vacuum-dried to obtain PLA-diol. To synthesize the PLA-*ran*-PMPDSe copolymers, PLA-diol of varying chain lengths and PMPDSe-diol were placed in a flask in equimolar amounts, and HDI was added at an NCO/OH molar ratio of 1.5 mol mol^{-1}. Subsequently, the mixture was heated at 180°C for 0.5 h with stirring (100 rpm) under a nitrogen atmosphere. The final product was dissolved in chloroform and poured into excess methanol for reprecipitation. The precipitate was filtered, washed with methanol, and vacuum-dried to obtain the PLA-*ran*-PMPDSe copolymers. For comparison, chain-extended PLA (PLA-CE) was prepared by placing PLA-diol in a flask, adding HDI at an NCO/OH molar ratio of 1.5 mol mol^{-1}, and heating at 180°C for 0.5 h with stirring under a nitrogen atmosphere. Similarly, PMPDSe-CE was prepared by adding PMPDSe-diol and HDI at an NCO/OH molar ratio of 1.5 mol mol^{-1} and heating under the same conditions as PLA-CE. Reprecipitation for PLA-CE and PMPDSe-CE was performed using chloroform and methanol.

3.2.4. Fabrication of Films

For the film fabrication methods applied in this section, please refer to Section 1.2.6 in Chapter 1.

3.2.5. Measurement

For ^{1}H NMR, SEC, tensile testing, and TGA methods applied in this section, refer to Section 1.2.7 in Chapter 1. For the WCA test and TGA methods applied in this section, refer to Section 2.2.10 in Chapter 1. T_g and melting temperatures (T_m) of the samples were measured by DSC using a thermal analysis system (DSC6220, Hitachi High-Tech Science Co., Tokyo, Japan). The sample (approximately 3 mg) was prepared (drying conditions: dried overnight at 90°C and then slowly cooled), heated from −80 °C to 200 °C at a heating rate of 10°C/min, and then kept at 200°C for 3 min to melt. After heating, the sample was cooled from 200 °C to −80 °C at a cooling rate of 10 °C/min. The temperature was maintained at −80 °C for 3 min. The sample was heated again from −80 °C to 200 °C at a heating rate of 10 °C/min. DSC measurements were performed under a nitrogen atmosphere at a flow rate of 50 mL/min. The crystallinity of PLA blocks in the copolymer was calculated as follows:

$$X_c\,(\%) = \frac{\Delta H_m - \Delta H_{cc}}{\Delta H_0 \times f_{PLA}} \times 100,$$

where X_c is crystallinity, f_{PLA} is the weight fraction of the PLA block in the copolymer, ΔH_m is the exothermic enthalpy, ΔH_{cc} is the endothermic enthalpy of cold in the reheating scan, and ΔH_0 is the theoretical melting enthalpy of the 100% crystalline PLA homopolymers, equal to 93 J/g.[42] Films were prepared (drying conditions: dried overnight at 90°C and then slowly cooled), and XRD analysis for films was performed using an XRD (RINT-Ultima, Rigaku Co., Ltd., Tokyo, Japan) operated at 45 kV and 200 mA. Data were collected within the range of scattering angles (2θ) of 5°–50° at the rate of 5°/min.

3.2.6. Disintegration Test of Films in Compost and Biodegradation Test of Films in Activated Sludge

For the disintegration test of films in compost applied in this section, please refer to Section 1.3.4 in Chapter 1. The biodegradability of the polymer in the activated sludge was evaluated according to the method described in JIS K6950:2000. Returned sludge from an urban wastewater treatment plant, obtained from the Osaka Research Institute of Industrial Science and Technology, which commissioned the evaluation, was added to 300 mL of the standard test culture to achieve an inoculum concentration of 30 mg/L. The films were cut, and small 30-mg pieces were used for testing. The test was conducted at a test temperature of 22°C for 28 days using an OM3100A Coulometer (Ohkura Electric Co., Saitama, Japan).

3.2.7. Biodegradation and Disintegration Tests of Films in Seawater

Film biodegradability in seawater was evaluated according to ASTMD6691-17 using a RESPIROMETRIC Sensor System 6 for Plastic Biodegradability (VELP Scientifica Srl, Usmate, Italy).[43] This technique quantifies the aerobic biodegradation capacity of organic matter by measuring the BOD,

which indicates the amount of oxygen consumed by microorganisms. Soda lime (1 g) containing sodium hydroxide was placed at the top of a sealed bottle as a CO_2 absorbent. The sealed bottle was placed in an incubator maintained at 30°C and stirred continuously in the dark for 2 months. The RESPIROMETRIC sensor transmits data directly to a PC, enabling real-time monitoring of the analysis curve. The seawater used in the BOD test was collected from Odaiba, Tokyo Bay, on the rainy evening of July 17, 2024. The collected seawater was filtered through a 77-μm mesh filter, and the conditions were adjusted by adding inorganic salts to achieve concentrations of 0.5 g/L ammonium chloride and 0.1 g/L potassium dihydrogen phosphate. Biodegradation tests were conducted under aerobic conditions at 30 °C for 2 months. The film samples (approximately 0.5 cm) were cut into small pieces, placed in 250 mL of test seawater, and stirred at 180 rpm. The C, H, and N contents (%) of the samples were analyzed in the CHN measurement mode using an organic element analyzer (Vario EL Cube, Elementar Ltd., Hanau, Germany). The O content was calculated by subtracting the C, H, and N contents from the total contents (**Table 6**). The results were used to calculate the ThOD of the sample. As a blank, a BOD test was performed using seawater without any added sample. The biodegradability of each film was calculated as follows:

$$\text{Biodegradability (\%)} = \frac{(\text{BOD (mg/L) of the sample} - \text{BOD (mg/L) of the blank}) \times \text{Test seawater volume (L)}}{\text{ThOD (mg/mg)} \times \text{Sample (mg)}} \times 100.$$

For the disintegration test in seawater, seawater was collected on the morning of August 9, 2024, from Odaiba, Tokyo Bay, on a clear day and adjusted in the same manner as mentioned above. Square films of size 2 cm and 250 mL of the adjusted seawater were placed in a 500-mL bottle and shaken at 30°C and 150 rpm for 3 months using a shaking incubator (Bio-Shaker BR-3000 L, TAITEC Co., Saitama, Japan). To investigate the amount of microorganisms in the seawater, biofilms attached to the films were suspended in the test seawater used for the 3-month disintegration test. Samples (100 mL) were aliquoted and filtered through mixed cellulose ester membranes with a pore size of 0.65 μm (Merck Millipore Inc., MA, USA) and polycarbonate track-etched membranes with a pore size of 0.2 μm (it4ip S.A., Louvain-la-Neuve, Belgium). Total DNA was extracted from both filters using ISOIL for Beads Beating kit (Nippon Gene Co., Toyama, Japan) and DNeasy PowerClean Pro Cleanup Kit (Qiagen Inc., Hilden, Germany) and analyzed for DNA concentration and A260/A280 in seawater using a NanoDrop ND8000 spectrophotometer (Thermo Fisher Scientific Inc., MA, USA). The collected samples were assessed for weight changes and visually inspected.

3.3. Results and Discussion

3.3.1. Synthesis of PLA–PMPDSe Alternating Multiblock (PLA-*alt*-PMPDSe) Copolymers

PLA–PMPDSe–PLA triblock copolymers were synthesized *via* the ring-opening polymerization of L-lactide using PMPDSe-diol as an initiator. PLA-*alt*-PMPDSe copolymers were synthesized *via* a chain-extension reaction. **Figure 2** shows the representative ^{1}H NMR spectra. The CH_2 signal of the terminal

group of the PMPDSe-diol was detected at 3.6 ppm (a), indicating that it was terminated with a hydroxyl group (**Figure 2a**). The PLA–PMPDSe–PLA triblock copolymer with the ring-opening polymerization of PMPDSe-diol exhibited typical PLA and PMPDSe signals (**Figure 2b**). The CH_3 and CH signals of the lactate repeating unit appeared as two strong signal peaks at 5.1 (j) and 1.5 (k) ppm, respectively. The CH_2 signal attributed to the sebacic acid unit of the PMPDSe chain was assigned to 2.2 (f), 1.6 (g), and 1.2 (h, i) ppm; the CH_3 signal attributed to the MPD unit to 0.9 (c) ppm; the CH_2 signal to 4.0 (e) and 1.5 (b); and the CH signal to 1.4 (d). The CH and CH_3 signals of the PLA chain end groups were detected at 4.3 ppm (j') and 1.4 ppm (k'), indicating that the triblock prepolymer was terminated with a hydroxyl group. The lactide conversion (%) in the ring-opening polymerization reaction was calculated using the integral ratio of the PLA-derived signal (5.1 ppm [l]) to the lactide-derived signal (5.0 ppm [j]), as shown in **Figure 2b**. The lactide conversion exceeded 95% in all samples, indicating successful ring-opening polymerization. Typical signals of the PLA and PMPDSe chains in the PLA-*alt*-PMPDSe copolymer are shown in **Figure 2c**. The CH_2OCONH signal adjacent to the urethane bond was assigned to 3.1 ppm (m), and the signals at the lactate terminus corresponding to 4.3 ppm (j') were infinitesimally small, indicating that the terminal hydroxyl group of the triblock prepolymer reacted with the isocyanate. **Table 1** presents a summary of the synthesis of the copolymers. The molecular weight of the PLA chain was determined by ^{1}H NMR using the ratio of the 5.1-ppm integral value (j) attributed to the lactate repeating unit to the 4.3-ppm integral value (j') of the lactate terminus. In addition, the molecular weight of the PMPDSe chain was determined by ^{1}H NMR using the ratio of the 4.3-ppm integral value (j') attributed to the repeating unit to the 4.0-ppm integral value (e) of the lactate terminus. The molecular weight of the entire PLA–PMPDSe–PLA triblock copolymer was calculated by summing the molecular weights of PLA and PMPDSe using ^{1}H NMR. PLA (%) was calculated from the molecular weight of the entire PLA–PMPDSe–PLA triblock copolymer and

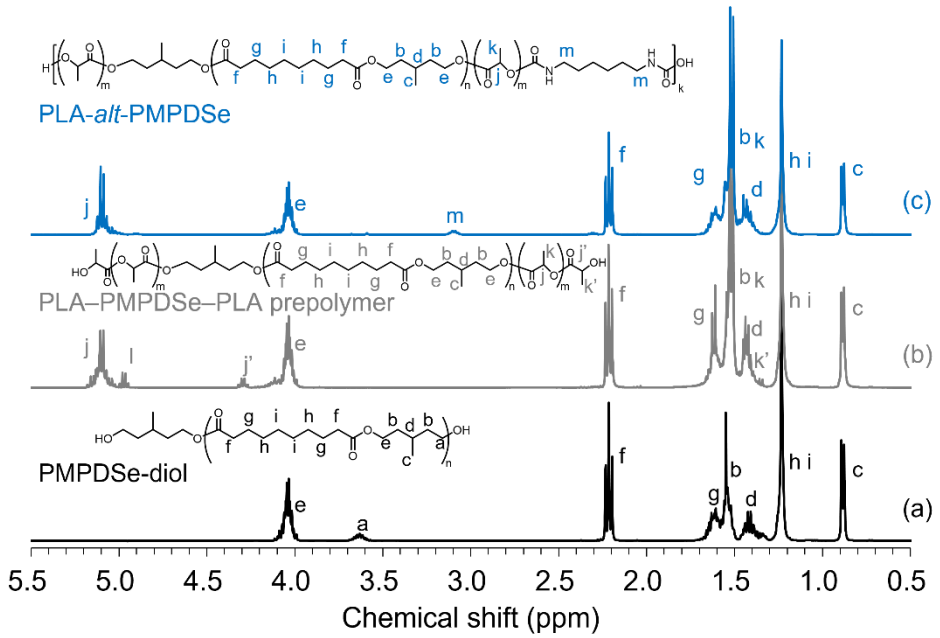

Figure 2. ^{1}H NMR spectra of (a) PMPDSe-diol, (b) PLA–PMPSe–PLA, and (c) PLA-*alt*-PMPDSe copolymers.

the PLA chain. Triblock copolymers with PLA chains of different lengths (M_n = 3,600, 4,800, 7,100, and 1,500) were synthesized by adjusting the stocking ratios of L-lactide. Subsequently, HDI was added at an NCO/OH molar ratio of 1.5 mol mol^{-1} to synthesize PLA-*alt*-PMPDSe copolymers (**Table 1**). The ^{1}H NMR spectrum of the PLA-*ran*-PMPDSe copolymers is shown in **Figure 3**. To match the PLA composition with the PLA-*alt*-PMPDSe copolymer, PLA-diol (M_n = 3,000, 4,200, 7,400, and 16,900) was synthesized by changing the L-lactide stock ratio, after which HDI was added to PLA-diol and PMPDSe-diol to synthesize PLA-*ran*-PMPDSe copolymers (**Table 1**).

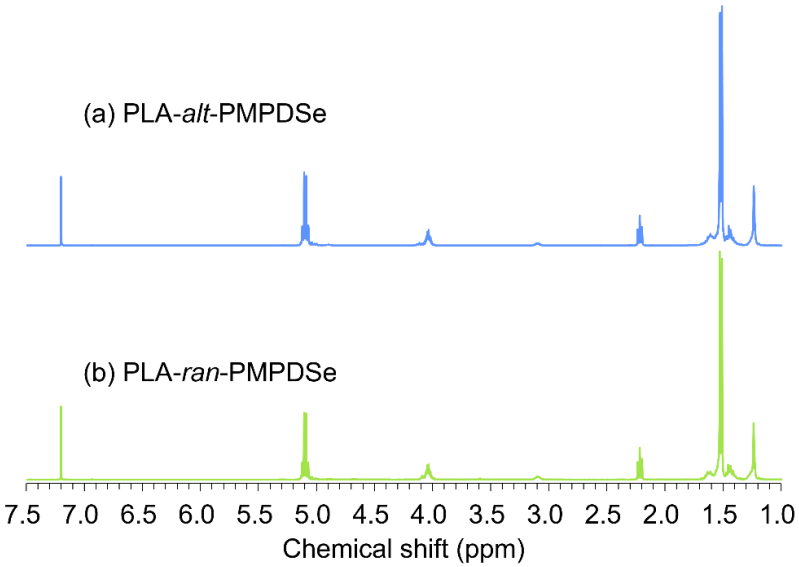

Figure 3. ^{1}H NMR spectra of (a) PLA-*alt*-PMPDSe and (b) PLA-*ran*-PMPDSe copolymer.

Table 1. Synthesis of the prepolymer by ring-opening polymerization and chain-extension reaction with HDI.

	Ring-opening polymerization[a]						Chain extension[b]				
	PLA[c] (%)	Oligomer[d] (Theo.) (g/mol)	Lactide conversion (%)	M_n [PLAe] (NMR) (g/mol)	M_n [Totale] (NMR) (g/mol)	Yield (%)	[NCO]/[OH][f] (mol/mol)	M_n[g] (SEC) (g/mol)	M_w[g] (SEC) (g/mol)	D[g]	Yield (%)
PMPD-CE	0	2,000	-	-	-	-	1.5	20,000	37,000	1.9	65
PLA-*alt*-	54	4,000	95	3,600	6,700	49	1.5	60,000	180,000	3.0	95
PMPDSe	61	6,000	95	4,800	7,900	55	1.5	53,000	130,000	2.5	94
	71	10,000	96	7,100	10,000	80	1.5	59,000	140,000	2.4	93
	85	18,000	98	15,000	17,700	83	1.5	48,000	120,000	2.5	96
PLA-*ran*-	59	2,000	96	3,000	-	59	1.5	35,000	96,000	2.7	79
PMPDSe	68	4,000	95	4,200	-	78	1.5	29,000	69,000	2.4	95
	79	8,000	97	7,400	-	85	1.5	32,000	60,000	1.9	94
	89	16,000	98	16,900	-	90	1.5	45,000	92,000	2.0	97
PLA-CE	100	8,000	97	7,400	-	85	1.5	41,000	76,000	1.9	95

[a]At 180°C for 3 h.
[b]At 180°C for 0.5 h.
[c]PLA-*alt*-PMPDSe copolymer: PLA (%) = PLA (determined by ^{1}H NMR)/overall (determined by ^{1}H NMR) × 100. PLA-*ran*-PMPDSe copolymer: preparation ratio of diols and HDI.
[d]Theoretical molecular weight of PLA synthesized by lactide ring-opening polymerization.
[e]Determined by ^{1}H NMR.
[f]Preparation ratio of HDI and diols.
[g]Determined by SEC (in chloroform).

3.3.2. Thermal Parameters of Each Sample

Figure 4 presents the evaluation results of the thermal properties as determined by DSC. The DSC curve of the PLA-*alt*-PMPDSe copolymer exhibited a single T_m because the crystallinity of the PMPDSe chains sandwiched in the triblock structure by the PLA chains was suppressed.[44] T_m and T_g increased with increasing PLA content and decreased with decreasing PLA content (**Figure 4a**). In the PLA-*ran*-PMPDSe copolymers, the PMPDSe and PLA chains were irregularly arranged, presumably resulting in the crystallinity of each block and multiple melting transitions (**Figure 4b**). Similar behavior was observed for other PLA-based TPUs.[44–46] In the case of the PLA-*ran*-PMPDSe copolymers containing 61%, the crystallinity of the PLA chains was suppressed because of the short PLA chain length, probably due to the PMPDSe chains, with a single T_m. The DSC results for the PLA-*alt*-PMPDSe copolymer, PLA-*ran*-PMPDSe copolymer, PLA-CE, PMPDSe-CE, and neat PLA are summarized in **Table 2**. The DSC curves of PLA-CE and PMPDSe are shown in **Figure 4c**. The PLA-*alt*-PMPDSe and PLA-*ran*-PMPDSe copolymers exhibited a single T_g and were miscible between blocks in the amorphous region.[24,47] The copolymers demonstrated lower T_g values than neat PLA and PLA-CE, indicating the effect of the introduction of PMPDSe chains (**Figure 4d**). In particular, in the case of the PLA-*alt*-PMPDSe copolymer, the units of the triblock structure are regularly arranged. It is assumed that the soft segments increase the overall mobility of the polymer, resulting in a significant decrease in T_g. In addition, the regular structure

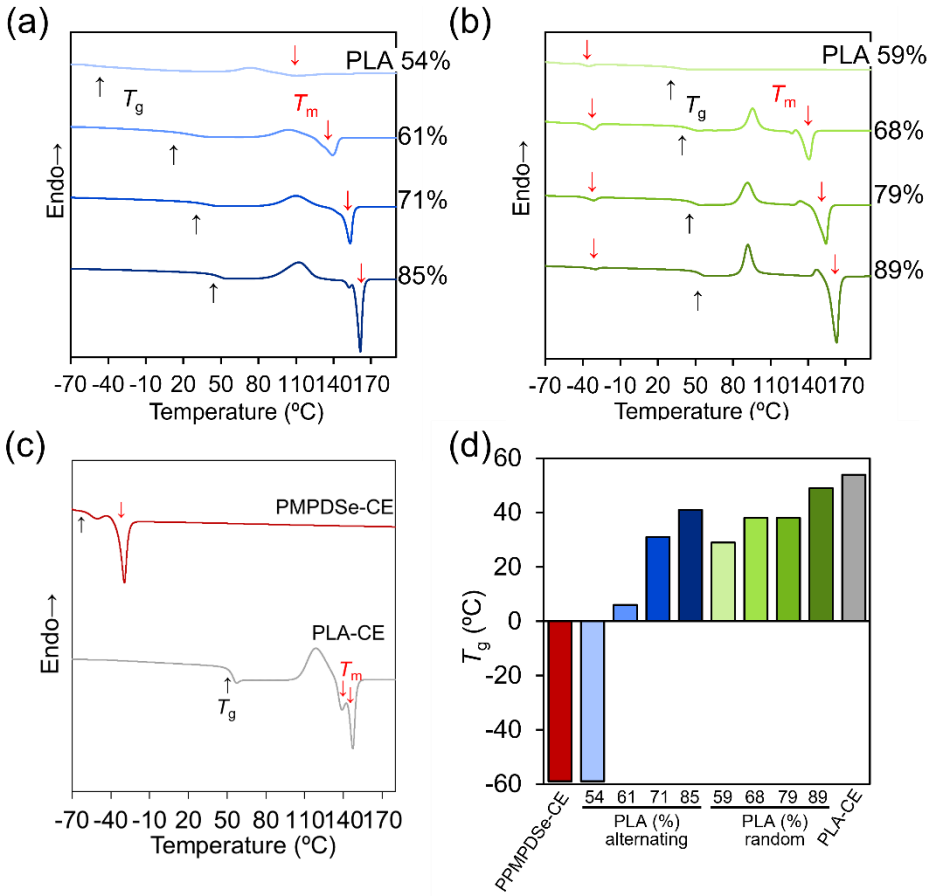

Figure 4. Thermal parameters of each sample. (a) Second heating curves of DSC for PLA-*alt*-PMPDSe copolymers, (b) PLA-*ran*-PMPDSe copolymers, (c) PMPDSe-CE and PLA-CE, and (d) T_g of each sample.

resulting from alternating multiblock leads to more flexible polymer chains and, consequently, lower T_g values.[24,44] Conversely, the PLA-*ran*-PMPDSe copolymers are assumed to have restricted molecular motion due to the irregular and localized arrangement of the rigid PLA units. The presence of these rigid units constrains the overall mobility of the polymer chains, resulting in higher T_g values, also correlating with the mechanical properties. **Figure 5** presents the first heating of DSC of the heat-treated film. The introduction of PMPDSe chains disrupted the alignment of the PLA chains,[48] resulting in higher crystallinity of the PLA-*alt*-PMPDSe and PLA-*ran*-PMPDSe copolymers with longer PLA chains (**Table 2**).

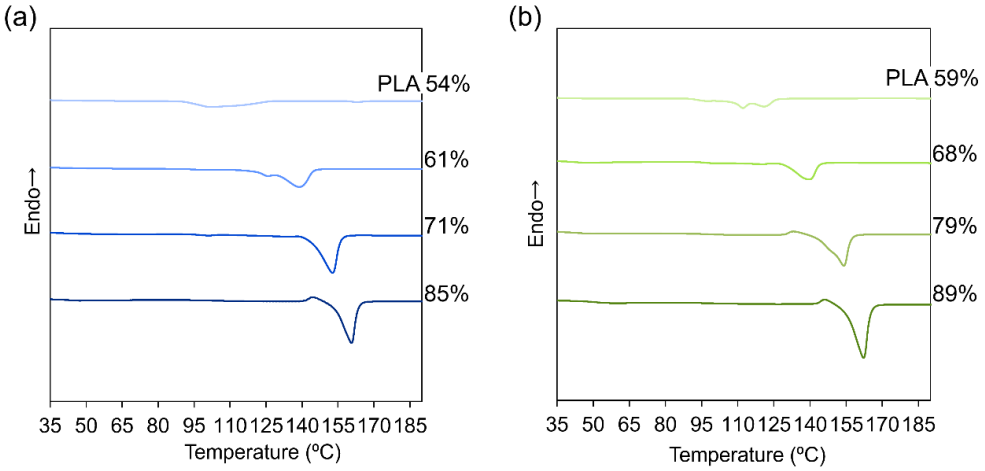

Figure 5. First heating curves of DSC for (a) PLA-*alt*-PMPDSe and (b) PLA-*ran*-PMPDSe copolymers.

The X_c value calculated from the XRD pattern was higher than that calculated from the DSC test (**Table 2**). However, these values cannot be directly compared because the two calculation methods are entirely different. **Figure 6a** and **6b** show the XRD patterns of the copolymers recorded after isothermal crystallization. PLA-CE has the typical diffraction peaks of PLA at $2\theta = 14.8°$ (010), 16.6° (200/110), 18.9° (203), and 22.2° (210). In all copolymers, the PLA chains were sufficiently long to form crystalline phases and had diffraction peaks. Although $2\theta = 16.6°$ is a strong peak, $2\theta = 22.2°$ is generally reported as a weak

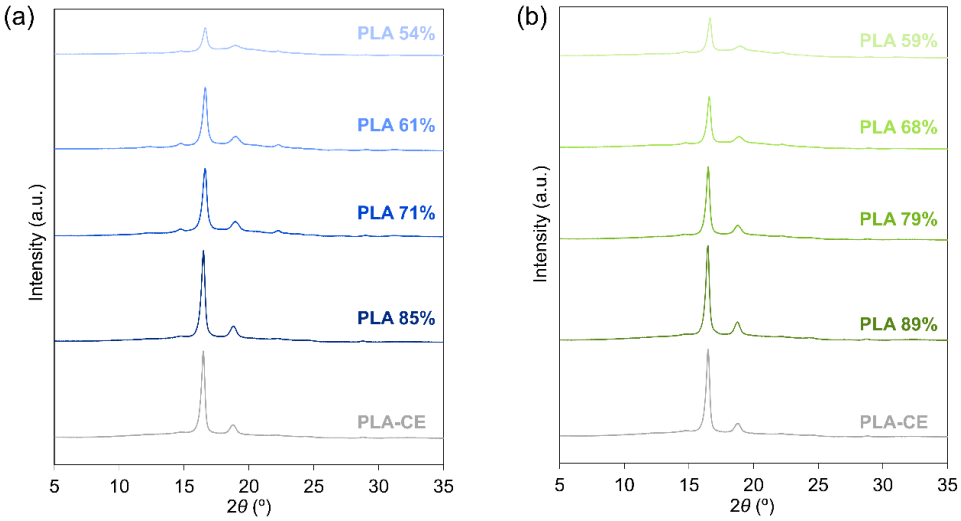

Figure 6. XRD patterns of (a) PLA-*alt*-PMPDSe and (b) PLA-*ran*-PMPDSe copolymers.

peak for PLA.[45] The copolymerization further weakened the PLA peaks; however, the peak at $2\theta = 22.2°$ remained slightly observed. Previous studies have revealed that polyurethanes containing branched-chain structures, such as MPD, often exhibit amorphous properties[49] and may have low crystallinity owing to hindered molecular packing. These copolymers demonstrated no differences in diffraction peak positions depending on the copolymerization method or composition and exhibited characteristics of semicrystalline polymers similar to the characteristic crystal structure of PLA. The PLA-*alt*-PMPDSe and PLA-*ran*-PMPDSe copolymers showed a decreasing trend in the intensity of the corresponding peaks with decreasing PLA chain length and crystallinity (**Table 2**).

Table 2. Thermal parameters of each sample by DSC. The degree of X_c of each sample determined by XRD.

		DSC			XRD
	PLA (%)	T_g (ºC)[a]	T_m (ºC)[a]	X_c (%)[b]	X_c (%)[c]
PMPDSe-CE	0	−59	−30	-	-
	54	−59	111	27	24.4
PLA-*alt*-PMPDSe	61	6	139	33	36.6
	71	31	153	33	39.4
	85	41	162	41	43.3
	59	29	−35	-	26	28.7
PLA-*ran*-PMPDSe	68	38	−32	140	31	33.1
	79	38	−32	154	37	38.6
	89	49	−30	160	37	42.6
PLA-CE	100	54	156		31	43.8
Neat PLA	100	55	152		30	45.5

[a]Determined by DSC.
[b]Degree of crystallinity of PLA from DSC first heating was calculated.
[c]Degree of crystallinity from XRD was calculated.

3.3.3. Thermal Stabilities of Each Sample

The thermal stability of the PLA−PMPDSe multiblock copolymers in a nitrogen atmosphere was evaluated using TGA. The TGA curves of the PLA-*alt*-PMPDSe and PLA-*ran*-PMPDSe copolymers are shown in **Figure 7a** and **7b**, respectively, and their respective DTGA curves are shown in **Figure 7c** and **7d**. Data such as the temperature at 5% weight loss ($T_{d,\,5\%}$) and the maximum decomposition temperature ($T_{d,\,max}$) are presented in **Table 3**. Nearly no residue remained after thermal degradation. Taking the degradation onset as starting at a temperature corresponding to $T_{d,\,5\%}$, neat PLA showed a degradation onset at 328°C, with $T_{d,\,max}$ located at 367°C, which is not substantially different from previous studies.[50,51] Compared to neat PLA, PLA-CE exhibited a lower thermal degradation temperature due to the shorter PLA chains, with a degradation initiation temperature of 255°C and a $T_{d,\,max}$ of 302°C, which is also not considerably different from previous studies (**Table 3**).[52] In contrast to simple homopolymers, the copolymers exhibited a two-step thermal degradation, with the PLA chains degrading in the first step, followed by the degradation of the introduced PMPDSe chains. All copolymers were thermally stable up to 246 °C, with $T_{d,\,max}$ exceeding 269 °C. A decrease in $T_{d,\,max\ PLA}$ was observed for copolymers with lower PLA content owing to shorter PLA chains. In contrast, the thermal degradation temperature of the PMPDSe chains in the copolymer was similar to that of PMPDSe-CE, which remained stable and unaffected by the presence of PLA. The thermal degradation temperature of the PLA-*ran*-PMPDSe copolymer was slightly

higher than that of the PLA-*alt*-PMPDSe copolymer, probably because of the longer PLA chains in the former.

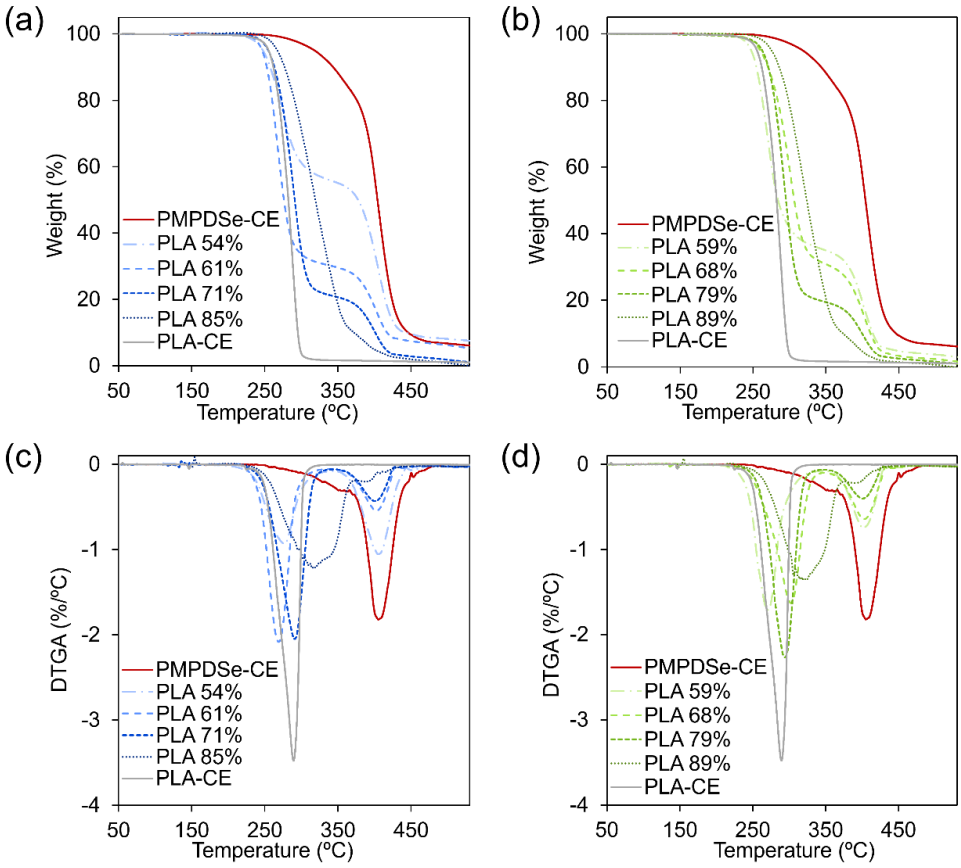

Figure 7. Thermal parameters of each sample. (a) TGA curves of PLA-*alt*-PMPDSe and (b) PLA-*ran*-PMPDSe copolymers. (c) DTGA curves of PLA-*alt*-PMPDSe and (d) PLA-*ran*-PMPDSe copolymers.

Table 3. Thermal parameters of each sample by TGA. Thermal degradation parameters of polymers in terms of the onset degradation temperature at a mass loss of 5 wt% ($T_{d,\ 5\%}$), maximum degradation rate (peak) temperature ($T_{d,\ max}$).

		Thermal properties (TGA)		
	PLA (%)	$T_{d,\ 5\%}$ (°C)	$T_{d,\ max\ PLA}$ (°C)	$T_{d,\ max\ PMPDSe}$ (°C)
PMPDSe-CE	0	318	-	404
PLA-*alt*-PMPDSe	54	248	276	405
	61	246	269	403
	71	255	292	402
	85	267	319	392
PLA-*ran*-PMPDSe	59	247	270	402
	68	260	301	403
	79	262	295	401
	89	275	321	393
PLA-CE	100	255	302	-
Neat PLA	100	328	367	-

3.3.4. Mechanical Properties of Hot-Pressed Films

The mechanical properties of the hot-pressed films were evaluated using tensile tests (**Figure 8**). **Figure 8a** shows the stress–strain curves of PLA-*alt*-PMPDSe copolymers containing 54%–85% PLA, and

Figure 8b shows the stress–strain curves of PLA-*ran*-PMPDSe copolymers containing 59%–89% PLA. A comparison of the toughness of the PLA-*alt*-PMPDSe copolymers with that of the PLA-*ran*-PMPDSe copolymers and PLA-CE is presented in **Figure 8c**. **Table 4** lists the results of the tensile tests. As shown in the DSC curves in **Figure 4c**, PMPDSe-CE has low T_m and is oil-like at room temperature, making film formation impossible. The XRD results revealed that crystallinity increased with an increasing number of PLA chains (**Figure 6**) and that the tensile strength of the PLA-*alt*-PMPDSe copolymer increased and became comparable to that of PLA-CE. In contrast, the elongation at break increased with decreasing PLA chain content, which was attributed to the influence of the soft segment and a decrease in crystallinity. The PLA-*alt*-PMPDSe copolymers containing 61% and 71% PLA maintained higher elongation at break and tensile strength and exhibited higher toughness than the PLA-*ran*-PMPDSe copolymers. Previous studies have reported that a regular, continuous structure, resulting from high molecular weight and chain extension, contributes to high toughness.[53] These results indicate that even with small amounts of PMPDSe chains, regularly arranged PLA-*alt*-PMPDSe copolymers exhibit excellent mechanical properties. Additionally, the tensile properties can be adjusted by controlling the composition, rendering it a highly versatile material.

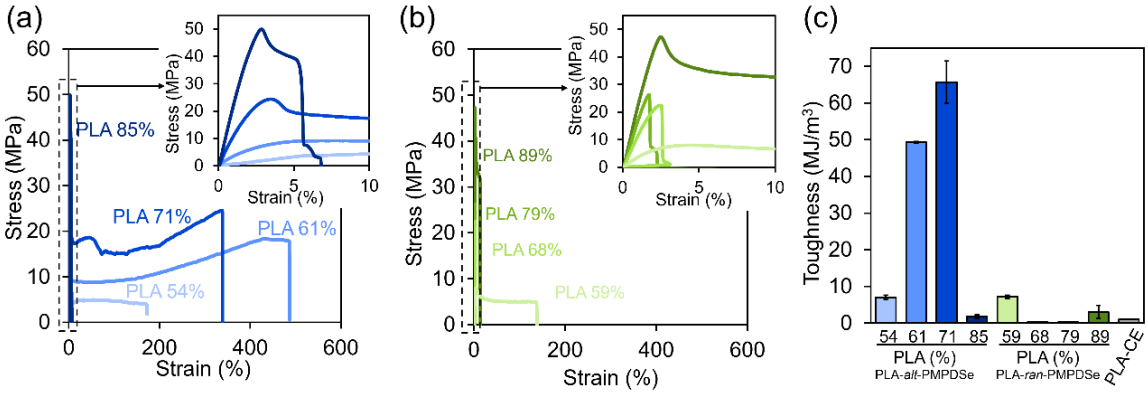

Figure 8. Stress–strain curves obtained by tensile tests of hot-pressed films of (a) PLA-*alt*-PMPDSe and (c) PLA-*ran*-PMPDSe copolymers. (c) Toughness obtained by a tensile test (average, three replicates).

Table 4. Mechanical properties of polymers.

		Mechanical properties (tensile test)			
	PLA (%)	Young's modulus (MPa)	Maximum stress (MPa)	Elongation at break (%)	Toughness (MJ/m^3)
PLA-*alt*-PMPDSe	54	110 ± 16	4.7 ± 0.3	200 ± 35	7.0 ± 0.6
	61	504 ± 11	19.4 ± 1.2	518 ± 31	49.3 ± 0.2
	71	1,520 ± 130	28.2 ± 3.1	331 ± 23	65.7 ± 5.7
	89	2,540 ± 75	46.3 ± 3.2	5.90 ± 1.90	1.80 ± 0.50
PLA-*ran*-PMPDSe	59	472 ± 21	8.43 ± 0.45	130 ± 10	7.20 ± 0.72
	68	1,290 ± 61	21.5 ± 0.8	2.90 ± 0.40	0.32 ± 0.01
	79	1,910 ± 67	24.8 ± 1.3	2.33 ± 0.45	0.26 ± 0.03
	89	2,440 ± 110	40.5 ± 5.9	11.6 ± 7.0	3.02 ± 1.83
PLA-CE	100	2,830 ± 110	52.6 ± 1.8	2.83 ± 0.21	1.00 ± 0.01
Neat PLA	100	2,880 ± 30	49.9 ± 3.2	2.26 ± 0.09	0.61 ± 0.06

3.3.5. Disintegration Test in Compost and Biodegradation Test in Activated Sludge

Figure 9 shows a simple appearance test of the PLA-*alt*-PMPDSe copolymer, PLA-*ran*-PMPDSe copolymer, and neat PLA films buried in compost to determine whether the films decomposed in 8 weeks. The characteristics of the compost used in the disintegration test are summarized in **Table 5**. Two weeks after the test began, all films became brittle and began to tear, although no significant weight changes were observed. After 4 weeks, all films had become more finely fragmented, and the samples with relatively lower PLA contents had lost more weight. In contrast, neat PLA and samples with high PLA content maintained weight. After 8 weeks, several samples were infinitesimally fine and were expected to disappear completely with an extension of the study period. In particular, the copolymers exhibited a more pronounced weight loss than PLA, indicating that degradation occurred more rapidly than in neat PLA because of the active microbial environment and high temperature and humidity of the compost. Previous studies have reported that PLA not only loses weight in compost[23,52] but also biodegrades completely. This study assumes that PLA and copolymers will also biodegrade in compost under these test conditions. The PLA-*alt*-PMPDSe copolymer containing 54% PLA, which showed significant disintegration in compost, BOD, and biodegradation in activated sludge compared to neat PLA, is shown in **Figure 10a** and **10b**. Biodegradability was calculated using ThOD (**Table 6**) determined from the CHNO content. After 28 days of incubation, the copolymer was biodegradable (12%); however, the neat PLA did not begin to degrade. The biodegradability of the copolymer increased after 28 days. Biodegradability would increase further with longer testing periods due to the low T_g of the PLA-*alt*-PMPDSe copolymers. In compost and activated sludge, the polymer chains become more flexible, accelerating hydrolysis and microbial attachment. Lower T_g and crystallinity make the amorphous regions of polymer chains more flexible, allowing more water to penetrate the interchain spaces and facilitating hydrolysis and microbial degradation.[13,15–17] Kumagai et al. reported that the introduction of long-chain dicarboxylic acids into nonmarine biodegradable plastics

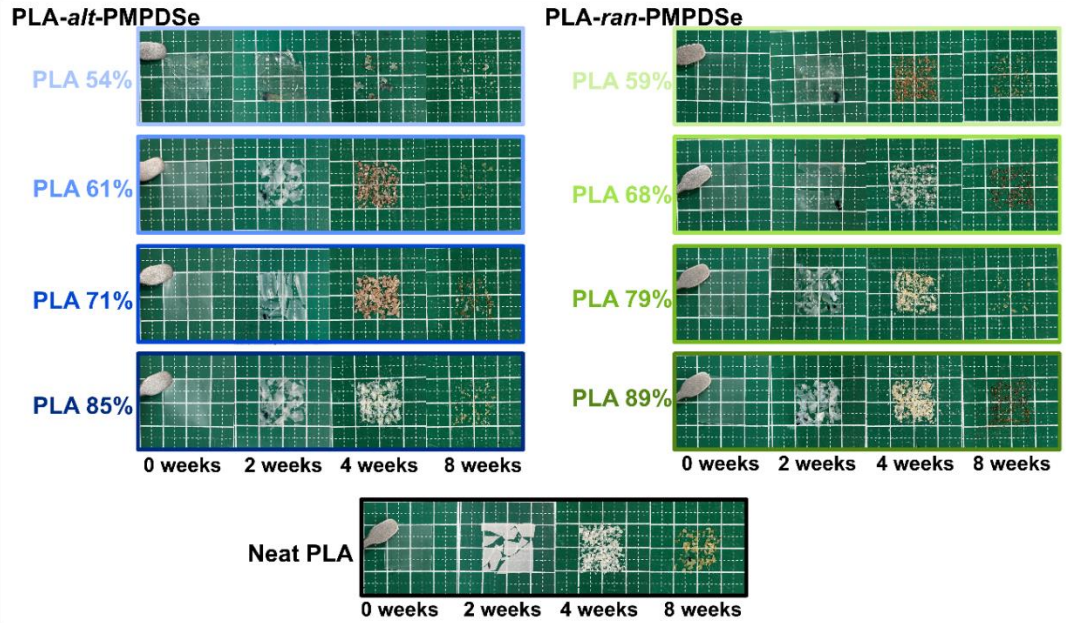

Figure 9. Disintegration tests of PLA-*alt*-PMPDSe copolymer, PLA-*ran*-PMPDSe copolymer, and neat PLA film in compost for 8 weeks.

improves biodegradability. However, crystallinity and glass transition temperature may not be the only influences and may have a role yet to be fully understood.[28] Further assessment of biodegradability and hydrophobicity in seawater was conducted to explore the possible influence of factors specific to long-chain dicarboxylic acids.

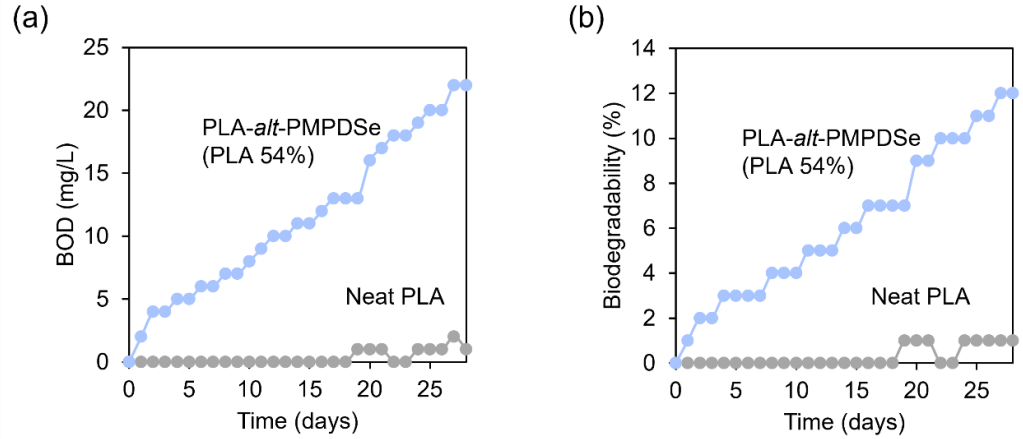

Figure 10. Measurements of changes in (a) BOD and (b) biodegradability for PLA-*alt*-PMPDSe copolymer and PLA in activated sludge. Activated sludge from a sewage treatment plant was used and tested for 28 days in test water at a concentration of 30 mg/L of sludge at 22°C, and the blank value was subtracted. Biodegradability was calculated using ThOD (**Table 6**) determined from the CHNO content.

Table 5. Characteristics of the compost used in the disintegration test.

Analysis in compost	Measured values
Total dry solids (%)[a]	45
Volatile solids (%)[b]	58
pH[c]	8

[a]Measured after drying at 115°C for 5 h.
[b]Measured after complete ashing of dried compost at 550°C.
[c]Measured by mixing compost with five times deionized water.

Table 6. The C, H, and N contents and ThOD of samples.

Sample	PLA (%)	Carbon (C) (%)	Hydrogen (H) (%)	Nitrogen (N) (%)	Oxygen (O) (%)	ThOD (mg/mg)
PLA-*alt*-PMPDSe	54	59.2	7.99	0.62	32.2	1.76
	61	54.9	6.90	0.57	37.6	1.56
	71	53.7	6.57	0.45	39.2	1.52
	85	51.8	6.10	0.34	41.7	1.44
PLA-*ran*-PMPDSe	59	56.6	7.46	1.36	34.6	1.68
	68	55.1	7.07	1.08	36.7	1.60
	79	53.4	6.57	0.75	39.2	1.52
	89	51.7	6.10	0.39	41.8	1.44
Neat PLA	100	50.0	5.61	-	44.4	1.33

3.3.6. Marine Biodegradation and Disintegration Test

Figure 11 shows the disintegration or biodegradation of the PLA-*alt*-PMPDSe and PLA-*ran*-PMPDSe copolymers in seawater compared to PLA. **Figure 11a** shows the change in film appearance in seawater for a PLA-*alt*-PMPDSe copolymer containing 54% PLA and a PLA-*ran*-PMPDSe copolymer

containing 59% PLA. The neat PLA film maintained its shape for 3 months in seawater. However, the PLA-*alt*-PMPDSe copolymer containing 54% PLA exhibited coloration, presumably due to microbial biofilms. The film changed shape and lost 15.3% of its weight over 3 months. The weight of the PLA-*ran*-PMPDSe copolymer containing 59% PLA decreased by 0.5%. **Figure 11b** shows the biodegradability of the PLA-*alt*-PMPDSe copolymer containing 54% PLA, the PLA-*ran*-PMPDSe copolymer containing 59% PLA, and neat PLA. The PLA-*alt*-PMPDSe copolymer containing 54% PLA and the PLA-*ran*-PMPDSe copolymer containing 59% PLA were selected based on the significant weight loss observed in the compost

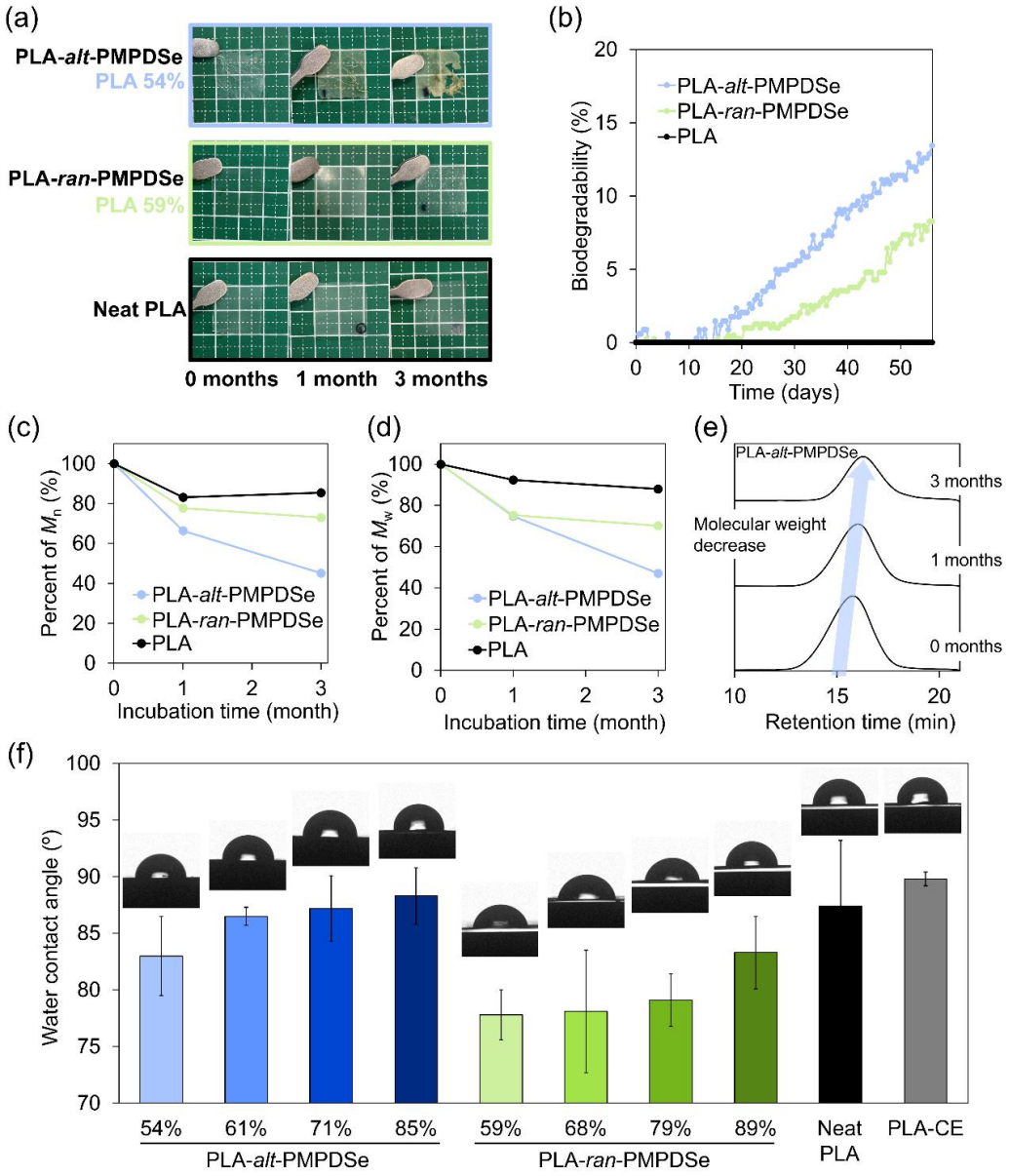

Figure 11. Marine biodegradation and disintegration tests of PLA-*alt*-PMPDSe copolymer containing 54% PLA, PLA-*ran*-PMPDSe copolymer containing 59% PLA, and neat PLA. (a) Changes in film appearance in seawater for 3 months. (b) Biodegradability of films cut into small pieces for 2 months. Biodegradability was calculated using ThOD determined from the CHNO content (**Table 6**). (c) M_n and (d) M_w change (%) of films in seawater over 3 months. (e) Molecular weight shifts of PLA-*alt*-PMPDSe copolymer containing 54% PLA by SEC. (f) WCA of each film of copolymers and PLA.

degradation test (**Figure 9**). Weight loss in seawater was observed in both samples. Consistent with the results of the disintegration test (**Figure 11a**), neat PLA showed almost no increase in biodegradation over 2 months. In contrast, the copolymer exhibited an increase in BOD, indicating oxygen consumption by microorganisms (**Figure 11b**). The biodegradability was 8.3% for the PLA-*ran*-PMPDSe copolymer and 17.2% for the PLA-*alt*-PMPDSe copolymer. The microbial concentration in seawater is lower compared to soil, compost, and fresh water.[17,19] Although the amount of DNA in the blank seawater was low, the amount of DNA increased significantly when measured after the disintegration test. PLA-*alt*-PMPDSe copolymers showed more than a twofold increase in DNA content compared to neat PLA and PLA-*ran*-PMPDSe copolymers, confirming an increase in microbial content (**Table 7**). Accordingly, the PLA-*alt*-PMPDSe copolymer formed a unique microbial community called the "plastosphere," which was distinct from the surrounding seawater.[54-57] It was inferred that the activation and growth of microorganisms were enhanced, thereby facilitating the biodegradation of the polymers. **Figure 11c** and **11d** show changes in molecular weight measured by SEC. The molecular weight of the PLA-*alt*-PMPDSe copolymer began to decrease from the beginning of the test. After 3 months, the values decreased from M_n = 20,300 g/mol and M_w = 48,800 g/mol to M_n = 9,100 g/mol and M_w = 23,000 g/mol, representing a significant 45.1% decrease from the initial M_n value. The molecular weight of PLA decreased from M_n = 53,300 g/mol and M_w = 121,000 g/mol to M_n = 45,600 g/mol and M_w = 106,000 g/mol while maintaining 85.4% of the initial M_n value. The molecular weight of the PLA-*ran*-PMPDSe copolymers decreased from M_n = 27,400 g/mol and M_w = 133,000 g/mol to M_n = 20,000 g/mol and M_w = 93,300 g/mol while maintaining 70.2% of the initial M_n value. **Figure 11e** shows changes in the molecular weight distribution curve of the PLA-*alt*-PMPDSe copolymer tested for 3 months. Although the SEC curve demonstrated no significant change in polydispersion, a peak shift was observed from the high-molecular-weight side to the low-molecular-weight side. **Figure S8** shows the SEC curves for PLA and PLA-*ran*-PMPDSe copolymers, with no significant peak shifts observed. Compared to neat PLA, multiblock copolymers exhibited lower T_g and crystallinity (**Table 2**), which may have reduced their molecular weight and facilitated biodegradation in seawater, similar to what occurs in compost and activated sludge. In the PLA-*ran*-PMPDSe copolymer, the PMPDSe and PLA chains were arranged irregularly. However, in the PLA-*alt*-PMPDSe copolymer, the PMPDSe chains were arranged regularly between the PLA chains, which may affect the hydrolysis efficiency and the possibility of low molecular weight.[23] For PLA to biodegrade, several bonds should be cleaved in the initial stages of degradation, reducing to oligomer sizes that can be metabolized by microorganisms.[16,22] According to this study, the degradation of the copolymer to low molecular weight in seawater affected its biodegradability. Although a few studies have evaluated the biodegradability of polyester polyurethanes, such as PLA-*alt*-PMPDSe copolymers, in marine environments, degradation has been reported to occur.[24,58] Additionally, microbial degradation has also been reported to occur under aerobic conditions in soil and compost.[23,58-62] This study evaluated biodegradability in simulated compost, activated sludge, and marine environments. Further enzymatic degradation experiments and field tests in natural environments are required. Furthermore, when the WCAs of the films were measured (**Figure 11f**), the contact angle tended to decrease as the number of PMPDSe chains containing sebacic acid increased. However, no penetration

of water droplets was observed, indicating that the film was fully functional. The contact angles of PLA, the PLA-*alt*-PMPDSe copolymer, and the PLA-*ran*-PMPDSe copolymer were 89.8 ± 0.6°, 83.0 ± 3.5°, and 77.8 ± 2.2°, respectively. A slight decrease in hydrophobicity may be a factor in improved hydrolysis and biodegradability. Although this improvement in marine biodegradability could not be fully elucidated, it is assumed to result from not only the crystallinity, hydrophobicity, and hydrolyzability of the polymers examined in this study, but also various factors, such as enzyme affinity caused by the presence of sebacic acid, a long-chain dicarboxylic acid, as reported in previous studies.[28]

Table 7. DNA concentrations and A260/A280 in 100 mL of test seawater after 3 months of disintegration testing. They were measured using a NanoDrop ND8000 spectrophotometer (Thermo Fisher Scientific Inc., MA, USA). Values below 2.5 ng/µl, the detection limit of the NanoDrop 8000 absorbance spectrophotometer, was listed as the limit of detection (LOD).

	DNA concentrations (ng/µL)	A260/280
Blank	LOD (<2.5)	-
PLA-*alt*-PMPDSe	12.2	1.42
PLA-*ran*-PMPDSe	4.9	1.30
PLA	5.5	1.39

3.4. Conclusion

To improve the brittleness and biodegradability of PLA, PLA-*alt*-PMPDSe copolymers were synthesized from biomass-derived PLA and PMPDSe containing sebacic acid as a structural unit. Compared with PLA-*ran*-PMPDSe copolymers, the thermal and mechanical properties of the resulting copolymers can be easily controlled by changing the length of the PLA chains. The PLA-*alt*-PMPDSe copolymers containing 61% or 71% PLA had significantly higher elongation at break and toughness compared with the PLA and PLA-*ran*-PMPDSe copolymers. Accordingly, the regularly arranged PMPDSe chains improved functionality. Biodegradability was highest in the PLA-*alt*-PMPDSe copolymers containing 54% PLA, with the films disintegrating in compost and seawater. Initial biodegradation was also observed in activated sludge. Even in seawater, the regular arrangement of PMPDSe chains between PLA chains promoted oligomerization, resulting in a biodegradation rate exceeding 17% in 2 months. In the WCA test, the water droplets did not penetrate immediately, and the contact angle of the PLA-*alt*-PMPDSe copolymers was comparable to that of neat PLA (>83°), indicating that it functioned well as a film. The improved biodegradability may be attributed not only to the crystallinity, hydrophobicity, and hydrolyzability of the polymer, but also to the long-chain dicarboxylic acid, sebacic acid. However, further studies are necessary to explore the possibility of complete mineralization. This study is expected to be deployed in various applications requiring high toughness and biodegradability, such as packaging, agricultural applications, and marine environments.

3.5. References

(1) OECD. Global Plastics Outlook: Policy Scenarios to 2060. *OECD Publishing* **2022** https://doi.org/10.1787/aa1edf33-en.
(2) Brandt, A.; Gräsvik, J.; Hallett, J. P.; Welton, T. Deconstruction of lignocellulosic biomass with ionic liquids. *Green Chem*. **2013**, *15*, 550–583. https://doi.org/10.1039/c2gc36364j.

(3) Carafa, R. N.; Foucher, D. A.; Sacripante, G. G. Biobased polymers from lignocellulosic sources. *Green Chem. Lett. Rev.* **2023**, *16*, 2153087. https://doi.org/10.1080/17518253.2022.2153087.
(4) Vanapalli, K. R.; Sharma, H. B.; Ranjan, V. P.; Samal, B.; Bhattacharya, J.; Dubey, B. K.; Goel, S. Challenges and strategies for effective plastic waste management during and post COVID-19 pandemic. *Sci. Total Environ*. **2021**, *750*, 141514. https://doi.org/10.1016/j.scitotenv.2020.141514.
(5) European Bioplastics, Bioplastics market development update 2023. *European Bioplastics* **2023**. https://www.european-bioplastics.org/market/ (accessed Dec 8, 2024).
(6) Jambeck, J. R.; Geyer, R.; Wilcox, C.; Siegler, T. R.; Perryman, M.; Andray, A.; Narayan, R.; Law, K. L. Marine Pollution. Plastic waste inputs from land into the ocean. *Science* **2015**, *347* (6223), 768–771. https://doi.org/10.1126/science.1260352.
(7) Walker, T. R. Drowning in debris: Solutions for a global pervasive marine pollution problem. *Mar. Pollut. Bull.* **2018**, *126*, 338, https://doi.org/10.1016/j.marpolbul.2017.11.039.
(8) Gilman, E.; Musyl, M.; Suuronen, P.; Chaloupka, M.; Gorgin, S.; Wilson, J.; Kuczenski, B. Highest risk abandoned, lost and discarded fishing gear. *Sci. Rep.* **2021**, *11* (1), 7195. https://doi.org/10.1038/s41598-021-86123-3.
(9) Worm, B.; Lotze, H. K.; Jubinville, I.; Wilcox, C.; Jambeck, J. Plastic as a Persistent Marine Pollutant. *Annu. Rev. Environ. Resour.* **2017**. *42*, 1-26. https://doi.org/10.1146/annurev-environ-102016-060700.
(10) Rhodes, C. J. Plastic Pollution and Potential Solutions. *Sci. Prog.* **2018**, *101* (3), 207–260. https://doi.org/10.3184/003685018X15294876706211.
(11) Lim, X. Z. Microplastics are everywhere — but are they harmful?, *Nature* **2021**, *593*, 207-260. https://doi.org/10.1038/d41586-021-01143-3.
(12) Yu, J.; Xu, S.; Liu, B.; Wang, H.; Qiao, F.; Ren, X.; Wei, Q. PLA bioplastic production: From monomer to the polymer. *Eur. Polym. J.* **2023**, *193*, 112076. https://doi.org/10.1016/j.eurpolymj.2023.112076.
(13) Karamanlioglu, M.; Preziosi, R.; Robson, G. D. Abiotic and biotic environmental degradation of the bioplastic polymer poly(lactic acid): A review. *Polym. Degrad. Stab.* **2017**, *137*, 122–130. https://doi.org/10.1016/j.polymdegradstab.2017.01.009.
(14) Takagi, A.; Hsu, Y.-I.; Uyama, H. Synthesis of High-Toughness Polyesters Using Xylose and Lactic Acid and Analysis of Their Biodegradability. *ACS Appl. Polym. Mater.* **2024**, *6* (21), 13307-13318. https://doi.org/10.1021/acsapm.4c02662.
(15) Stloukal, P.; Pekařová, S.; Kalendova, A.; Mattausch, H.; Laske, S.; Holzer, C.; Chitu, L.; Bodner, S.; Maier, G.; Slouf, M.; Koutny, M. Kinetics and mechanism of the biodegradation of PLA/clay nanocomposites during thermophilic phase of composting process. *Waste Management* **2015**, *42*, 31–40. https://doi.org/10.1016/j.wasman.2015.04.006.
(16) Souza, P. M. S.; Morales, A. R.; Marin-Morales, M. A.; Mei, L. H. I. PLA and Montmorilonite Nanocomposites: Properties, Biodegradation and Potential Toxicity. *J. Polym. Environ.* **2013**, *21* (3), 738–759. https://doi.org/10.1007/s10924-013-0577-z.
(17) Haider, T. P.; Völker, C.; Kramm, J.; Landfester, K.; Wurm, F. R. Plastics of the Future? The Impact of Biodegradable Polymers on the Environment and on Society, *Angew. Chem. Int. Ed.* **2019**, *131* (1), 50–63. https://doi.org/10.1002/ange.201805766.
(18) Albertsson, A.-C.; Hakkarainen, M. Designed to degrade. *Science* **2017**, *358* (6365), 872–873. https://doi.org/10.1126/science.aap8115.
(19) Wang, G.-X.; Huang, D.; Ji, J.-H.; Völker, C.; Wurm, F. R. Seawater-Degradable Polymers—Fighting the Marine Plastic Pollution. *Adv. Sci*. **2021**, *8*, 2991121. https://doi.org/10.1002/advs.202001121.
(20) Min, K.; Cuiffi, J. D.; Mathers, R. T. Ranking environmental degradation trends of plastic marine debris based on physical properties and molecular structure. *Nat. Commun.* **2020**, *11* (1), 727. https://doi.org/10.1038/s41467-020-14538-z.
(21) Stubbs, C. J.; Worch, J. C.; Prydderch, H.; Wang, Z.; Mathers, R. T.; Dobrynin, A. V.; Becker, M. L.; Dove, A. P. Sugar-Based Polymers with Stereochemistry-Dependent Degradability and Mechanical Properties. *J. Am. Chem. Soc.* **2022**, *144* (3), 1243–1250. https://doi.org/10.1021/jacs.1c10278.
(22) Seok, J. H.; Iwata, T. Effects of Molecular Weight on the Marine Biodegradability of Poly(L-lactic acid). *Biomacromolecules* **2024**, *25* (7), 4420–4427. https://doi.org/10.1021/acs.biomac.4c00454.
(23) Takagi, A.; Hsu, Y.-I.; Uyama, H. Biodegradable poly(lactic acid) and polycaprolactone alternating multiblock copolymers with controllable mechanical properties. *Polym. Degrad. Stab.* **2023**, *218*, 110564. https://doi.org/10.1016/j.polymdegradstab.2023.110564.

(24) He, M.; Hsu, Y.-I.; Uyama, H. Superior sequence-controlled poly(L-lactide)- based bioplastic with tunable seawater biodegradation. *J. Hazard. Mater.* **2024**, *474*, 134819. https://doi.org/10.1016/j.jhazmat.2024.134819.
(25) Chen, X.; Wang, L.; Shi, J.; Shi, H.; Liu, Y. Environmental Degradation of Starch/Poly(Lactic Acid) Composite in Seawater. *Polym. Polym. Compos*. **2011**, *19* (7), 559-566. https://doi.org/10.1177/096739111101900705.
(26) Huang, D.; Hu, Z.-D.; Liu, T.-Y.; Lu, B.; Zhen, Z.-C.; Wang, G.-X.; Ji, J.-H. Seawater degradation of PLA accelerated by water-soluble PVA. *e-Polym*. **2020**, *20* (1), 759–772. https://doi.org/10.1515/epoly-2020-0071.
(27) Rheinberger, T.; Wolfs, J.; Paneth, A.; Gojzewski, H.; Paneth, P.; Wurm, F. R. RNA-Inspired and Accelerated Degradation of Polylactide in Seawater. *J. Am. Chem. Soc.* **2021**, *143* (40), 16673–16681. https://doi.org/10.1021/jacs.1c07508.
(28) Kumagai, S.; Hayashi, S.; Katsuragi, A.; Imada, M.; Sato, K.; Abe, H.; Asakura, N.; Takenaka, Y. Improving the marine biodegradability of poly(alkylene succinate)-based copolymers. *Polym. J.* **2024**, *56*, 419-429. https://doi.org/10.1038/s41428-023-00871-9.
(29) Jeon, W.-Y.; Jang, M.-J.; Park, G.-Y.; Lee, H.-J.; Seo, S.-H.; Lee, H.-S.; Han, C.; Kwon, H.; Lee, H.-C.; Lee, J.-H.; Hwang, Y.-T.; Lee, M.-O.; Lee, J.-G.; Lee, H.-W.; Ahn, J.-O. Microbial production of sebacic acid from a renewable source: production, purification, and polymerization. *Green Chem*. **2019**, *21* (23), 6491–6501. https://doi.org/10.1039/c9gc02274k.
(30) Frone, A. N.; Popa, M. S.; Uşurelu, C. D.; Panaitescu, D. M.; Gabor, A. R.; Nicolae, C. A.; Raduly, M. F.; Zaharia, A.; Alexandrescu, E. Bio-Based Poly(lactic acid)/Poly(butylene sebacate) Blends with Improved Toughness. *Polymers (Basel)* **2022**, *14* (19). 3998. https://doi.org/10.3390/polym14193998.
(31) Briassoulis, D.; Mistriotis, A.; Mortier, N.; Tosin, M. A horizontal test method for biodegradation in soil of bio-based and conventional plastics and lubricants. *J. Cleaner Prod.* **2020**, *242*, 118392. https://doi.org/10.1016/j.jclepro.2019.118392.
(32) Briassoulis, D.; Pikasi, A.; Papardaki, N. G.; Mistriotis, A. Aerobic biodegradation of bio-based plastics in the seawater/sediment interface (sublittoral) marine environment of the coastal zone – Test method under controlled laboratory conditions. *Sci. Total Environ.* **2020**, *722*, 137748. https://doi.org/10.1016/j.scitotenv.2020.137748.
(33) Asada, K.; Fukano, K.; Yamashita, K.; Nakanishi, E. Improved heat and solvent resistance of a pressure-sensitive adhesive thermally processable by isocyanate dimer dissociation. *J. Appl. Polym. Sci.* **2015**, *132* (6), 41444. https://doi.org/10.1002/app.41444.
(34) Kuraray Press Release, Kuraray Acquires ISCC PLUS Certification. 3-Methyl-1.5-Pentanediol (MPD) produced at Niigata Plant. *Kuraray*. **2024**, https://www.kuraray.com/news/2024/240117 (accessed Dec 5, 2024).
(35) Xiong, M.; Schneiderman, D. K.; Bates, F. S.; Hillmyer, M. A.; Zhang, K. Scalable production of mechanically tunable block polymers from sugar. *Proc. Natl. Acad. Sci. U.S.A.* **2014**, *111* (23), 8357–8362. https://doi.org/10.1073/pnas.1404596111.
(36) Spanjers, C. S.; Schneiderman, D. K.; Wang, J. Z.; Wang, J.; Hillmyer, M. A.; Zhang, K.; Dauenhauer, P. J. Branched Diol Monomers from the Sequential Hydrogenation of Renewable Carboxylic Acids. *ChemCatChem* **2016**, *8* (19), 3031–3035. https://doi.org/10.1002/cctc.201600710.
(37) European Commission, A sustainable approach to transforming residual biomass into high-value biopolymers, Horizon 2020 - the Framework Programme for Research and Innovation (**2014-2020**). https://doi.org/10.3030/760802 (accessed Dec 11, 2024).
(38) Szliszka, E.; Czuba, Z. P.; Domino, M.; Mazur, B.; Zydowicz, G.; Krol, W. Ethanolic Extract of Propolis (EEP) Enhances the Apoptosis- Inducing Potential of TRAIL in Cancer Cells. *Molecules* **2009**, *14* (2), 738–754. https://doi.org/10.3390/molecules.
(39) Slivniak, R.; Domb, A.J. Stereocomplexes of enantiomeric lactic acid and sebacic acid ester-anhydride triblock copolymers, *Biomacromolecules* **2002**, *3*, 754–760. https://doi.org/10.1021/bm0200128.
(40) Modi, S.; Jain, J.P.; Domb, A.J.; Kumar, N. Copolymers of pharmaceutical grade lactic acid and sebacic acid: Drug release behavior and biocompatibility, *Eur. J. Pharm. Biopharm.* **2006**, *64*, 277–286. https://doi.org/10.1016/j.ejpb.2006.05.013.
(41) Gazzotti, S.; Hakkarainen, M.; Pagnacco, C.A.; Manenti, M.; Silvani, A.; Farina, H.; Arnaboldi, L.; Ortenzi, M.A. Poly(alditol sebacate)-PLA copolymers: enhanced degradability and tunable surface properties, *Polym. Chem.* **2024**, *15*, 2081–2093. https://doi.org/10.1039/d4py00307a.

(42) Rasselet, D.; Ruellan, A.; Guinault, A.; Miquelard-Garnier, G.; Sollogoub, C.; Fayolle, B. Oxidative degradation of polylactide (PLA) and its effects on physical and mechanical properties. *Eur. Polym. J.* **2014**, *50* (1), 109–116. https://doi.org/10.1016/j.eurpolymj.2013.10.011.
(43) ASTM D6691-17, Standard Test Method for Determining Aerobic Biodegradation of Plastic Materials in the Marine Environment by a Defined Microbial Consortium or Natural Sea Water Inoculum (2018 updated). https://doi.org/10.1520/D6691-17.
(44) Cohn, D.; Hotovely-Salomon, A. Biodegradable multiblock PEO/PLA thermoplastic elastomers: molecular design and properties. *Polymer (Guildf)* **2005**, *46* (7), 2068–2075. https://doi.org/10.1016/j.polymer.2005.01.012.
(45) Fabbri, M.; Soccio, M.; Costa, M.; Lotti, N.; Gazzano, M.; Siracusa, V.; Gamberini, R.; Rimini, B.; Munari, A.; García-Fernández, L.; Vázquez-Lasa, B.; San Román, J. New fully bio-based PLLA triblock copoly(ester urethane)s as potential candidates for soft tissue engineering. *Polym. Degrad. Stab.* **2016**, *132*, 169–180. https://doi.org/10.1016/j.polymdegradstab.2016.02.024.
(46) Navarro-Baena, I.; Marcos-Fernández, A.; Fernández-Torres, A.; Kenny, J. M.; Peponi, L. Synthesis of PLLA-*b*-PCL-*b*-PLLA linear tri-block copolymers and their corresponding poly(ester-urethane)s: effect of the molecular weight on their crystallisation and mechanical properties. *RSC Adv.* **2014**, *4* (17), 8510–8524. https://doi.org/10.1039/c3ra44786c.
(47) Imre, B.; Pukánszky, B. Compatibilization in Bio-Based and Biodegradable Polymer Blends. Eur. Polym. J. **2013**, *49*, 1215–1233. https://doi.org/10.1016/j.eurpolymj.2013.01.019.
(48) Saeidlou, S.; Huneault, M. A.; Li, H.; Park, C. B. Poly(lactic acid) crystallization. *Prog. Polym. Sci.* **2012**, *37*, 1657–1677. https://doi.org/10.1016/j.progpolymsci.2012.07.005.
(49) Sur, S.-H.; Choi, P.-J.; Ko, J.-W.; Lee, J.-Y.; Lee, Y.-H.; Kim, H.-D. Preparation and Properties of DMF-Based Polyurethanes for Wet-Type Polyurethane Artificial Leather. *Int. J. Polym. Sci*. **2018**, *2018*, 7370852. https://doi.org/10.1155/2018/7370852.
(50) Phuong, V. T.; Coltelli, M. -B.; Cinelli, P.; Cifelli, M.; Verstichel, S.; Lazzeri, A. Compatibilization and property enhancement of poly(lactic acid)/polycarbonate blends through triacetin-mediated interchange reactions in the melt. *Polymer (Guildf)* **2014**, *55* (17), 4498–4513. https://doi.org/10.1016/j.polymer.2014.06.070.
(51) Tejada-Oliveros, R.; Gomez-Caturla, J.; Sanchez-Nacher, L.; Montanes, N.; Quiles-Carrillo, L. Improved Toughness of Polylactide by Binary Blends with Polycarbonate with Glycidyl and Maleic Anhydride-Based Compatibilizers. *Macromol. Mater. Eng.* **2021**, *306* (12), 2100480. https://doi.org/10.1002/mame.202100480.
(52) Bianchi, E.; Guidotti, G.; Soccio, M.; Siracusa, V.; Gazzano, M.; Salatelli, E.; Lotti, N. Biobased and Compostable Multiblock Copolymer of Poly(L-lactic acid) Containing 2,5-Furandicarboxylic Acid for Sustainable Food Packaging: The Role of Parent Homopolymers in the Composting Kinetics and Mechanism. *Biomacromolecules* **2023**, *24* (5), 2356–2368. https://doi.org/10.1021/acs.biomac.3c00216.
(53) Zheng, L.; Li, C.; Wang, Z.; Wang, J.; Xiao, Y.; Zhang, D.; Guan, G. Novel Biodegradable and Double Crystalline Multiblock Copolymers Comprising of Poly(butylene succinate) and Poly(ε-caprolactone): Synthesis, Characterization, and Properties. *Ind. Eng. Chem. Res.* **2012**, *51* (21), 7264–7272. https://doi.org/10.1021/ie300576z.
(54) Zettler, E. R.;Mincer, T. J.; Amaral-Zettler, L. A. Life in the "Plastisphere": Microbial Communities on Plastic Marine Debris. *Environ. Sci. Technol*. **2013**, 7137–7146. https://doi.org/10.1021/es401288x.
(55) Dash, H.R.; Mangwani, N.; Chakraborty, J.; Kumari, S.; Das, S. Marine bacteria: potential candidates for enhanced bioremediation, *Appl. Microbiol. Biotechnol*. **2013**, *97*, 561–571. https://doi.org/10.1007/s00253-012-4584-0.
(56) De Tender, C.A.; Devriese, L.I.; Haegeman, A.; Maes, S.; Ruttink, T.; Dawyndt, P. Bacterial Community Profiling of Plastic Litter in the Belgian Part of the North Sea, *Environ. Sci. Technol.* **2015**, *49*, 9629–9638. https://doi.org/10.1021/acs.est.5b01093.
(57) Urbanek, A.K.; Rymowicz, W.; Mirończuk, A.M. Degradation of plastics and plastic-degrading bacteria in cold marine habitats, *Appl. Microbiol. Biotechnol.* **2018**, *102*, 7669–7678. https://doi.org/10.1007/s00253-018-9195-y.
(58) Gunawan, N.R.; Tessman, M.; Zhen, D.; Johnson, L.; Evans, P.; Clements, S.M.; Pomeroy, R.S.; Burkart, M.D.; Simkovsky, R.; Mayfield, S.P. Biodegradation of renewable polyurethane foams in marine environments occurs through depolymerization by marine microorganisms, *Sci. Total. Environ.* **2022**, *850,* 158761, https://doi.org/10.1016/j.scitotenv.2022.158761.

(59) Kim, Y.D.; Kim, S.C. Effect of chemical structure on the biodegradation of polyurethanes under composting conditions, *Polym. Degrad. Stab*. **1998,** *62*, 343-352. https://doi.org/10.1016/S0141-3910(98)00017-2.
(60) Howard, G.D. Biodegradation of polyurethane: a review, *Int. Biodeterior. Biodegrad.* **2002**, *49*, 245-252. https://doi.org/10.1016/S0964-8305(02)00051-3.
(61) Akiba, M. Desterioration and Stabilization of Polyurethane, *J. Adhes. Soc. Jpn.* **2004**, *40*, 241-252. https://doi.org/10.11618/adhesion.40.241 (in Japanese).
(62) Xie, F.; Zhang, T.; Bryant, P.; Kurusingal, V.; Colwell, J.M.; Laycock, B. Degradation and stabilization of polyurethane elastomers, *Prog. Polym. Sci.* **2019**, *90,* 211–268. https://doi.org/10.1016/j.progpolymsci.2018.12.003.

Concluding Remarks

This study aimed to address the challenges of the brittleness and biodegradability of PLA to promote the widespread adoption of bioplastics. The results of the synthesis and biodegradability of sustainable PLA-based block copolymers were summarized.

Chapter 1 developed high-toughness biomass polyesters derived from wood-based xylose and lactic acid. PAX-*co*-PLA was synthesized using xylose, lactic acid, and aliphatic diols with carbon numbers ranging from 2 to 6. Compared to PLA, PAX-*co*-PLA exhibited improved toughness and heat resistance. The biodegradability of PHX-*co*-PLA, which showed the highest toughness, was evaluated. PAX-*co*-PLA contributed to the effective utilization of resources and demonstrated potential biodegradability in compost and seawater, thereby contributing to the reduction of environmental impact.

In Chapter 2, PLA-*alt*-PCL with different PLA chain lengths was synthesized *via* ring-opening polymerization of lactide and chain-extension reactions. The simplified one-pot reaction process enabled the synthesis of PLA-*alt*-PCL with a regular sequence, which is expected to reduce manufacturing costs by efficiently utilizing PLA production plants in anticipation of mass production. Additionally, PLA-*alt*-PCL exhibited controllable mechanical properties, high toughness, and high biodegradability in compost, as well as a decrease in molecular weight in seawater, with significant degradation observed in the early stages.

PLA-*alt*-PMPDSe with improved marine biodegradability and mechanical properties was synthesized in Chapter 3. The copolymers of PLA and PMPDSe—based on biomass-derived sebacic acid—exhibited excellent mechanical properties and potential biodegradability in compost, activated sludge, and seawater, indicating their suitability for various applications, including packaging materials and agricultural films.

Inspired by PLA production techniques using wood resources, this study developed PLA-based block copolymers that address the weaknesses of PLA through copolymerization. The results obtained are promising in terms of contributing to the future expansion of bioplastic applications and solving various environmental issues.

List of publications

Chapter 1

Synthesis of High-Toughness Polyesters Using Xylose and Lactic Acid and Analysis of Their Biodegradability

Atsuki Takagi, Yu-I Hsu*, Hiroshi Uyama*

ACS Applied Polymer Materials **2024**, 6 (21), 13307–13318.

DOI : 10.1021/acsapm.4c02662

Chapter 2

Biodegradable poly(lactic acid) and polycaprolactone alternating multiblock copolymers with controllable mechanical properties

Atsuki Takagi, Yu-I Hsu*, Hiroshi Uyama*

Polymer Degradation and Stability **2023**, *218*, 110564.

DOI : 10.1016/j.polymdegradstab.2023.110564

Chapter 3

Biomass-derived poly(lactic acid) and poly(3-methyl-1,5-pentanediol sebacate) alternating multiblock copolymers with improved marine biodegradability and mechanical properties

Atsuki Takagi, Yu-I Hsu*, Hiroshi Uyama*

Polymer Degradation and Stability **2025**, *236*, 111301.

DOI : 10.1016/j.polymdegradstab.2025.111301

Other publications

Mutant β-fructofuranosidase synthesizing blastose [β-D-Fru*f*-(2→6)-D-Gl*cp*]

Atsuki Takagi, Takayoshi Tagami, and Masayuki Okuyama*

Enzyme and Microbial Technology **2024**, *180*, 110500.

DOI : 10.1016/j.enzmictec.2024.110500

Acknowledgements

This research was conducted as a collaborative research and doctoral research at the Uyama Lab., Department of Applied Chemistry, Graduate School of Engineering, the University of Osaka, and the Biochemical Research Center, Innovation Promotion Devision, Oji Holdings Co., from September 2021 to July 2025. I would like to express my sincere gratitude to all those who have supported me.

First and foremost, I would like to extend my deepest appreciation to my research supervisor, Prof. Hiroshi Uyama, for his expertise, constructive criticism, and guidance, which enabled me to achieve the results of this research. I am profoundly grateful for his unwavering support, mentorship, and trust in me. In particular, I am grateful to Prof. Takashi Hayashi and Prof. Satoshi Minakata for their valuable advice and insightful feedback during the dissertation review process.

I am indebted to Associate Prof. Yu-I Hsu for her meticulous guidance on experimental techniques, research progression, and academic writing. Her support was invaluable throughout this research. I would like to extend my sincere thanks to all the members of the Uyama Lab., especially Assistant Prof. Akihide Sugawara, Ms. Yoko Uenishi, Ms. Tomoko Shimizu, Ms. Chikako Abe, Dr. Manjie He, Dr. Yuxiang Jia, Dr. Kazuki Shibasaki, Dr. Judit Rebeka Molnar, Dr. Ying Yao, Dr. May Myat Noe, Dr. Hasinah Binti Mohamed Rafiq, Ms. Izzah Durrati Binti Haji Abdul Hamid, Ms. Sooyeon Noh, Mr. Yi-ho Chen, Mr. Yuji Kiba, Mr. Takeshi Hiraoka, Mr. Motoi Oda, Mr. Kaita Kikuchi, Mr. Hajime Fujimori, Ms. Suzune Miki, Ms. Rika Ohnishi, Mr. Shotaro Yano, Mr. Hiroshi Hasegawa, Mr. Sota Nakagawa, and Mr. Naoaki Ishihara, for their support ranging from creating a comfortable laboratory environment to assisting with experimental measurements. Their kindness and encouragement have been greatly appreciated.

I would like to extend my heartfelt gratitude to the members of the Biochemical Research Center, Innovation Promotion Division, Oji Holdings Co., for their unwavering support. They were always there to help me when I faced obstacles. I am also deeply grateful to the members of the Innovation Promotion Division, including Taketo Okutani, Corporate Officer, Yosuke Uchida, General Manager, Yuichi Noguchi, Deputy General Manager, Takeshi Kawai, Deputy General Manager, Hirotaka Nakamura, Group Manager, Ryosuke Hirakawa, Group Manager, Naoyuki Okuda, Senior Researcher, Mr. Atsushi Koizumi and Mr. Mugito Kato. In particular, I would like to express my deepest gratitude to Deputy General Manager, Yuichi Noguchi for his valuable advice, unwavering support, and trust in me. Additionally, I am grateful to Kohei Michikawa, former General Manager, for providing the opportunity for joint research with the Uyama Lab.

I was also greatly indebted to Professor Atsuo Kimura, Professor Masayuki Okuyama, and Associate Professor Takayoshi Tagami of the Graduate School of Agriculture, Hokkaido University, who guided me during my master's program and helped me take my first steps as a researcher.

Finally, none of this would have been possible without the love and support of my family. I am deeply grateful to my father Hiromi, my mother Yuko, my sister Chisato, my brother Shunsuke, and my wife Eri for their unwavering support and encouragement.

2025. 7

Atsuki Takagi